2016-01-01

Geology and Mineralization Controls Surrounding the Palmarejo Mining District - A Compilation of Remote and Hands on Exploration Techniques

Castulo Molina Sotelo
University of Texas at El Paso, cacho_molina@hotmail.com

GEOLOGY AND MINERALIZATION CONTROLS SURROUNDING THE PALMAREJO MINING DISTRICT - A COMPILATION OF REMOTE AND HANDS ON EXPLORATION TECHNIQUES

CÁSTULO MOLINA SOTELO

Doctoral Program in Geological Sciences

APPROVED:

Philip C. Goodell, Ph.D., Chair

Terry L. Pavlis, Ph.D.

Laura F. Serpa, Ph.D.

Richard P. Langford, Ph.D.

Raed E. Aldouri, Ph.D.

Charles Ambler, Ph.D.
Dean of the Graduate School

GEOLOGY AND MINERALIZATION CONTROLS SURROUNDING THE PALMAREJO MINING DISTRICT - A COMPILATION OF REMOTE AND HANDS ON EXPLORATION TECHNIQUES

by

CÁSTULO MOLINA SOTELO, MS, IG.

DISSERTATION

Presented to the Faculty of the Graduate School of

The University of Texas at El Paso

in Partial Fulfillment

of the Requirements

for the Degree of

DOCTOR OF PHILOSOPHY

Department of Geological Sciences

THE UNIVERSITY OF TEXAS AT EL PASO

December 2016

Acknowledgements

My deepest gratitude to Philip Goodell and Michael Krebs, whose encouragement and support made the achievement of this milestone possible.

Abstract

Exploration is the base of the mining industry, and it is often taken as synonymous with "finding a mine". In reality it is a more complex process; where the selection, evaluation, screening and testing of successively smaller areas lead to the discovery of an economic deposit. Once the deposit is found, the economic factors become more important than the geological ones, and then the exploration becomes a tool to give sustainability to the mining operation through time.

The key to a continued and successful exploration are the correct answers to the basic questions: What kind of deposit is this? How can it be classified? Which are the mineralization controls, and where are they located? What are the conditions for a high-grade material, and how can those conditions be identified in the field?

Once the basic questions are answered, and the geological model of mineralization is correctly identified, the remaining question is about where we are located with respect to the whole system, in order to efficiently target the exploration in specific locations as well as at a regional scale. It is at this time when the exploration becomes an inter-disciplinary effort, where the remote and hands on exploration techniques convene to give continuity and balance between finding ores and producing metals.

The successful re-discovery of the Palmarejo District by an Australian Junior in 2003 was founded on basic information and entrepreneurial drive (Masterman et al, 2005). The drilling at the intersection of two outcropping veins (La Blanca and La Prieta) ended with the definition of the first resource in the Rosario area. The exploration drilling then continued along the veins, and the richest, hidden orebody (Clavo 76) was found. The knowledge gleaned from this area and the use of different exploration tools, were applied to target the drilling, and eventually led to the discovery and outline of the blind deposits of Guadalupe, Los Bancos and Independencia.

The mining of such deposits is currently ongoing, and as mineral resources are depleted, the exploration task is to refresh resources, in order to maintain long term operations. To give sustainability to the business, the exploration foot print needs to expand to outlying areas, in order to increase the feasibility of the mine.

In order to unravel the geological associations and controls of mineralization on any scale, it is at this stage when studies go back and forth from millimeters to meters and eventually kilometers. Using a series of five chapters, three of them focused on the mine, and two at regional level, this author will show the geology and mineralization controls at different scales within the study area. Once the mineralization controls at regional and mine scales are known, the combination of previous knowledge with the right tools, helps the explorer to decide where to wisely and effectively spend the resources.

Table of Contents

List of Tables

List of Figures

Chapter 1: Geology and Exploration History of the Palmarejo Silver and Gold District, Chihuahua, México.

1.1 ABSTRACT

The silver and gold deposits of the world-class Palmarejo District are typical, intermediate sulfidation- style epithermal, precious metal occurrences, hosted in Cretaceous- to Tertiary-aged volcanic and intrusive rocks of the Lower Volcanic Complex (LVC), and host one of the newest and largest silver and gold producers in Mexico. The district and mining operations are owned and operated by Coeur Mining Inc. through its wholly-owned subsidiary, Coeur Mexicana.

The Palmarejo deposit is centered at the intersection of the La Prieta and La Blanca structures – a zone called the Rosario Clavo (shoot), while the other ore shoots are extending to the south-east along both structures. To date there are five known silver and gold-bearing clavos in the Palmarejo deposit termed Rosario, 76, 108, Tucson and Chapotillo. Subsequent work by Bolnisi and Coeur led to the discovery and definition of Guadalupe, Los Bancos, La Patria, and Independencia, as well as numerous new targets in the +12,000 hectare Palmarejo District.

1.2 INTRODUCTION AND LOCATION

Palmarejo is located in the southwest portion of the State of Chihuahua in the Sierra Madre Occidental (SMO) epithermal belt (Figure 1.1). The district contains multiple silver and gold occurrences in at least four wide, northwest-trending structural belts. The largest deposits known today are the Palmarejo, the Guadalupe and the La Patria occurrences. The Palmarejo and Guadalupe deposits are the location of the current surface and underground mining operations.

The history of exploration and mining in the Palmarejo District spans a period of time from the early 1800's to the present day. However, activities were conducted only sporadically by small-scale operators and the district was not consolidated into a cohesive, one-owner land package until the early part of the 21st century.

Initial modern-day reconnaissance and exploration of the Palmarejo District, commenced in 2003 by Bolnisi Gold NL (Bolnisi), an Australian junior exploration company. Bolnisi drilled

its first exploration holes in what is now known as the Palmarejo deposit and mine area in late 2003, and completed the first mineral resource estimate for the Palmarejo deposit in July of 2004 (Beckton, 2004). In December 2007, Coeur d'Alene Mines Corporation (Coeur) acquired the property and produced the first gold and silver Dore in March 2009.

According to Gonzalez Reyna (1956), the modern day development status of the Palmarejo District was preceded by the earliest explorer Valentin Ruiz, who in 1818, envisioned the area for high-grade silver-gold mining. However, mining only commenced on Ruiz' concept after 1853. Ownership of the prospects and incipient mining operations passed from several different parties, including the English company Palmarejo and Mexican Gold Fields, who commenced operations in the early 1910`s. During this time, production capacity was 125 tonnes (metric units) per day of mining and processing of high-grade ores from Rosario. The company built a mill at the Chínipas River, put an aqueduct to produce electrical power and completed the railroad connection between the mine and the mill in 1896. Mining ceased temporarily in 1912 with the onset of the Mexican Revolution (United Nations, 2006). After the First World War armistice, Palmarejo and Mexican Gold Fields resumed operations at Palmarejo, and produced 14 kilograms of gold and 1233 kilograms of silver from 1271 tonnes of high- grade ore. The company operated intermittently from 1922 until the silver price and recovery problems forced the closure of the operations in 1927 (Gonzalez Reyna, 1956).

Minas Uruapa, a private Mexican mining company, acquired the property in 1964, but it was not until 1985 that production recommenced at a rate of 120 tonnes per day. Minas Uruapa operated a flotation mill, located near the small town of Palmarejo until 1992, when the operation became marginal and forced the closure of the mine (Masterman et al, 2005). Estimated past production from the district, through 1992, was 68,000 tonnes of ore and over 695,500 and 3,200 troy ounces of silver and gold, respectively (Coeur d'Alene Mines Corporation corporate public filings on www.sedar.com, February, 2010).

At the time of Coeur's acquisition of the district, the total mineral resource was 1.47 million troy ounces of gold and 130.8 million troy ounces of silver, contained in over 22,300 million tonnes

or ore (at a cutoff grade of 0.67 grams per tonne of gold equivalent grade; gold equivalent equals gold grade plus silver grade divided by 57). Subsequent exploration by Coeur management had increased the total mineral resource to over 1.7 million troy ounces of gold and nearly 99 million troy ounces of silver effective December 31, 2013. This, after having produced over .5 and 33.5 million troy ounces of gold and silver, respectively, since 2009, the first year of modern mining and ore processing by Coeur (Rasmussen et al, 2014).

1.3 REGIONAL GEOLOGIC SETTING

The Palmarejo mining district is located in the Sierra Madre Occidental (SMO), a Cretaceous- to Tertiary-aged volcanic field in northwestern Mexico, approximately 270 km southwest of Chihuahua City (Figure 1.1). The SMO consists of a north- to northwest-trending volcanic plateau, about 1,200 km long and 300 km wide, averaging 2,000 m above sea level. This igneous province is considered the result of Cretaceous-Cenozoic magmatic and tectonic episodes related to the subduction of the Farallon Plate beneath North America and the opening of the Gulf of California (Ferrari et al, 2005). The Palmarejo vein system is set at elevations from 900 to 1200 meters above sea level (masl).

Other authors consider the SMO to be the least deformed, silicic, large igneous province on Earth, as well as the largest of Cenozoic age (Bryan, 2007; Bryan and Ernst, 2008). The province also hosts several world-class epithermal precious-metal deposits, (Dreier, 1984; Staude and Barton, 2001) for instance, the currently active mines Palmarejo, Pinos Altos, Ocampo, Sauzal, and Dolores, as well as several developing projects of great interest for exploration juniors and major precious metals producers.

1.3.1 Geologic framework of the SMO province

Geology of the SMO is divided into the Lower Volcanic Complex (LVC) and Upper Volcanic Supergroup (UVS). The LVC is characterized by a series of andesitic, volcanic and sedimentary rocks, inter-layered with felsic pyroclastic units deposited between 46 and 35 Ma (McDowell and Keizer, 1977; Wark, et al, 1990), and estimated to be approximately 2 km thick

(McDowell and Keizer, 1977). Calc-alkaline granodioritic to granitic batholiths and stocks have intruded volcano-sedimentary rocks of the LVC.

Geochemical data show that the SMO rocks form a typical calc-alkaline rhyolite suite with intermediate to high K and relatively low Fe content. The Late Eocene to Miocene volcanism is clearly bimodal, but silicic compositions are dominant in the upper volcanic sequence rocks (Ferrari, et al, 2005). The LVC rocks are interpreted to have formed in a magmatic arc environment during the Late Cretaceous- to Early Tertiary-aged Laramide Orogeny (Staude and Barton, 2001). The large porphyry copper-molybdenum deposits in southern Arizona (USA) and northern Sonora (Mexico), were emplaced during this episode of convergence, whereas ignimbrites of the UVS were deposited during rift-type magmatism induced by Mid-Tertiary steepening of the subducted slab beneath western Mexico (Staude and Barton, 2001).

1.3.2 Tectonic setting of Palmarejo

North of the Temoris area (Figure 5.23), mapping from different mining companies and researchers such as Busby (2008), have identified a series of surge- like volcanics with thick layers of ignimbrite breccias, interstratified with thick, silicic lava flows. The epithermal deposits in this part of the SMO are hosted in the LVC along fault- fissure zones and appear to be related to the silicic plug-type intrusions. A similar association between silicic intrusions and mineralization in the SMO is discussed by Bryan et al, (2008). Portions of Palmarejo, Guadalupe and La Patria in the district show these characteristics.

The regional extensional structures trend northwest-southeast and resulted in the development of horsts and grabens throughout the SMO. Late Eocene- to early Oligocene- aged hydrothermal fluids, spatially and temporally associated with deposition of the lower parts of the UVS, exploited the extensional architecture (Goodell, 1995). Ore bodies are probably present throughout the province, but are only visible in the bottoms of the canyons since the overlying, upper volcanic rocks provide a thick cover and obscures detection. The continuity of the structural

system is located southwards on a southeast-northwest trend, developing a set of gold and silver mineralized structures (Rasmussen et al, 2014).

The Late Eocene to early Oligocene time was the major metallogenic episode in western Mexico (McDowell and McIntosh, 2012). The principal types of ore deposits formed are vein-style, low and intermediate sulfidation Ag- Au ±Pb-Zn-Cu (e.g., Palmarejo, Pinos Altos), as well as disseminated high-sulfidation Au-Cu (e.g., Mulatos and El Sauzal), and high- temperature, carbonate-hosted Ag-Pb-Zn (e.g., Naica and Santa Eulalia in, Clark and de la Fuente, 1978, Staude and Barton, 2001). The genetic classification of Palmarejo is consistent with the definitions of low to intermediate sulfidation, gold-silver deposits, coined by Hedenquist et al (2000), and discussed in Sillitoe and Hedenquist (2003), and Einaudi et al (2003).

1.4 PALMAREJO DEPOSIT

Two main ore deposits have been defined to date in the Palmarejo district: Palmarejo and Guadalupe ore deposits, both part of the northwest-trending belt of gold and silver vein deposits typical of the SMO (Figure 1.2). The Palmarejo deposit is formed by two main sets of southwest dipping structures, La Prieta, which is a WNW striking fault zone and La Blanca, a NW striking structure (Figure 1.3). In addition, a broad zone of sheeted, quartz-vein stockwork mineralization, forms, at the intersection of the two structures known as the Clavo Rosario (Gustin, 2005).

1.4.1 Alteration and mineralization

Wall rock alteration in Palmarejo district is characterized by illite at deeper levels, grading upwards to illite-smectite on prominent outcrops which reveal unexposed structures underneath (e.g., Los Bancos area; Molina, 2008). Hematite box works after pyrite are also developed within wall rocks. Other alteration assemblages are represented by regional propyllite wall rock characterized by pyrite, calcite, chlorite and local epidote. Kaolin clays, as alteration products, are recognized within mineralized portions of La Blanca, evidencing acidic conditions of circulating fluids (Corbett, 2004). Additional surface sampling from La Prieta Vein shows the presence of local dickite-illite clay pairs, along with manganese-rich carbonates (Molina, 2010).

Acidic alteration conditions are particularly well developed at Espinazo del Diablo, located west of Palmarejo (Figure 1.2), consisting of NW trending silicic structures with halos of advance argillic alteration, characterized by quartz-alunite as well as dickite, pyrophyllite, kaolinite, diaspore, and barite (Sillitoe, 2010; Hedenquist, 2014). Au-Ag mineralization is hosted within quartz veins and vein breccias and vary from pervasive silicification to quartz fill expansion breccias and sheeted vein systems (Corbett, 2006). Quartz in the breccias and veins occurs as multiple cross-cutting events and vary from chalcedony to comb quartz (Figure 1.4).

1.4.2 Structures and mineralization

The main structure-controlled veins, La Prieta and La Blanca, have been mapped for more than 2.0 kilometers and 1.5 kilometers respectively. The mineralized strike length is 1,500 meters on La Prieta and 1,000 meters on La Blanca (Figure 1.3). Several steep plunging, high-grade, mineralized shoots, known as clavos, have been defined on each structure (Figure 1.2).

Ore shoots in Palmarejo include Clavo 076 and Clavo 108, contained in La Blanca Vein. La Prieta Vein hosts Rosario, Tucson and Chapotillo ore shoots. Both La Blanca and La Prieta are the main faults controlling and hosting gold-silver mineralization. Clavo Rosario lies at the intersection of these faults, which dip moderately to steeply, to the southwest (Rhys, 2009) and host the bulk of precious metals at Palmarejo. Average grades in Palmarejo are 2.1 grams/tonne Au, and 164 grams/tonne Ag (Coeur, 2013). According to Rasmussen et al, the 076 clavo is a sub vertical, plunging ore shoot, localized at a strike inflection on the La Blanca fault (Figures 1.2 and 1.3). Stratigraphic contacts also impart control on mineralized widths (Figure 1.3). The veins evolved from the early stages, characterized by high grade sulphide content, into veins with progressively lower sulphide content that in turn evolve from quartz-adularia-dominant to carbonate-dominant (Figure 1.4). The composition of carbonates evolves from early dolomitic to late calcite-dominant stages (Ross, 2009).

1.4.3 Mineralogy and fluid inclusions

Ore minerals in Palmarejo include electrum as the main gold-bearing mineral; the silver-bearing minerals are varied, but the most common are copper-silver sulphides, jalpaite, mckinstryte and stromeyerite. Acanthite is also present, but subordinated to Ag-Cu sulphides. Gold and silver minerals are usually associated with other base metal sulphide minerals such as sphalerite, chalcopyrite, galena, and bornite. Additional sulphosalts are also present, such as tennantite, and pearceite. Selenides and tellurides are found sporadically in isolated areas of the vein system (Ross, 2009; Melchor, 2005). The vein system is interpreted to have formed from at least eight mineralization events, recognized though cross-cutting relationships of veinlets, which aid in the understanding of the paragenesis (Rhys, 2009). Microthermometric studies in quartz at La Blanca Vein reveal tight homogenization temperatures in the range of 260°C to 270°C, in a sub horizontal pattern (Rubio and Albinson, 2005), which implies no telescoping of the mineralization. Additional thermometric data by Galvan (2012) in a sphalerite host, show a span of homogenization temperatures from 270° to 320°C, and salinities from 1.2 to 7.4 wt. % NaCl equivalent, interpreted as different mineralization pulses recorded in the sulphide mineral phases. Boiling evidence in fluid inclusions in quartz was recorded by petrographic observations (Melchor, 2005, Figure 1.7). Additional boiling evidence is observed on blade-type textures displayed by the carbonate minerals contained in the hypogenic stages.

1.5 GUADALUPE DEPOSIT

The Guadalupe vein system comprises four main centers along a NW-striking fault system known as Guadalupe Norte, Guadalupe Centro, Las Animas, and La Curra (Figure 1.5). The structure is characterized by exposed quartz-carbonate veins and breccias ranging from centimeters to tens of meters in width and unexposed features highlighted by the clay-smectite-rich fault system oriented northwest and dipping 55° to 60° to the northeast (Molina, 2008). This regional feature is wide and made up of multiple fault strands over several tens of meters. Slivers of various

lithologies are present between shear zones adjacent to the main structure, that differ from the surrounding hanging wall or foot wall of the fault. (Rhys, 2009).

1.5.1 Alteration

Both extrusive and intrusive rocks, exposed along the hanging wall and footwall of the structure, are weakly to pervasively altered by quartz, carbonate, kaolinite, montmorillonite, illite, muscovite, chlorite and epidote. Kaolinite and montmorillonite are ubiquitous in outcropping altered rocks and fault zones. Exposed quartz veins and breccias are spatially associated with a major NW-striking fault zone and in the footwall block. Vein and breccia infill material comprises amorphous silica and fine- grained quartz, fine and coarse grained platy carbonate (with quartz pseudomorphs), kaolinite, illite, iron oxides (dominantly hematite and goethite) and manganese oxides. Quartz vein textures include massive, sugary, bladed, comb, crustiform, and colloform, opaline and drusy quartz. Multiphase breccias show typical cockade textures (Figure 1.4C). Alteration styles identified at the Guadalupe project typically include a central, multiphase quartz-carbonate assemblage and an outer propyllite halo consisting of epidote-chlorite- pyrite-carbonate assemblage.

According to Rhys (2009), the quartz-carbonate assemblage is spatially associated with the principal structure and comprises at least five main alteration/infill events: 1) Cryptocrystalline grey quartz and potassic feldspar are the oldest assembly. The event is typically characterized by centimeter-wide planar to sinuous veins with narrow alteration selvages; 2) A microcrystalline sugary white quartz alteration/infill phase crosscuts the early phase and is characterized by centimeter to tens of meters wide quartz veins. Illite replacement of potassic feldspar, rhodocrosite and bladed carbonate after former barite crystals are also observed; 3) The third alteration/infill event comprises coarse-grained, amethyst quartz infill; 4) Ubiquitous carbonate flooding characterizes the fourth phase, containing calcite, rhodocrosite, and manganocalcite; 5) The final phase comprises late breccia and fracture hematite ± carbonate infill. This final phase probably produced the high gold grades, related to supergene enrichment of gold. Ubiquitous propyllite

assemblage containing epidote-chlorite-pyrite-carbonate alteration develops a halo around the inner quartz- carbonate assemblage.

1.5.2 Mineralization and mineralogy

Mineralization extends for more than 3.5 km along strike and up to 300 meters down dip (Figure 1.8). The Guadalupe veins hosts gold-silver ore shoots containing minor amount of copper-lead-zinc ores. Ore shoots are preferentially developed in fault linking zones and adjacent to a rhyolite flow dome complex (Figure 1.6), where the fault steepens and thickens becoming parallel to extension vein sets which strike parallel to the main vein (Rhys, 2009). Average grades of 2.11 grams/tonne Au and 138 grams/tonne Ag are present in hypogenic native gold, electrum, local native silver, Ag-rich sulphides acanthite, jalpaite, and sulphosalts (Figure 1.8A), pearceite, freibergite, in addition to supergene-related gold hosted in iron oxides (Melchor, 2010). The chemistry of the deposit could be addressed as an Au-Ag-Cu-As (+/- Zn-Pb) hydrothermal system. Copper sulphide minerals are also present in minor amounts, those are chalcopyrite, bornite, and trace amounts of chalcocite. The Guadalupe deposit is the next main silver and gold producer of the Palmarejo mining district, with mineral resources in excess of 65 million ounces of silver and 0.95 million ounces of gold (Coeur, 2013).

1.5.3 Gold and silver metal zoning

Precious metal distributions show three vertically zoned metal windows at the Guadalupe Project; they are characterized by an upper silver-base metal-rich, a middle gold-silver-rich and a lower gold-silver-base metal-rich ore (Masterman et al, 2005). Precious metal zonation is evident within all the district structures, with gold/silver ratios typically decreasing towards the lower boundary. Gold/silver ratios above 1:100, and elevated silver values, occur in the upper portions of the vein, whilst the lower portion (often of 1-3 m or 10% of the vein thickness), usually contains a gold/silver ratio below 1:100; in some portions of the ore shoots the ratio drops to 1:10. The prominent zonation is associated with increasing gold endowment towards the lower boundary.

Quartz and carbonates are the main vein infill gangue materials, formed by amorphous opaline silica, sugary and drusy quartz, blade- type carbonates and minor barite relicts. All of them are emplaced on multiple events developing comb, crustiform, breccias and cockades open space vein textures, typical of the epithermal environment. Thermometry measurements by Rubio and Albinson (2005), obtained two homogenization temperature clusters within the quartz host, the first group in the range of 190°C, and a second one at 220°C +/-3°C. Further petrology and geochemistry of the district is to be addressed to solve for metal distribution and zonation pursuing the development of additional targets that may be present within the Palmarejo District, and may contribute to the increase of resources.

1.6 ACKNOWLEDGMENTS

The article is a combined effort of all the members of the exploration team headed by the author, and it describes the history of the district, the regional geologic setting, the mineralogical associations and mineralization controls of both Palmarejo and Guadalupe deposits. Portions of this article were published by the Society of Economic Geologists in the Guidebook Series, Volume 42; “Gold and Silver Mines of the Sierra Madre Occidental, Mexico”. It was originally published in 2010 (Birak, et al, 2010), and the revised version in 2014 (Rasmussen et al, 2014). The publication of this paper was possible thanks to the support of the senior management of Coeur Mining: Mitch Krebs (CEO), Don Birak and Hans Rasmussen, Exploration VP’s in 2010 and 2014, respectively. Gratuity goes to the geologists who contributed directly in these papers and to those, who with restless discussions, have contributed to the better understanding of the geologic knowledge of the Palmarejo district.

CHAPTER 1 FIGURES

Figure 1.1 Location of the Palmarejo district. The figure is also showing important geographic references, as well as the location of other significant epithermal deposits inside the Sierra Madre Occidental province.

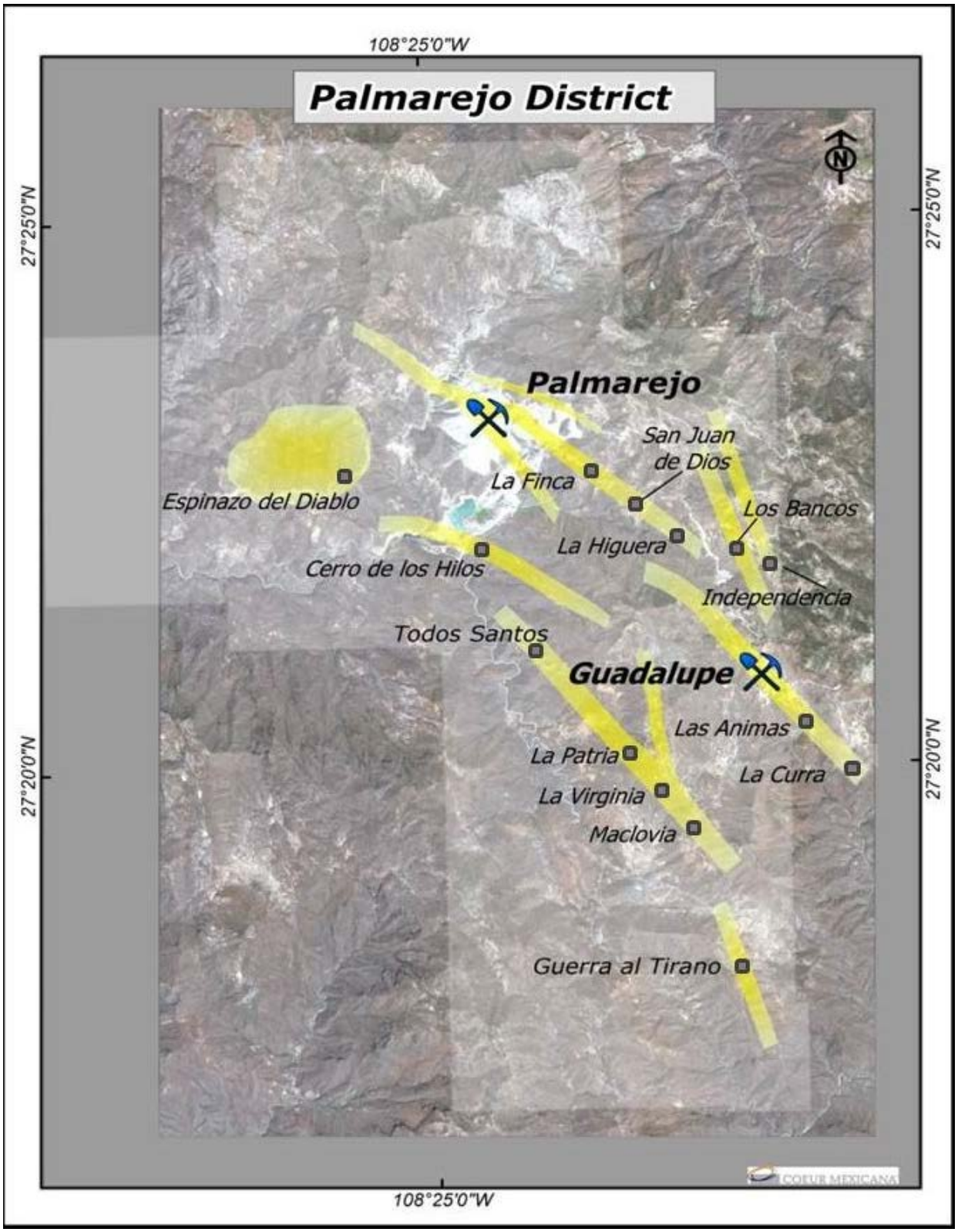

Figure 1.2 Palmarejo mining district. Figure showing mineral occurrences, and the regional structural and mineralization trends in the Palmarejo District.

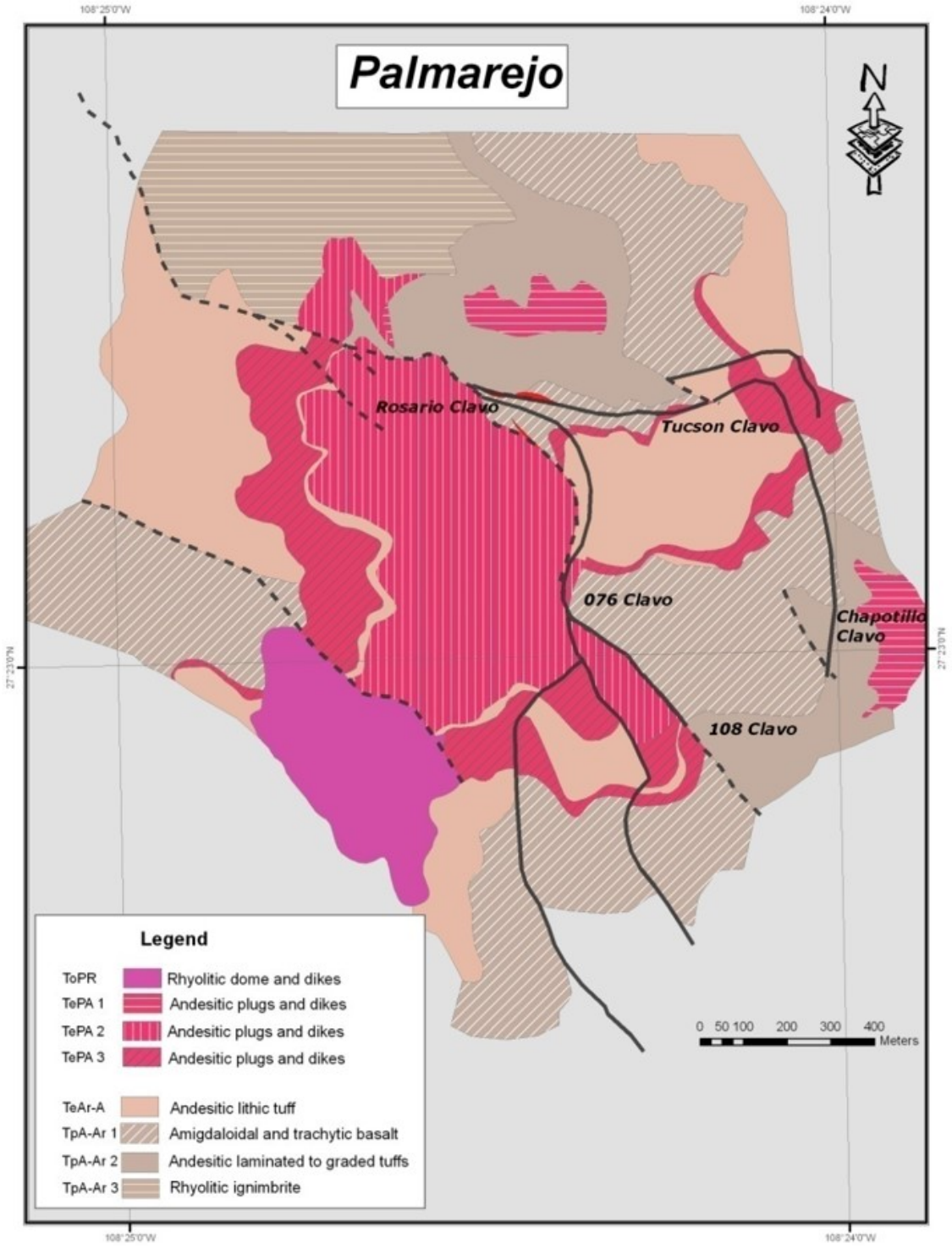

Figure 1.3 Geologic map of Palmarejo. Showing the main lithologies and the location of the main orebodies that conform the Palmarejo deposit. Note the location of orebodies at the intersection of structures (e.g. Rosario and 076 clavos), and/or changes in direction (e.g. Tucson, 108 and Chapotillo clavos).

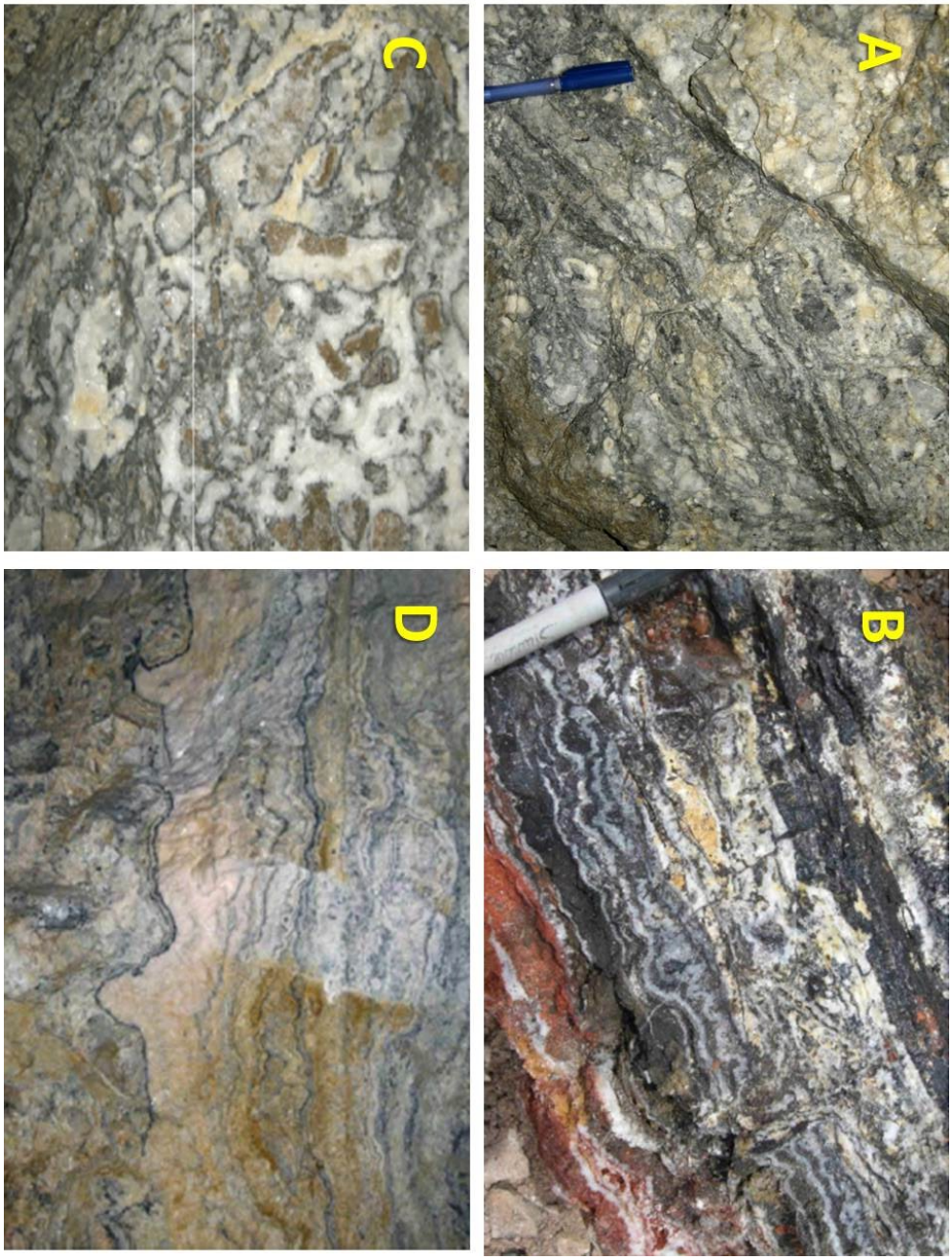

Figure 1.4. Mineralization in the Palmarejo vein. A.- Cataclastic (fault) breccia textures in mineralized areas within 76 Clavo. B.- Main stage mineralization: early sulphide-rich phases, locally brecciated in later vein phases. Dark grey crustiform bands and fragments comprise sphalerite > galena + pyrite + chalcopyrite with accessory Ag-sulphide + Ag-Cu minerals and electrum as the main Ag-Au phases. C.- Intermediate vein phases (76 Clavo): Quartz matrix breccia contains fragments of early sulphides, and cockade breccias with sulphide-sulphosalt overgrowth on fragments. D.- Late calcite phases and textures (76 Clavo). Early sulphide-rich phases and intermediate phase quartz breccia fill with sulphides and late pinkish calcite at center of the photo; from Rhys, D, 2009.

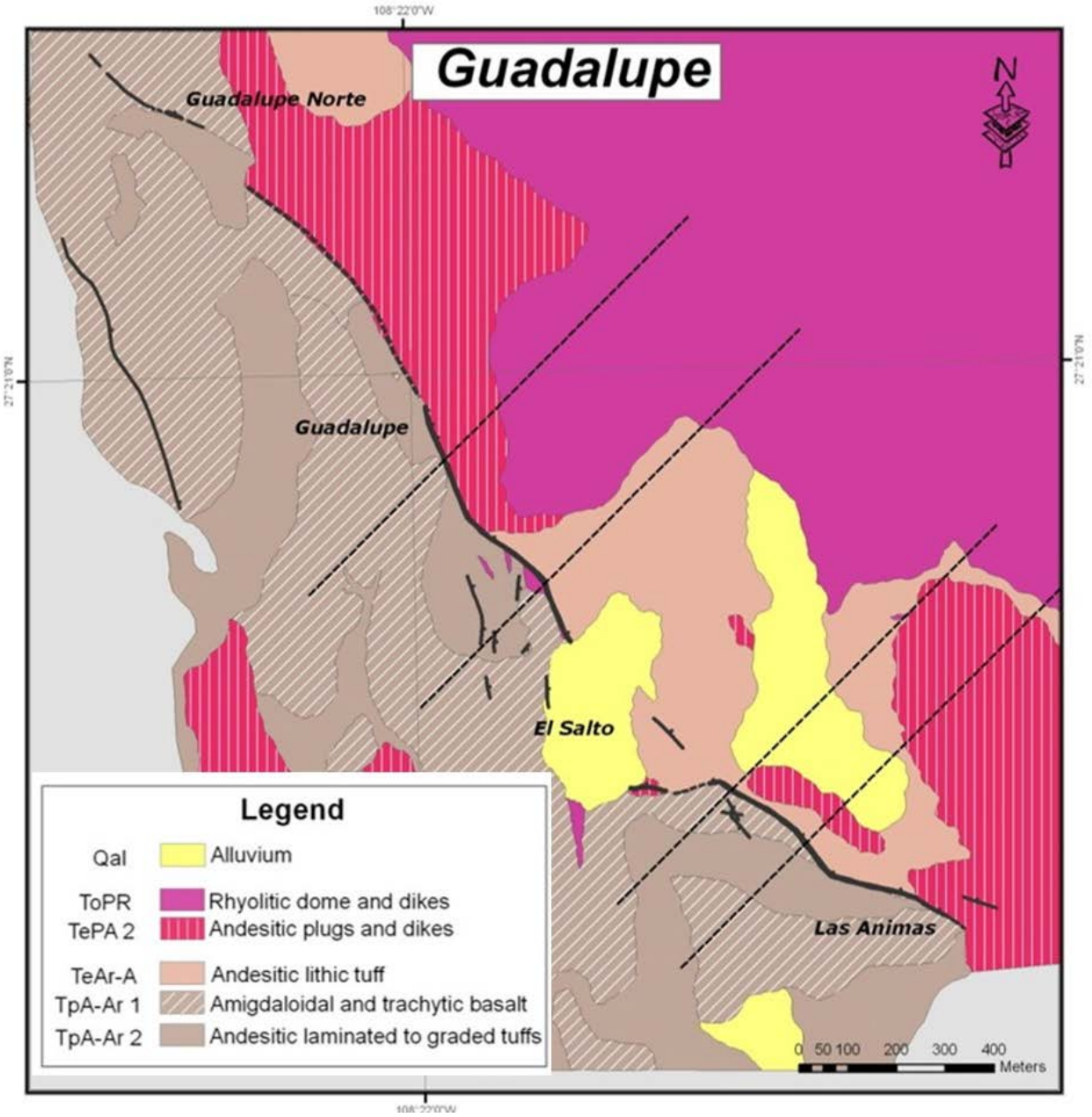

Figure 1.5 Geologic map of the Guadalupe deposit. Showing the main lithologies and the location of the most important orebodies (Guadalupe Norte, Guadalupe, and Las Animas). Note the location of orebodies at the changes of strike and/or intersection of structures, and their spatial relationship with the Rhyolitic dome and dikes.

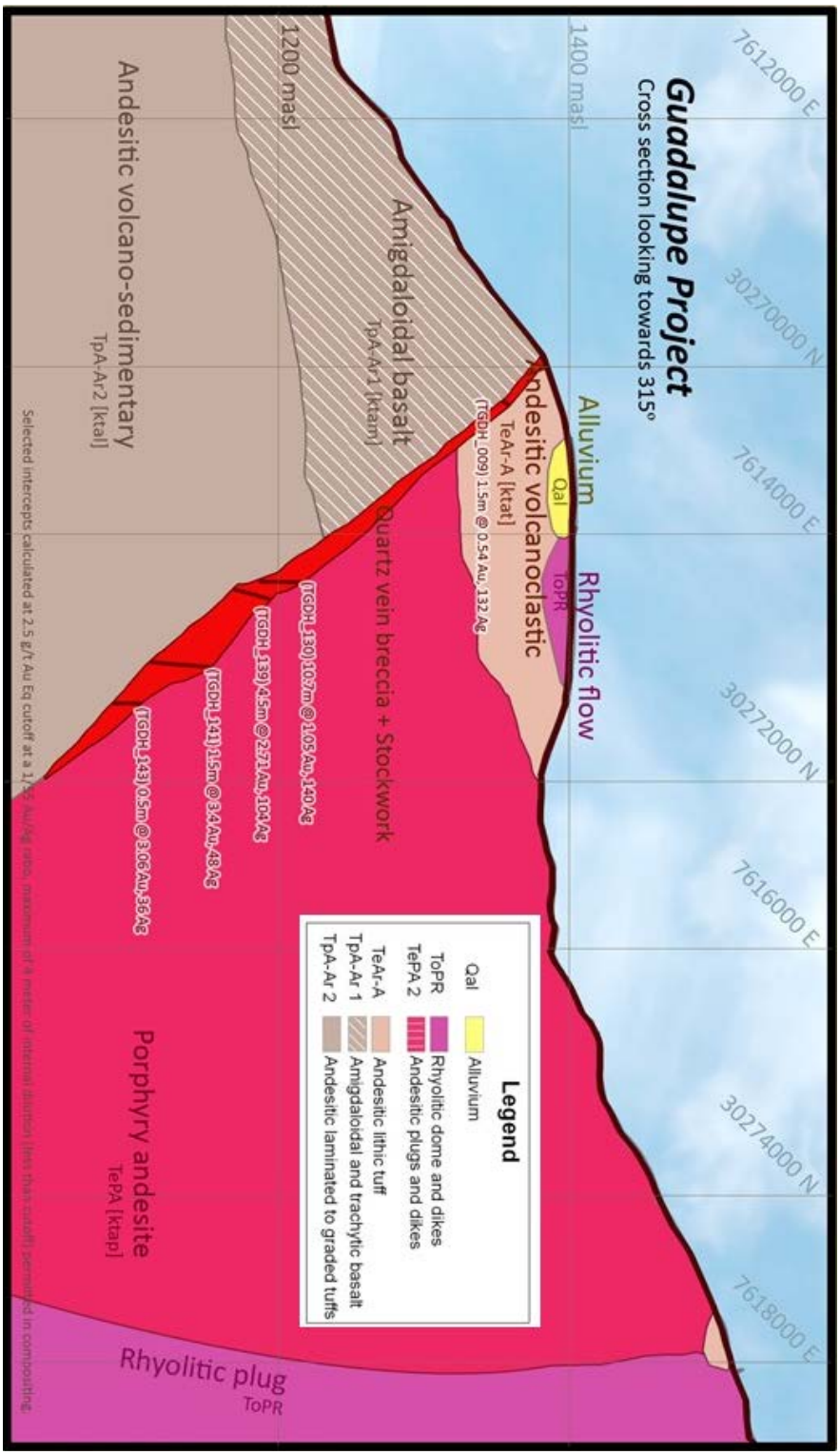

Figure 1.6 Geologic section of the Guadalupe deposit. The different lithologies at the footwall and hanging wall are showing the big dislocation of units caused by the normal faulting dipping NE, now hosting the mineralization. Inside the vein several intercepts are shown labeled with the hole ID, thickness, gold and silver grades.

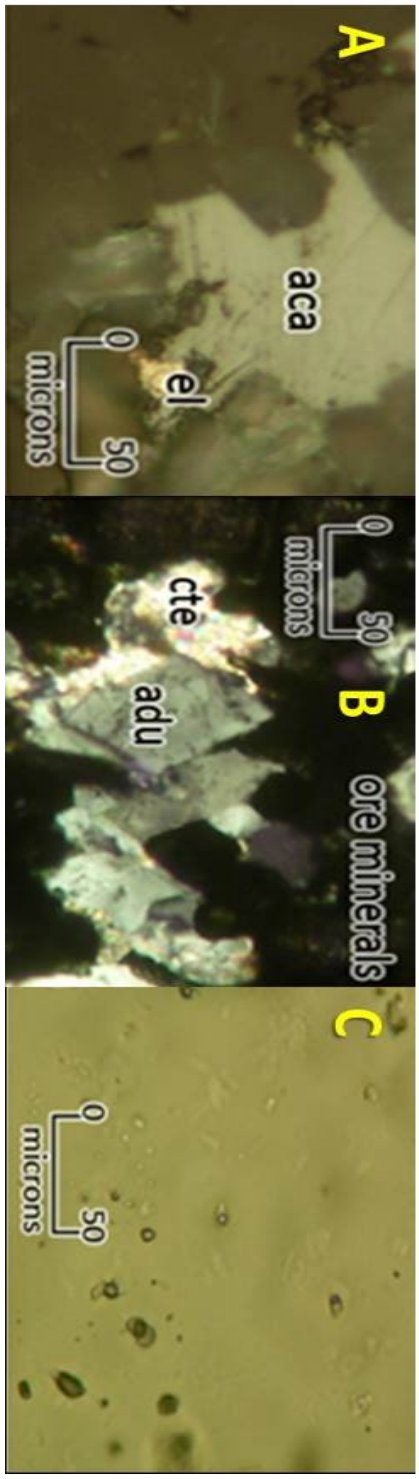

Figure 1.7 Microscopy of Palmarejo mineralization. Photomicrographs A and B under the microscope are showing ore and gangue minerals in Palmarejo deposit; A.- Electrum (el) and acanthite (aca) in quartz (qz) matrix B.- Adularia (adu) and calcite (cte) gangue in ore minerals. C.- Fluid inclusions showing variable liquid vapor ratios in quartz host; from Melchor (2005).

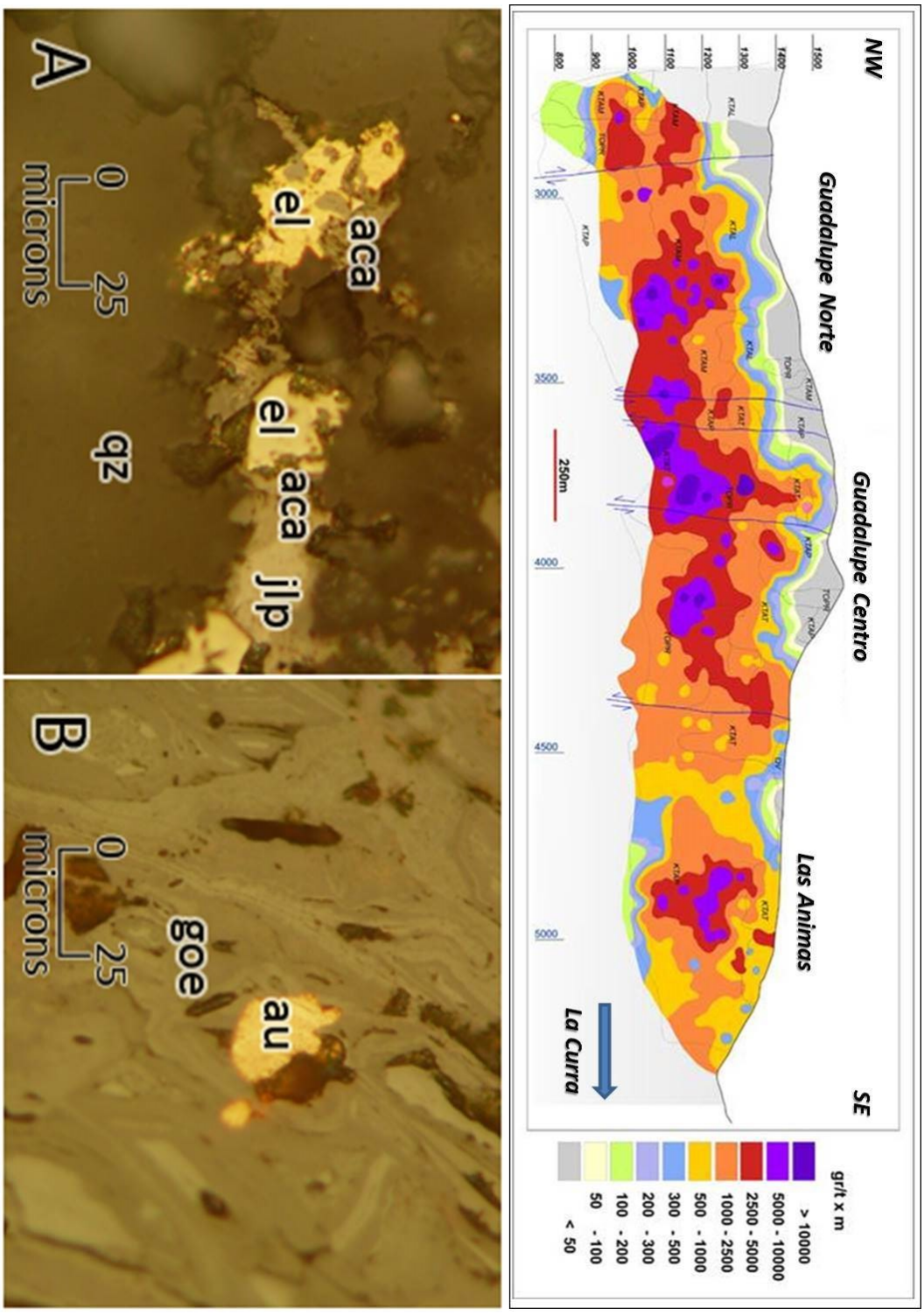

Figure 1.8 Mineralization in the Guadalupe vein. The upper figure is showing the distribution of the high-grade mineralization along the Guadalupe vein, by graphing the silver equivalent grade, multiplied by the vein thickness. Figure 1.8A is showing hypogene electrum (el), acanthite-jalpaite (aca-jlp) in quartz host. Figure 1.8B is showing gold (au) in supergene goethite (goe); from Melchor (2010).

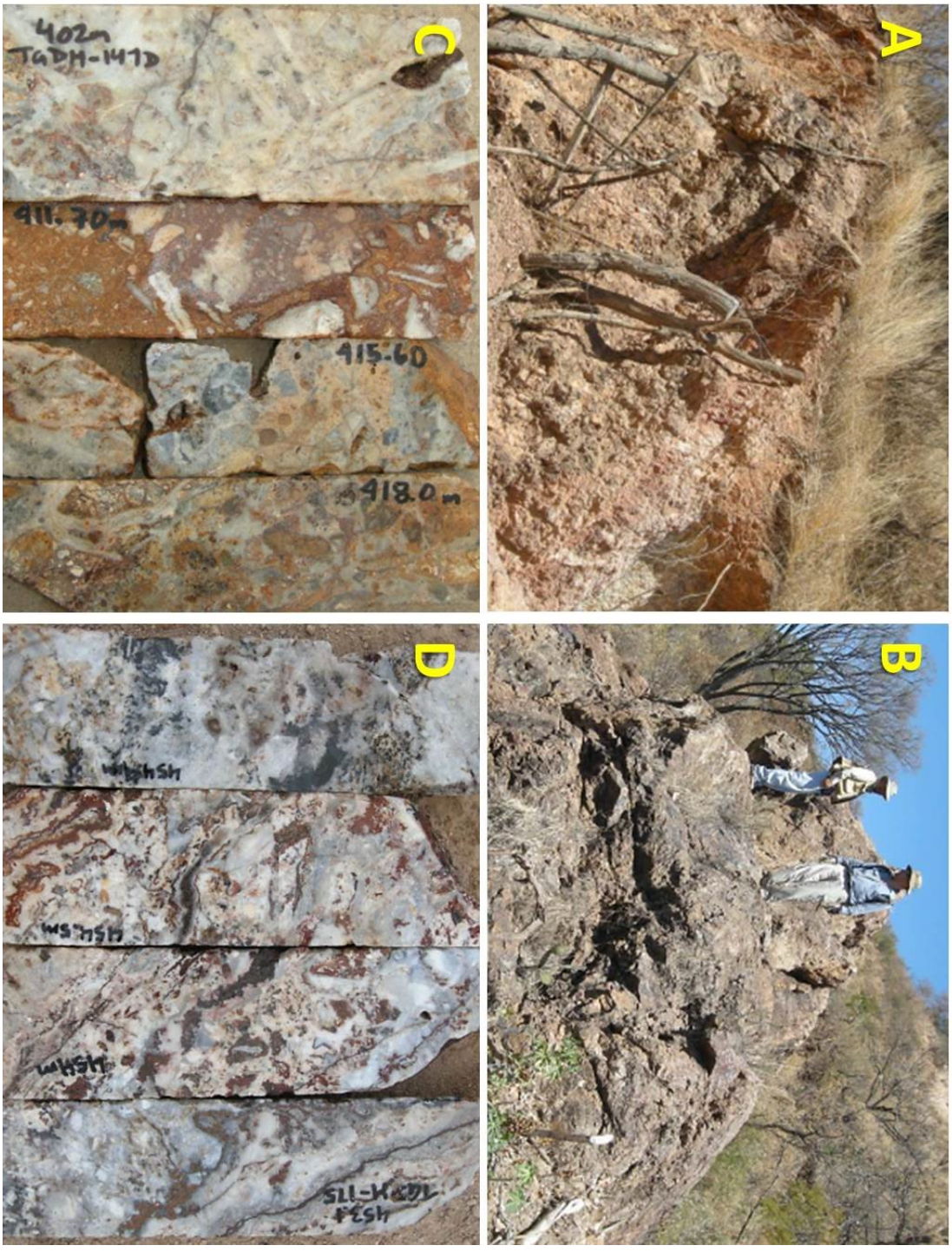

Figure 1.9 Surface expressions of the Guadalupe vein. Photos 1.9A and B are showing the surface expressions of the Guadalupe vein (A: pervasive silicic-argillic altered vein-fault outcrop at Guadalupe Centro. B: NE dipping adularia-silica altered outcrop at Las Animas). Photos 1.9C and D are showing core. (C: vein and breccia styles including oxidized cataclastic breccia. D: high grade hydrothermal breccia vein fill). From Rhys (2009).

Chapter 2: Geostatistical Analysis of the mineralization at the Guadalupe Mine, Palmarejo District, Chihuahua, Mexico.

2.1 ABSTRACT

Mineralization at Guadalupe is a structurally controlled, intermediate-sulfidation deposit of epithermal affinity. During the exploration stage, the zonation of the gold and silver values became evident. Ag/Au metal ratios are above 100, and high silver grades occur in the upper portions of the vein, whereas in the lower portions of the system the ratios are below 100 and even as low as 10. The most important mineralization window in Guadalupe is located between 900 and 1500 meters of elevation and the vertical zoning of the precious metals is fully documented. The present study concludes that the analysis of the variations of the silver-gold ratios is a useful tool for this type of deposit to locate the position within the mineralized system. A multi-element geo-statistical analysis, from data obtained by a handheld X-ray fluorescence analyzer, is also presented. This study uses univariate, bivariate and multivariate analysis techniques, and demonstrates the importance of the quality of the assay data, particularly when data does not have a normal distribution. Therefore, bivariate plots and factor analysis are not reliable enough when the accuracy and precision of the assays isn't first-class. It is concluded that the use of this analytical methodology is limited, although it helps to show some trends, it can easily lead to erroneous conclusions, or simply show a lack of correlation.

2.2 INTRODUCTION

The Guadalupe mine, in the Palmarejo mining district, is located on the western border of the state of Chihuahua, between the municipalities of Chínipas and Guazaparez (Figure 2.1). Guadalupe is Coeur's most recent mine in exploitation in Mexico. The Guadalupe deposit is a typical intermediate-sulfidation, epithermal deposit (Sillitoe, 2010), contained in a main fault structure, striking to the northwest and hosted in a volcano-sedimentary sequence of andesitic composition.

The present study focuses on the geochemistry of the deposit. Analysis of metal ratios, as well as a multi-elemental geostatistical analysis were performed. The analysis is based on

laboratory findings as well as data obtained by means of a portable X-Ray fluorescence analyzer (Niton XL3t). The samples used for the data came from drill hole intersections within the Guadalupe vein, and were compiled from 359 drill holes made during the exploration stage between 2005 to 2012. The extraction points of the samples are distributed along 2.6 kilometers of the structure, with a vertical extension of 505 meters, between 980 to 1485 meters above sea level (masl), with an average elevation of 1236 masl.

Data from ten chemical elements were investigated for the geostatistical analysis using univariate and multi-variable methods. These methods are very useful for the simplification of large data bases and to help recognize tendencies in the behavior of the elements (Reimann et al, 2008), even though it is widely recognized that when trying to explain natural phenomena, the geochemical data rarely has a normal distribution (Reimann and Filzmoser, 2000). Most frequently they group in various sub-groups (Aitchison, 1986), due to the fact that the elements are expected to correlate with each other. It is for this reason that this study's principal objective is to document, with the data available, the possible correlation of the elements through the process of mineralization and its spatial distribution

2.3 GEOLOGY AND MINERALIZATION

The lithology at Palmarejo mining district is diverse in type and age. At the bottom of the sedimentary sequence, there are limestones, shales and sandstones deposited in a marine environment. These sedimentary units are interbedded with volcano-sedimentary rocks. The age of the rocks varies from the Cretaceous to the Quaternary, with a large predominance of volcanic and igneous rocks from the Tertiary age (Figure 2.2).

The stratigraphy of the area is composed, at the bottom, of a recrystallized limestone (KaCz-Ar) which has been designated Albian in age by the Mexican Geological Service (CRM, 2004). Its lower contact does not outcrop, while its upper contact is discordant with a polymictic conglomerate (KTCg), primarily made up of fragments of volcanic and calcareous composition. It

is unconformable, covering either the limestone or a granodioritic intrusive (KTGd), which is intruding into the limestone and the previously described conglomerate.

Upon the previously mentioned units, resting in a discordant manner, is the Lower Volcanic Complex (LVC). Within the study area the LVC group is represented by diverse types of rock from sedimentary to volcanic and intrusive in origin. The primary andesitic composition is the common denominator within this diverse lithology. The main units within this group are comprised of a basal member that is characterized by a predominance of andesitic lapilli (TpA-Ar), most likely deposited during the Paleocene, and an upper member characterized by andesitic tuffs (TeAr-A) from the Eocene. Both members are intruded upon by an andesitic dome and dike complex (TePA).

The Upper Volcanic Complex (UVC) is discordantly covering the Lower Volcanic Complex. The rhyolites of this Complex cover most of the higher elevations of the Sierra Madre Occidental, while the rocks of the Lower Volcanic Complex are restricted to the barrancas (wide ravines), where most of the mineralization occurs. The UVC is mainly constituted by rhyolitic tuffs and ignimbrites at its base (ToTR), rhyolitic domes and dikes (TmPR), rhyodacitic tuffs (ToRDd) and basaltic flows (TmB) on top. The control of the mineralization in the Palmarejo District is of a structural type, where the mineralization occurs mainly as infilling veins and stockwork associated with extensional faulting. The high grade orebodies are located at the inflections and intersections of structures, where the greatest dilation zones occur.

The deposits in the Palmarejo district are of an epithermal origin. This is evidenced by the internal textures of the deposit and the presence of illite and adularia as minerals associated with the alteration and mineralization zones. The mineralogy is transitional toward the upper portion of the system to low temperature minerals, such as smectite and chlorite. According to Sillitoe (2013), the deposits are assigned to the category of intermediate-sulfidation, based on the copper, lead, and zinc content, the association of chalcopyrite - tennantite, the low iron sphalerite and the abundance of carbonate minerals, including species rich in manganese and rhodonite (manganese silicate). If the deposits were classified as low sulfidation type, then they should demonstrate a

lower total sulfide and base metal content (>3% by volume), the presence of pyrrhotite and arsenopyrite, high iron sphalerite, lower quantities of carbonate minerals, the absence of rhodonite, and a higher adularia content as components of the deposit.

The paragenesis of the metals is typically characterized by an early phase appearance of silver with the base metals, followed by a gold and silver mineralization event. In the Guadalupe deposit, three main vertical zoning areas have been identified. The mid-superior part is characterized by sulfides and a predominance of silver. The middle part is rich in gold and silver, while the lowest portion of the system is characterized by a high sulfide content and lower metal ratios between silver and gold.

2.4 METHODOLOGY

A total of 4182 vein samples from the Guadalupe deposit were considered for the metallic ratio analysis (Table 2.1). These samples were analyzed by ALS Global Lab in Vancouver Canada, and prepared at their Chihuahua, México facilities. The packages used for these samples were code numbers Au-ICP21 and ME-GRA21. The first is a fire assay for gold and finalized with ICP-AES, which has a detection limit of 0.001 ppm Au. The second is a package with fire assay for gold and silver, and finalized by gravimetric analysis. This package has a detection limit for gold of 0.05 ppm, while the silver detection limit is 5 ppm.

For the metallic ratios analysis, the data was analyzed using an Excel table. All of the assays below the detection limit were substituted with 0.075 ppm for gold and 7.5 ppm for silver. Then, the basic statistics and the metallic ratios were calculated. The last step was to plot in graphics, the ratio values against their spatial distribution, for their visual interpretation.

For the multi-element analysis, a database of intervals selected from 292 holes, with a total of 2865 samples, was compiled. The leftover pulps from the earlier analysis were analyzed using a mobile Niton™ GOLDD™ (Niton, 2008), X-Ray fluorescence analyzer. According to manufacturer, the GOLDD technology delivers vast improvements in sensitivity and provide lower detection limits than similar XRF analyzers on the market, without specifying such limits. The

silver and gold values obtained by this method were substituted for the analytical analysis from ALS, mostly due to the better detection limit of gold.

The exploratory data analysis (EDA, Kurlz, 1988) was first conducted using the Microsoft Excel™ and the SPSS™ program afterwards (Sall et al, 2005), where the statistics of the basic exploratory analysis were obtained. This step included the analysis of undetermined values, the median, the mean, the standard deviation, the maximum and minimum values, the range and percentiles (Table 2.2). Following the methodology of Zumlot et al (2008), the box diagrams (Figure 2.7), histograms (Figure 2.3), and quantile-quantile standard graphs (Q-Q plots) were created in SPSS™ for each element (Figure 2.8). These graphs were used to determine elements with sufficient number of samples with values above the detection limit, as well as identify the outliers and the normality of the data. The values below the detection limit were replaced with the lowest half value for each element (Zumlot et al, 2008, Zhang et al, 2005). The Kolmogorov-Smirnov trial (Stephens, 1974) was used in order to determine normality. This information was also useful in selecting the elements for the multi variable analysis, using the SPSS™ program.

2.5 RESULTS

Table 2.1 shows the statistical summary of gold and silver fire assays from ALS Global Lab. It is important to note the average grade within the vein of 108 ppm of silver and 1.83 ppm of gold. The metallic content versus depth graphs, show a reduction in the silver grades as the depth is increased (Figure 2.4), while the gold values have an inverse behavior (Figure 2.5).

Upon plotting the metal ratios with respect to the elevation, it can be remarked how the silver/gold ratio decreases with depth (Figure 2.6), and also how the main mineralization window is located between the elevations of 1200 and 1400. This last observation is supported by the highest values of dispersion, (Figures 2.4, 2.5) due to the proportional effect related to the high-grade ore. Figure 2.6 is showing a logarithmic graph of metallic Ag/Au ratios versus elevation in which the silver/gold gradient relation is accentuated according to the depth of the system. Additionally, several Ag/Au ratio graphs versus coordinates were elaborated in order to see

variations with respect to the location of samples at the same elevation, but all turned to be horizontal. This test determined that there are no substantial variations in metallic Ag/Au ratios along the length of the structure.

From the analyses of data and elevations, it was observed that the precious metal ratios above 100 occur at the upper part of the deposit. The deposit narrows in the lower portions, and the Ag/Au metallic ratios are less than 100, and can reach a Ag/Au ratio as low as 10. In general terms, the sulfide phase with silver is localized above 1300-meters elevation, and it is constituted of early argentite with fine-grained black sulfides, low-iron (white) sphalerite, pyrite and fine-grained galena.

The intermediate zone, which is rich in gold and silver, is located between the elevations of 1150 and 1300 masl. This zone is associated with the early phase of base metals with silver (acanthite, fine-grained black sulfides, yellow sphalerite, galena and pyrite), followed by a gold-rich mineralization stage, in form of electrum. Visible gold and electrum are associated with honeycomb textures in zones with higher hematite content. The deepest economical mineralization zone is localized below the 1150 masl elevation, and is associated with black sulfides, high-iron (brown) sphalerite, chalcopyrite, and coarse-grained galena.

For the Geostatistical analysis, the analytical values of gold and silver from ALS were considered and attached with the multi-element assays obtained through the use of X-Ray fluorescence. Table 2.2 shows the percentiles of the original elements and in an equally important manner, the elements for which there are not a sufficient number of samples to perform a reliable multivariable analysis. There are insufficient samples above the detection limit for molybdenum, zirconium, rubidium, copper, and antimony. Based on this selection, the elements silver, gold, strontium, lead, arsenic, zinc, iron, manganese and barium were included in the factorial analysis.

As expected, the graphs inform that the total data is not evenly distributed. The skewness and kurtosis values do not fall within the normal parameters, and the histograms with normal distribution support this conclusion. Five of the 14 elements analyzed have more than 25% of their samples below the detection limit (Table 2.2).

Although antimony has 43% of its data below the detection limit, this element was included in the multi-element analysis due to its importance in the precious metal deposits. Table 2.3 shows only those elements whose data is considered admissible for the analysis. Skewness and kurtosis are also shown to prove the normality of the data. For the univariate analysis, box histograms and diagrams were elaborated for each element, although only some were selected to be presented in Figure 2.7.

Quantile-Quantile graphs (Q-Q) were elaborated for each element. Due to their relative importance the gold and silver graphs were selected to be shown in Figure 2.8, where their outliers are pointed out in the red circles. These traditional Q-Q box plots are compared with Q-Q plots with no normal tendencies, for the purpose of identifying outliers, and for visualization and identification of diverse populations. Figure 2.9 is a graph with the purpose of comparing box diagrams between elements.

Some tendencies are evident with a bivariate correlation analysis. The most notable aspect is that most of the elements (except for Pb/Zn and As/Fe) do not show correlation, as exposed in Figure 2.10. The graphs generally have a cloud of data in an “L” shape. The elements that have a positive correlation are arsenic/iron and lead/zinc, the latter, above all, shows the strongest positive correlation. None of the elements show a negative correlation.

For the multi-variate analysis, the principle component methodology was used. The results of the factorial analysis are presented in Table 2.4. The factorial components with values above 1 were chosen, which gave a total of four factors. The elements with values above 0.5 were included in the component, with the exception of silver in factor 4, which has a weight of 0.498.

The first component, which encompasses 77% of the variance, includes silver, lead, and zinc, and is associated with the primary mineralization of sulfides. The second component includes lead, arsenic, zinc, iron, and barium, and is interpreted as a second stage of sulfide mineralization, with an important contribution of iron, probably associated with arsenopyrite. The third component includes manganese, and strontium, and is interpreted as an association to the host rock. The fourth

factorial component is probably related to the deposit of precious metals in native form, such as electrum.

2.6 CONCLUSIONS

The mineralization in the Guadalupe mine corresponds to an intermediate sulfidation, epithermal type and is structurally controlled. The main ore bodies are located within faults with higher displacement, mainly at intersections with other structures. The most important mineralization window is located between 900 and 1500 meters of elevation, and the zoning of the precious metals is predictable, where the silver/gold ratio decreases as it approaches the lower limit of the mineralization window. Reasoning these observations, it was concluded that the variation of the ratios of silver-gold are useful in locating our position within the mineralization system inside an intermediate sulfidation deposit. Besides gold, silver, lead, and zinc, iron is an important element in the deposit, and its analysis is useful to identify different stages of pyritization. Although the data reveals certain tendencies in the geochemistry of the Guadalupe deposit, with this trial methodology many elements have values below the detection limit. For this reason, the Fluorescent X-Ray analysis is not recommended to conduct a robust multivariable analysis.

2.7 ACKNOWLEDGMENTS

This article is a scientific collaboration with Philip C. Goodell. It was originally written in Spanish to be published and presented at the XXXI AIMMGM International Mining Convention in October 2015, under the title: “Análisis Geoestadístico de la Mineralización en la Mina Guadalupe, Distrito Palmarejo, Chihuahua, México” (Molina and Goodell, 2015).

We express our profound appreciation to Mitch Krebs and Frank Hanagarne, leaders of Coeur Mining. Special thanks to Valente de Leon, Erick Kappus, for the analysis of the multivariable data, Rana Asher for translation, Enrique Fuentes, for revision and suggestions, Miguel Saenz, for drafting, and especially to the entire exploration team at Coeur in Mexico for their hard work and continual support.

CHAPTER 2 TABLES

Table 2.1 Statistical summary of the gold and silver assays.

Element	Samples	Min	Max	Mean	Std. Deviation	Kurtosis
Ag	4182	6.00	4420	109	211	125
Au	4182	0.06	315	2	9	695
Ag/Au	4182	0.02	9067	54	295	301

Table 2.2 Statistical summary of raw data from the Guadalupe vein.

Statistics

	N								Percentiles			
	Valid	Missing	Mean	Median	SD	Range	Min	Max	25	50	75	95
Ag	2984	1	108.79	58.00	200.9	4415	5	4420	21.00	58.00	127.00	358.75
Au	2984	1	1.5542	.4700	7.930	300.00	.00	300.00	.1600	.4700	1.2175	4.6700
Mo	1338	1647	10.15	3.04	49.500	1394	2	1395	2.15	3.04	5.32	28.86
Zr	2082	903	42.16	27.67	46.586	313	2	315	9.58	27.67	56.36	142.19
Sr	2984	1	54.18	40.13	49.808	1174	4	1178	24.88	40.13	67.23	141.46
Rb	1780	1205	28.00	20.62	24.461	133	2	134	7.23	20.62	44.08	75.58
Pb	2746	239	127.33	51.32	394.8	11009	3	11012	24.70	51.32	104.73	416.90
As	2513	472	55.92	37.21	58.972	792	6	799	20.97	37.21	67.05	163.46
Zn	2911	74	231.44	104.53	599.3	17015	6	17022	60.17	104.53	203.90	720.90
Cu	651	2334	56.79	28.82	92.284	1181	11	1192	18.91	28.82	53.14	195.14
Fe	2984	1	13353	9479	10917	73291	719	74011	5895	9479.3	17399	37354.5
Mn	2788	197	2407	1748	2235	22987	65	23052	915.2	1748.4	3187	6675.74
Ba	2818	167	523.21	304.97	865.7	28072	38	28109	150.8	304.97	681.01	1457.46
Sb	1699	1286	36.64	30.70	21.144	159	11	170	21.43	30.70	45.35	79.41

Table 2.3 Statistical summary of admissible assays of the Guadalupe vein.

Element	Samples	Range	Min	Max	Mean	Std. Deviation	Variance	Skew	Kurtosis
Ag	2985	4415	5	4420	109	201	40360	10	157
Au	2985	300	1	300	2	8	63	24	760
Sr	2985	1177	2	1178	54	50	2481	6	96
Pb	2985	11010	2	11012	117	380	144547	15	309
As	2985	795	3	799	48	57	3299	4	26
Zn	2985	17019	3	17022	226	593	351569	13	274
Fe	2985	73651	360	74011	13348	10918	119206463	2	3
Mn	2985	23015	38	23052	2251	2239	5012511	2	11
Ba	2985	28091	19	28109	495	849	720990	16	436
Sb	2985	165	5	170	23	22	500	2	4

Table 2.4 Results of factor analysis, extraction method of PCA using four components. Factor loading above 0.5 are highlighted

Element	Component			
	1	2	3	4
Ag	0.581	0.188	0.295	0.498
Au	0.287	0.192	0.127	0.815
Sr	-0.485	0.398	0.558	-0.087
Pb	0.755	0.526	0.064	-0.322
As	-0.354	0.565	-0.461	0.253
Zn	0.729	0.555	0.028	-0.345
Fe	-0.334	0.684	-0.432	0.083
Mn	-0.317	0.237	0.723	-0.009
Ba	-0.314	0.514	-0.13	-0.065
Sb	0.367	-0.295	-0.341	0.064

CHAPTER 2 FIGURES

Figure 2.1 Location map for the Palmarejo district, showing the political boundaries and important geographic localities.

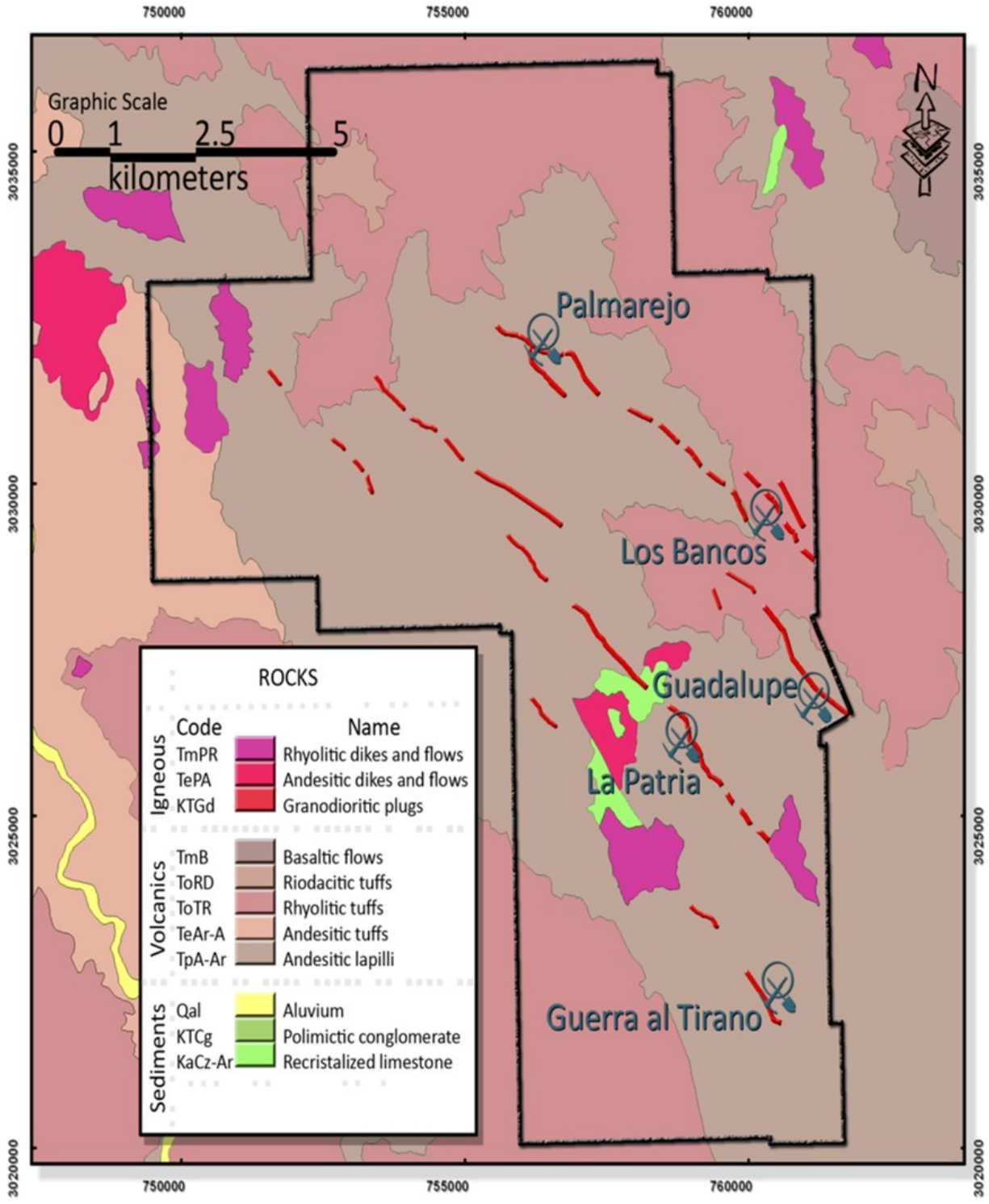

Figure 2.2 Geologic map of the Palmarejo district, showing the main lithologic units and the location of the most important veins and mines.

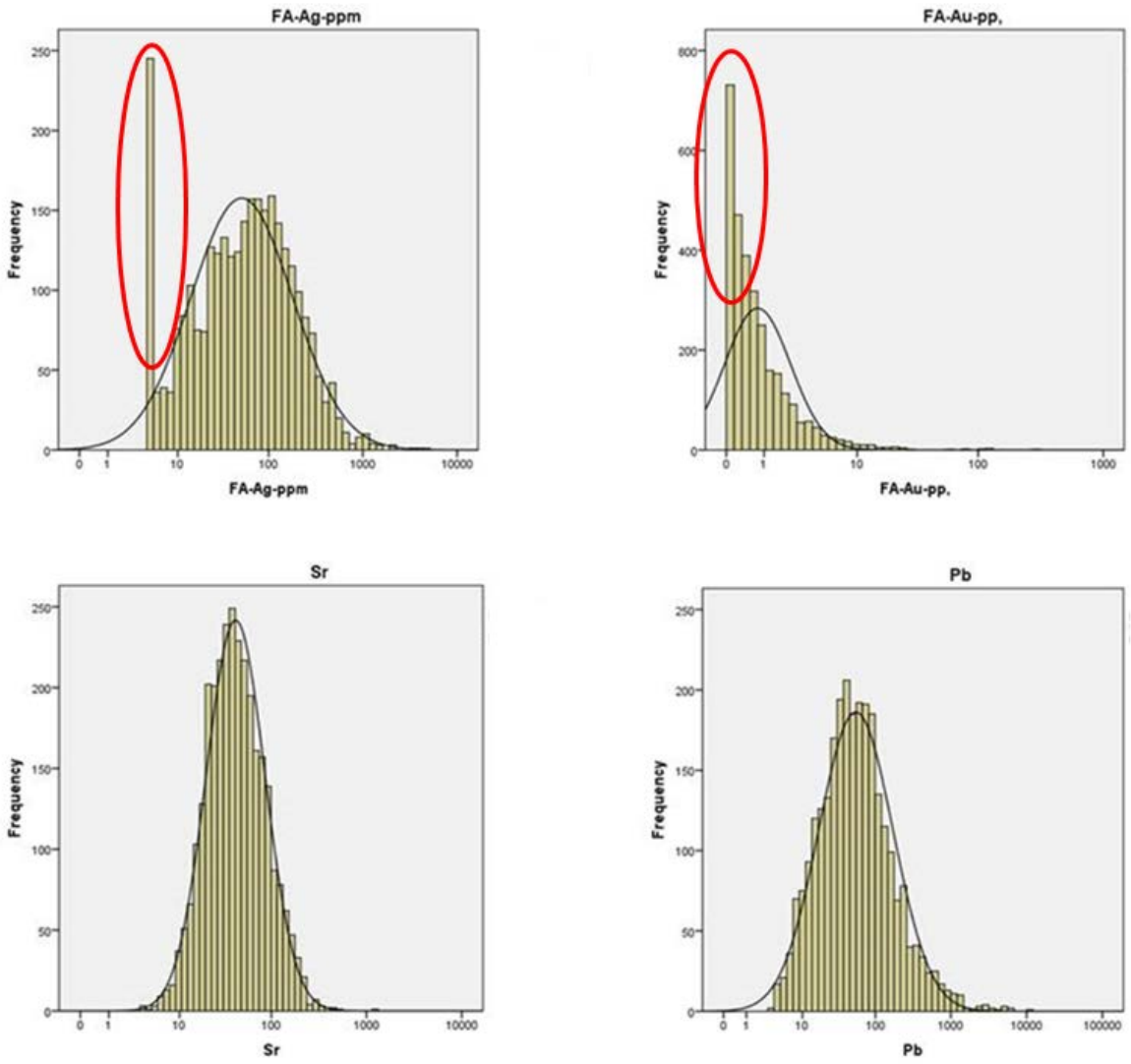

Figure 2.3 Histograms for silver, gold, strontium, and lead. The red circles show those values below the detection limit, which were substituted by 7.5 ppm for silver, and 0.075 ppm for gold.

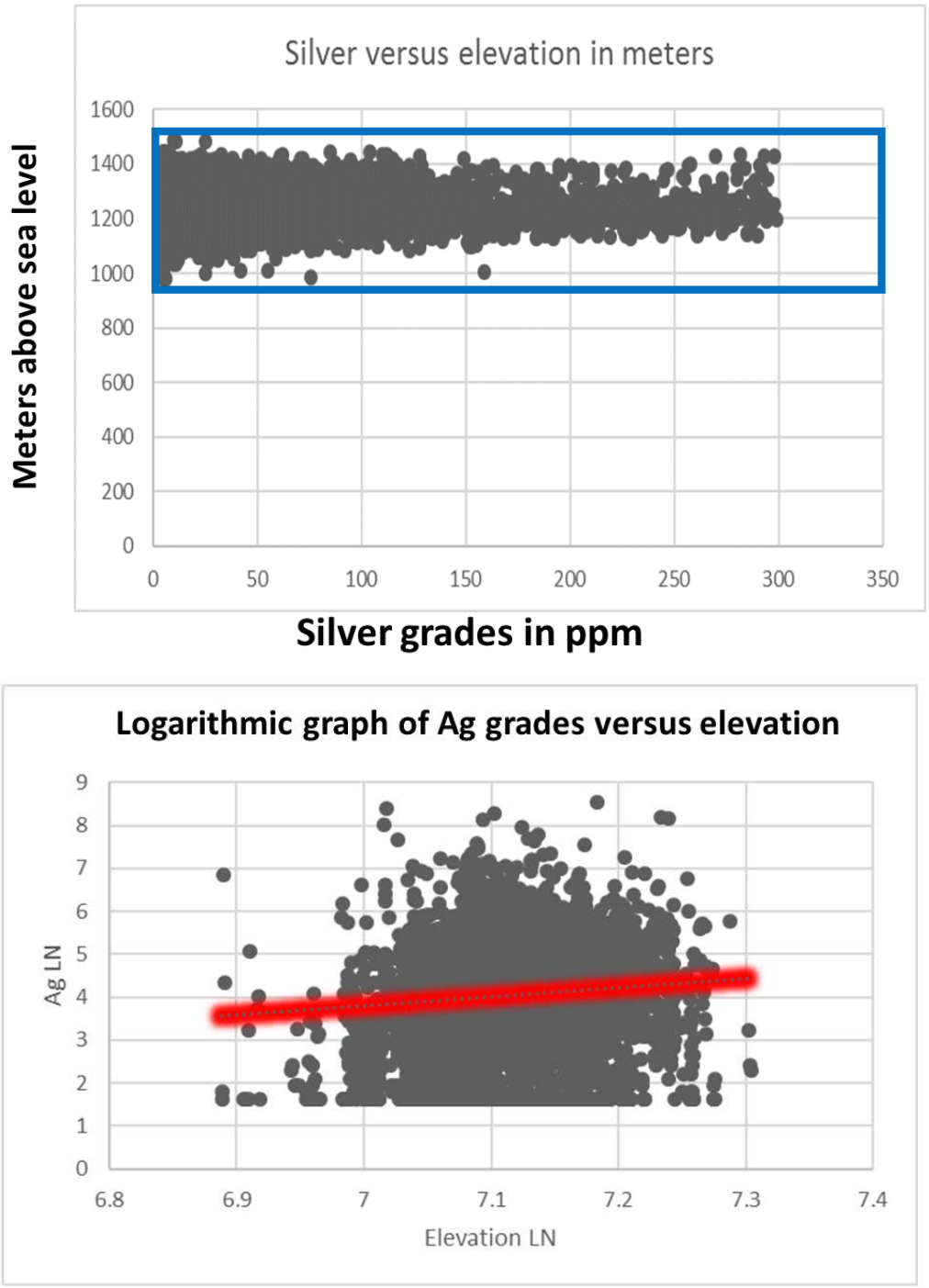

Figure 2.4 Graph showing the silver grade distribution versus elevation. The upper figure is showing the grade in ppm and elevation in meters above sea level (masl). Blue area indicates the mineralization window and the high dispersion values. The lower figure is in logarithmic scale, and is showing the tendency of the silver grades to increase with elevation.

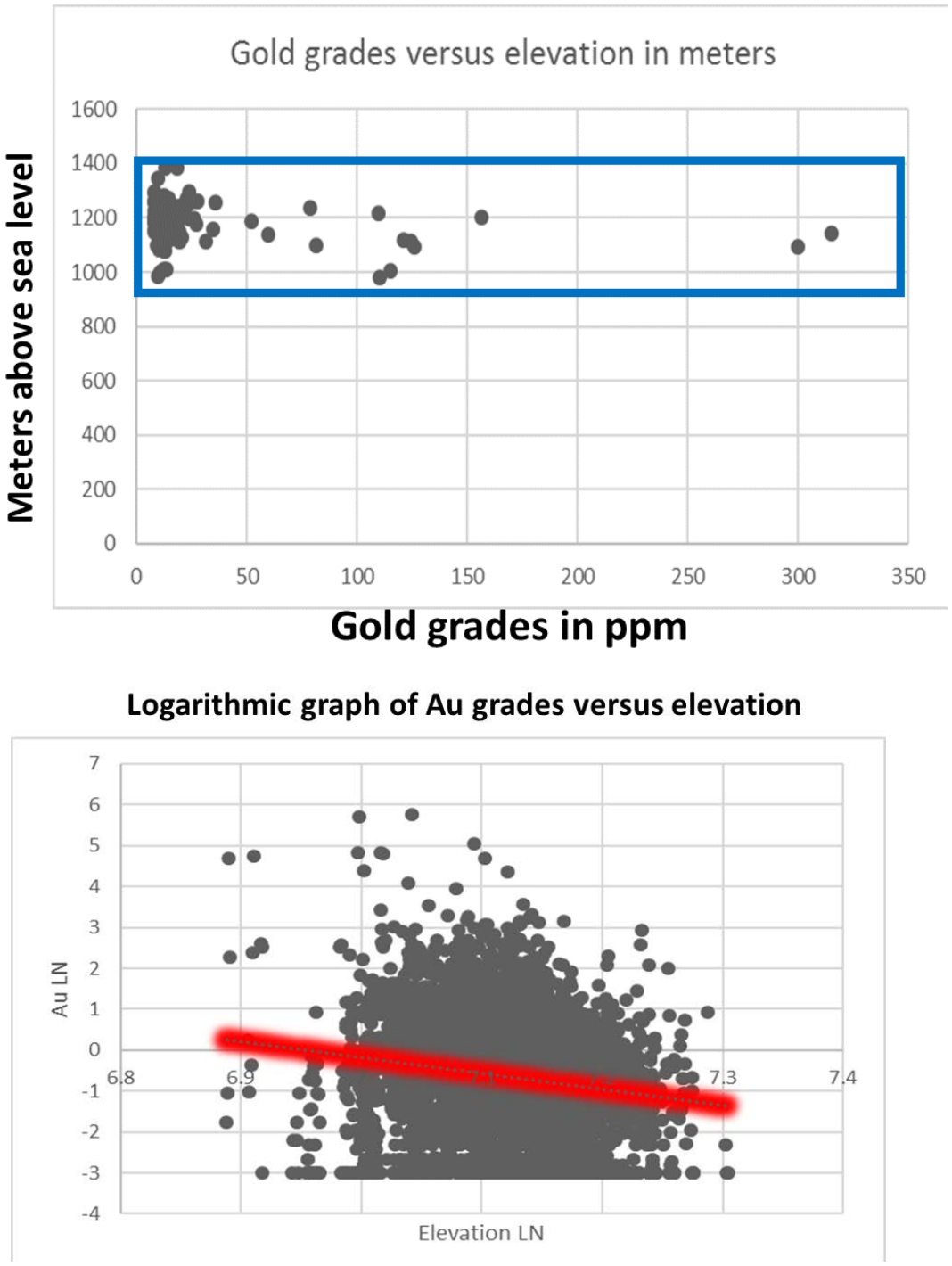

Figure 2.5 Graph showing gold grade distribution versus elevation. The upper figure is showing the grade in ppm and the elevation in masl. Blue area indicates the mineralization window and the high dispersion values. Lower figure is in logarithmic scale.

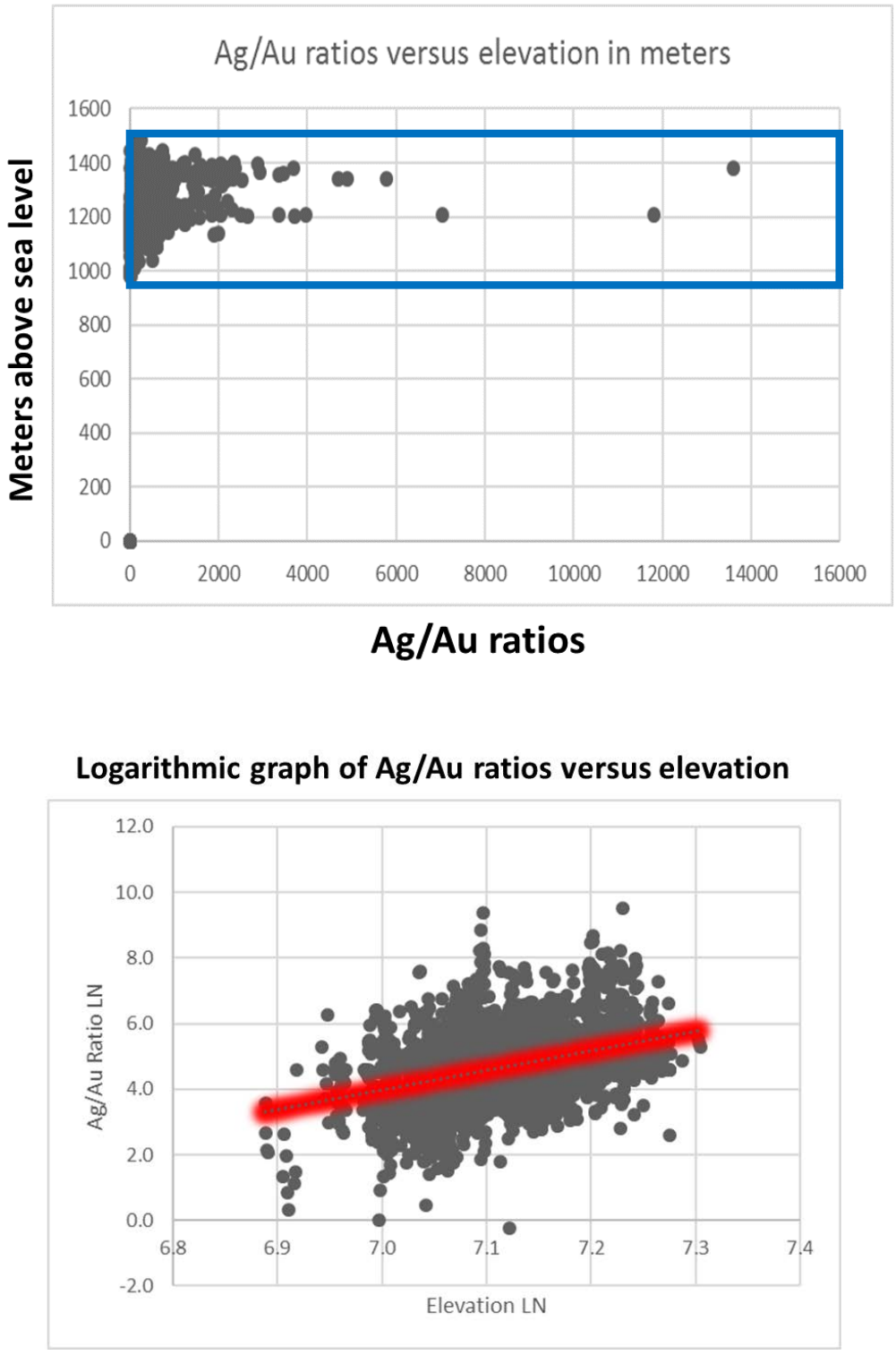

Figure 2.6 Graph showing the silver/gold ratio versus elevation. The upper figure is showing the ratios versus the elevation in masl. Lower figure is in logarithmic scale. Note the gradient versus depth, showing the zonation of the mineralization.

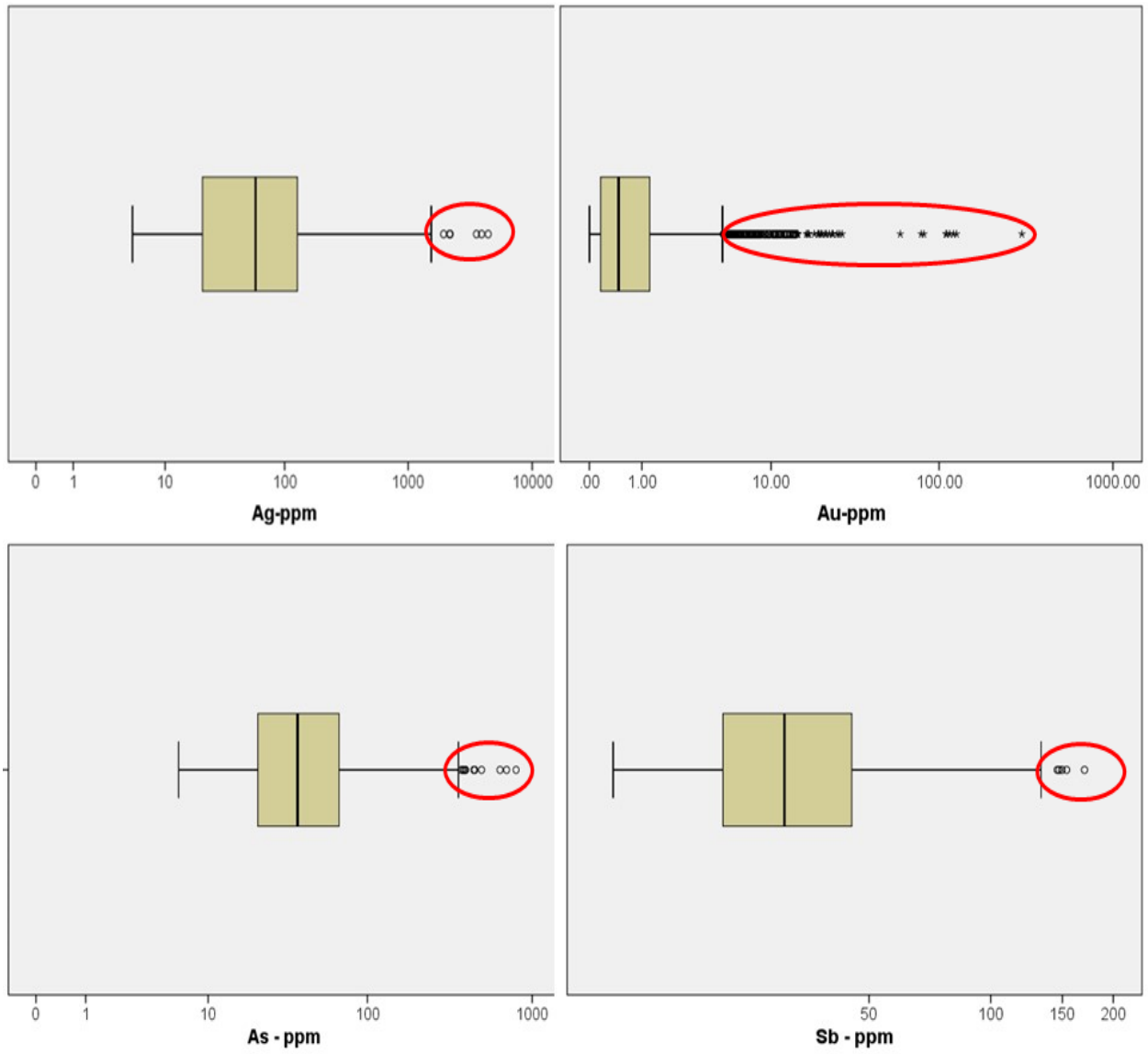

Figure 2.7 Box diagrams of silver, gold, arsenic and antimony. The red circles indicate the outliers.

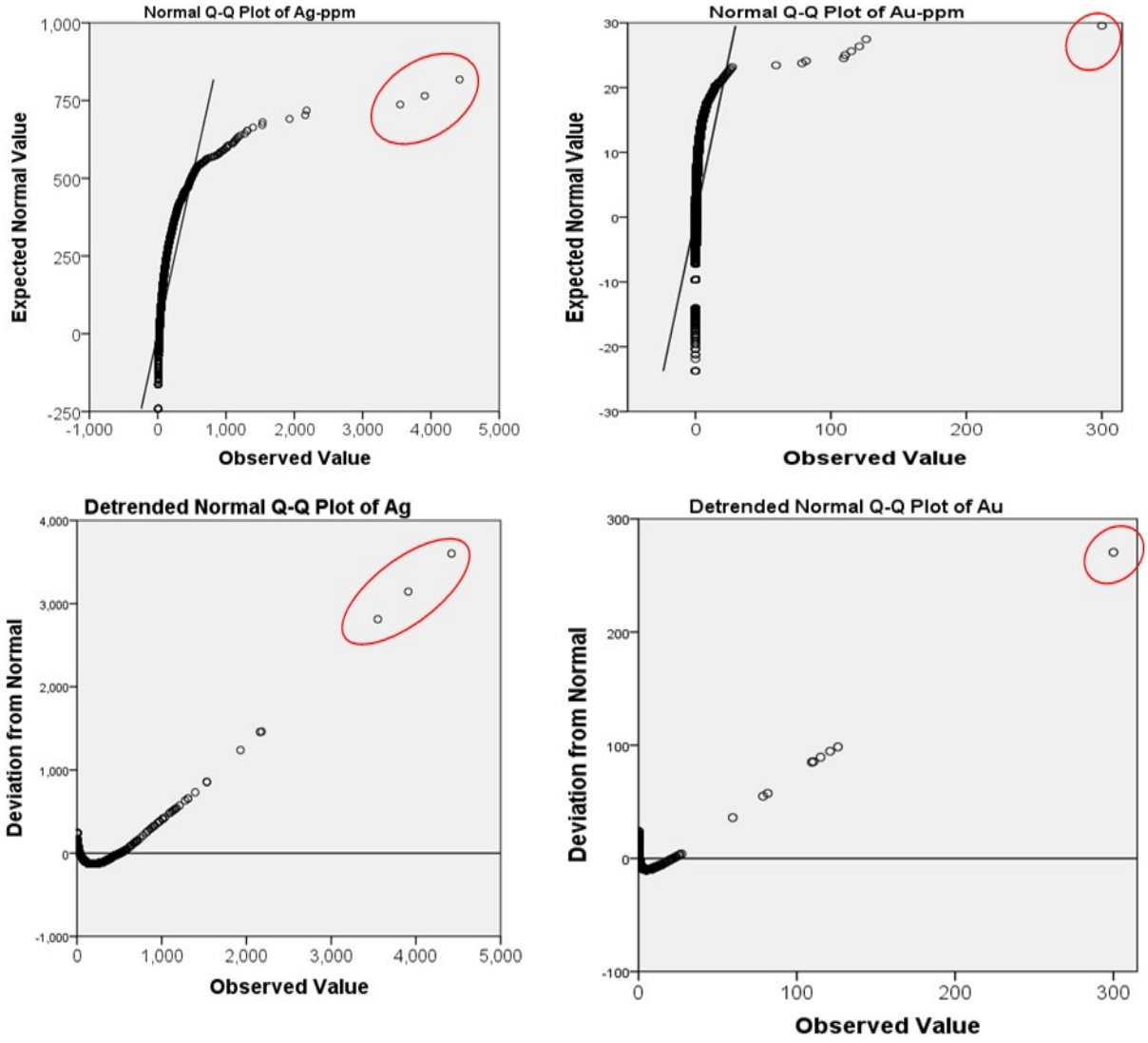

Figure 2.8 Normal Q-Q plots for silver and gold compared with the de-trended normal Q-Q plots for the same two elements. The outliers are marked within the red circles.

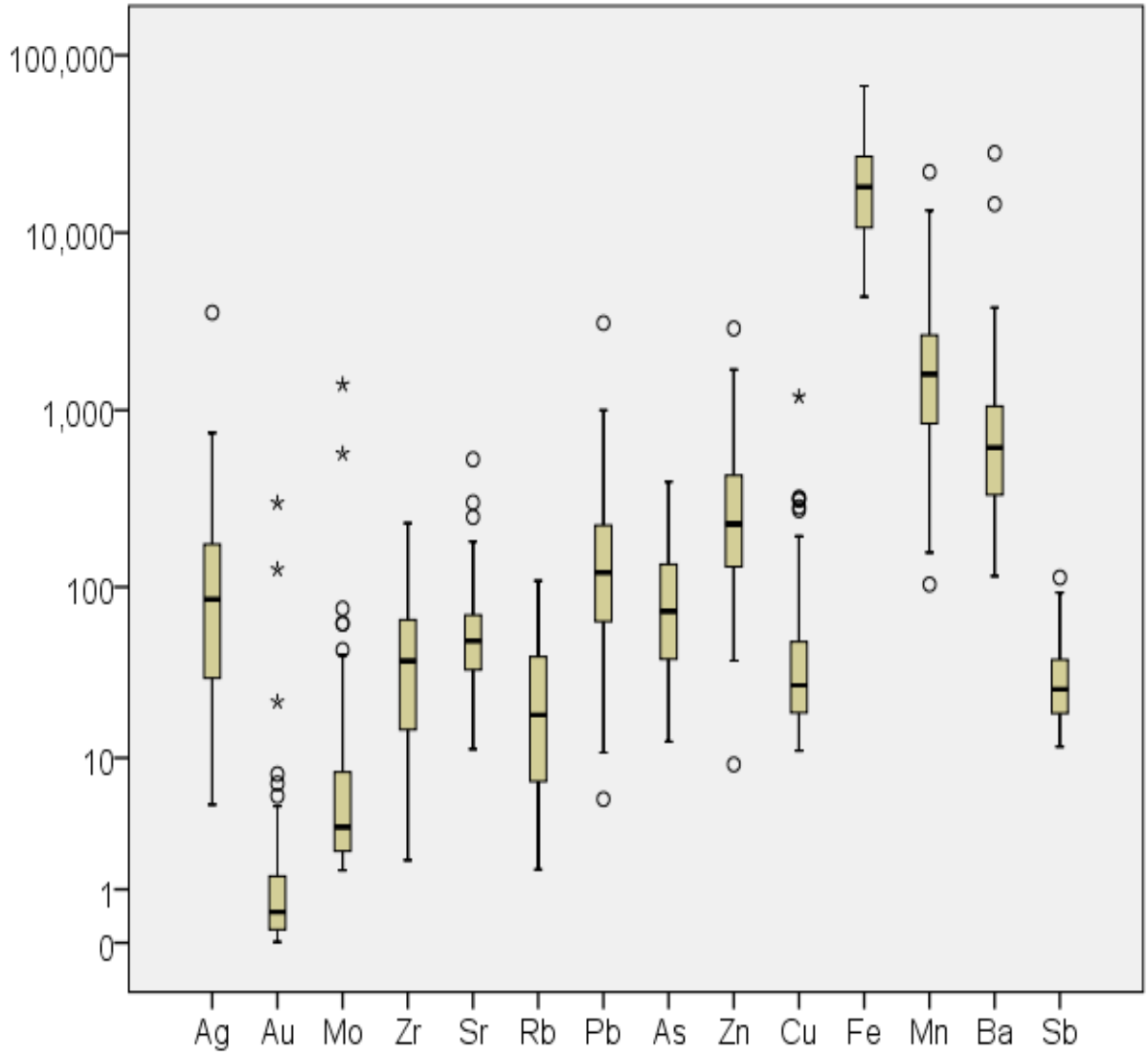

Figure 2.9 Comparative graph of the box diagrams for each element in the raw dataset.

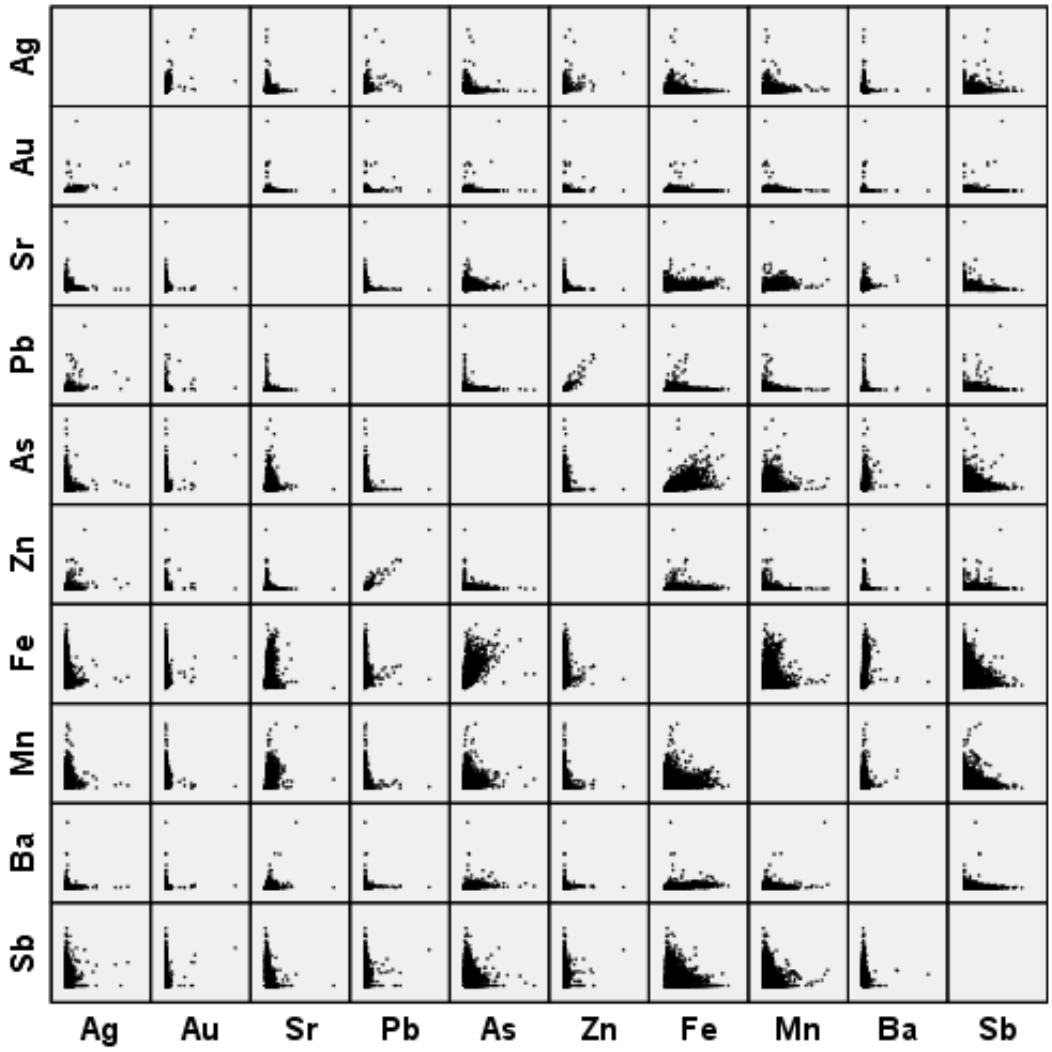

Figure 2.10 Bivariate graph for silver, gold, strontium, lead, arsenic, zinc, iron, manganese, barium, and antimony.

Chapter 3: Geology and Mineralization of the Independencia – Los Bancos (ICA) Ag-Au Epithermal Vein Systems in the Palmarejo District, Chihuahua, Mexico.

3.1 ABSTRACT

The finding of the ore deposits at Los Bancos and Independencia (ICA) was the product of applying technology and knowledge. It happened after the discovery of the hidden orebodies in Palmarejo and Guadalupe, and used the advantage of the recently acquired knowledge. The Independencia – Los Bancos (ICA) is the new mine of Coeur in Mexico; it started production in early 2016. The ICA deposit is composed of two semi parallel veins, about 300 meters apart, striking roughly N 40º to 45º W, and dipping between 60º to 80º to the southwest. The argillic alteration was identified and mapped in 2005 (Molina, 2005), but it was not until 2007 that the first hole was spudded in at the top of this non-mineralized, argillic alteration. ICA deposit, like Palmarejo and Guadalupe, are typical epithermal, intermediate-sulfidation, style. The mineralization is structurally controlled and normal faulting follows the northwest regional orientation, dipping from 45º (La Patria) to 75 º (Los Bancos) to either northeast or southwest. Normal faults serve as paths for the fluid migration and host the mineralization, especially at intersections with other structures or in areas of dilation due to inflection points, by changing strike and/or dip. The conclusions of this research are that the mineralization at ICA is genetically linked to the mineralization in the rest of the district. New zircon U-Pb geochronological data from Ramirez (2016) recognized two rhyolitic shallow intrusive pulses in the area; the first at 28.1 ± 1.0 Ma, and the second at 23.4 ± 0.4 Ma. The oldest one is pre-mineralization rhyolitic domes, whereas the youngest belongs to dikes associated to the mineralization event, giving a likely mineralization age of Early Miocene.

3.2 INTRODUCTION AND LOCATION

Ideally, the exploration for minerals is the process of finding ore by the application of successive techniques like remote sensing, geologic mapping, sampling, geochemistry, and geophysics, in order to target where the appropriate conditions exist, and thus test by drilling in

the places with more probabilities to contain economic mineralization. In reality, this process is unlikely to occur. Usually exploration success involves a mix of opportunity and serendipity.

Conversely, the finding of the ore deposits at Los Bancos and Independencia (ICA) was the product of applying technology and knowledge. It happened after the discovery of the hidden ore bodies in Palmarejo and Guadalupe, and used the advantage of the recently acquired knowledge of the associated conditions to this kind of mineralization. Similarly, to the 76 Clavo in Palmarejo and the Guadalupe deposit, the economic mineralization at ICA does not outcrop, and the only insight at surface is the presence of extensive argillic alteration. This alteration, along with some others, was detected using ASTER imagery (Molina, 2005).

The surface sampling of the Los Bancos and Independencia veins returned no values on precious metals. The argillic alteration was also sampled and analyzed with a TerraSpect^{TM} spectrometer and smectite was identified. The presence of smectite as an indicator of hidden mineralization was first documented on top of the 76 Clavo in Palmarejo in 2005, and guided the exploration to target the hidden orebodies in Guadalupe. First pass drilling on the ICA area was done in August of 2007, targeting both the Independencia (Don Ese) and Los Bancos veins. The purchase of Paramount Gold in 2014 opened the development of this area, as they share property boundaries where the Independencia deposit is contiguous to the Don Ese deposit, and production from ICA started in January 2016, as current mining activities in the Palmarejo district are were transitioning to underground mining in Guadalupe and ICA.

The ICA deposits are defined as an intermediate-sulfidation epithermal affinity. The regional stress regimes that affected the Palmarejo district region in southwest Chihuahua, allowed for the NW-SE trending emplacement of mineralization along normal faults caused by Tertiary extension in the northwestern SMO. This study focuses on the geological relationship between the ICA deposits and the rest of the Palmarejo district, the regional tectonic setting, geology, mineralization, as well as the documentation of the timing of the ignimbrites from the UVS, and the relationship of those to the most likely age of mineralization.

The study area is located in the Coeur Mining Inc. Palmarejo property, latitude 27^0 23'N, longitude 108^0 24'W, in the state of Chihuahua, Mexico, within the Temoris and Guazaparez mining districts of northern Mexico (Figure 3.1).

3.3 REGIONAL GEOLOGY

The ICA mine, inside the Palmarejo district, is located in the western boundary of the Sierra Madre Occidental geologic province. This province is characterized by a thick volcanic package from Cretaceous to Tertiary in age, whose emplacement was the result of the subduction at the Pacific coast of the Farallon plate (Ferrari et al, 2002) and the relaxation that followed during the opening of the Gulf of California by transcurrent faulting which occurred between 14 to 12 Ma (McDowell and Keizer, 1977). The SMO covers an area of over half a million square kilometers, from Arizona to the center of Mexico. The SMO is composed by two main groups, named the Lower (LVS) and Upper (UVS) Volcanic Supergroups by McDowell and Keizer (1977). In general terms, the LVS is composed of granodioritic batholiths at the base, and igneous rocks of predominantly andesitic composition, while the UVS is predominantly rhyolitic in composition (Ferrari et al, 2002).

3.3.1 Magmatism

The magmatism of the SMO has been divided into five main events by Ferrari et al (2007). The oldest occurred between 90 to 40 Ma and is related to the Laramide orogeny, where the subduction and the associated magmatic activity produced granodioritic plutonic bodies, and volcanic rocks of predominantly andesitic composition, which constitute the bulk of the LVS package (Damon et al, 1983). The second is an ignimbritic event during the Eocene, from 46 Ma to 42 Ma (McDowell and McIntosh, 2012) which constitutes the top of the LVS. The latest three volcanic events lie unconformably on top of the former group. It is a thick sequence of predominantly rhyolitic ignimbrites, interbedded with mostly silicic, and in lesser amounts mafic and intermediate, tuffs and lavas emplaced from the Oligocene to the Early Miocene (McDowell

and Keizer, 1977). Periods of bimodal volcanism has been documented by Cameron et al (1989), between the ignimbritic pulses, ranging from 33 to 17.6 Ma.

3.3.2 Tectonism

The west coast of North America has been a subduction margin since the mid Paleozoic until the present time. This portion of the Cordillera was subject to intense compressional stress during the Laramide, but the later, extensional deformation, occurred from Oligocene to Eocene (Ferrari et al, 2007) obscuring the original compressional features. The switching from compressional to extensional regime occurred around 33 Ma (McDowell and Mauger, 1994), as marked by the peralkaline ignimbrites and basalts related to the Basin and Range extensional event. The epithermal mineralization of the SMO has been associated to this extensional regime, and Goodell (in Prep.) states that the presence of pull-apart basin geometries are the main ground preparation causes for some of the mining districts (e.g. Temoris-Guazaparez Basin, El Sauzal - Cuenca de Oro) of southwestern Chihuahua. The orientation of these proposed pull-apart basins is associated to the kinematics of the opening of the Gulf of California.

3.3.3 Metallogeny of the Sierra Madre Occidental

The SMO metallogenic province hosts a variety of ore deposits. Jurassic to Early Cretaceous deposit types were mainly intrusion-related copper, skarns, volcanogenic iron, and shear-zone Au-bearing quartz veins, located in the LVS (Damon et al, 1983; Staude and Barton, 2001; Clark and Fitch, 2009). The Late Eocene to Oligocene is another period of mineralization, mainly low-sulfidation Ag-Au (±Pb-Zn- Cu) epithermal veins, high-sulfidation Au-(Cu), and high-temperature carbonate-hosted deposits (Staude and Barton, 2001; Clark and Fitch, 2009). The epithermal mineralization in this portion of the SMO belongs to this second period (Late Eocene to Oligocene). The preferential orientation of mineralization of this event is NW, congruent with the extensional event described before, and totally reflected in the Palmarejo district.

3.4 PALMAREJO DISTRICT GEOLOGY

The regional geology is composed of rocks of diverse origin, from marine (limestone, sandstone, and mudstones) intercalated with volcano sedimentary andesitic, volcanic, sub-volcanic, and intrusive rocks. The ages range from Cretaceous to recent, with a large predominance of volcano-clastic, igneous and volcanic rocks of Tertiary age (Figure 3.2) widely recognized as the Lower and Upper Volcanic Series. The present paper uses the stratigraphic nomenclature used by Coeur's geologists in different reports, and the main units are locally subdivided for more detail and listed from oldest to youngest as follows: A Cretaceous limestone-sandstone sequence (KaCz-Ar) is covered by a mainly andesitic, polymictic conglomerate (KtalCg) at the base. Covering the former are laminated andesitic siltstones and fine-grained sandstones (Ktal), of Cretaceous age, interbedded by andesitic rhyolites (KtalRHY) and amygdaloidal andesitic flows (Ktam). On top of the former units, are andesitic sandstones and conglomerates (Ktat). All these volcano-sedimentary sequences are related to the LVS, and except for the limestone and conglomerates at the base, the rest of the sequence constitutes the host rock for the mineralization in the Palmarejo district. The former package is overlain by rhyolites (ToTR), rhyodacites (ToRD), and basalts (TmB) of Tertiary age, which correspond to the UVS (Figure 3.3). The intrusive units documented within the district are Cretaceous granodioritic intrusions (KsGd) outcropping south of La Patria mine, Cretaceous andesitic porphyries (Ktap), and a Tertiary rhyolitic porphyries (ToPR), all of the above covered by Quaternary alluvium (Qho).

3.5 PALMAREJO DISTRICT MINERALIZATION

The largest precious metal ore body in the Palmarejo district is the Clavo 76, at the Palmarejo mine complex. Other important occurrences in the same mine are; Clavo Rosario, Tucson, 108, and Chapotillo. Clavos Rosario and Chapotillo, which were exposed, while 76 and 108 were blind. The second largest occurrence is the Guadalupe trend, which contains the Guadalupe Norte, Central, South, Las Animas, and La Curra ore shoots. At the Guadalupe trend, only Las Animas and La Curra were touching the surface. Just north of the Guadalupe Norte ore

shoot, in two parallel structure are Los Bancos and Independencia ore bodies, both of hidden mineralization. The La Patria trend is composed of the Cerro de los Hilos, Todos Santos, La Patria and Maclovia deposits, all of which are exposed at the surface.

The emplacement and mineralogy of all these mineral occurrences is consistent with the characteristics of the intermediate-sulfidation type described by Hedenquist et al (2000). All the deposits are structurally controlled, and hosted mostly in andesites of the LVS, and closely associated to the conspicuous rhyolitic dikes and domes, as discussed by Bryan et al (2008) and Kerr et al, (2015), and to porphyry intrusive bodies, like the one below the Espinazo del Diablo lithocap (Sillitoe, 2010). The mineralization is structurally controlled and normally faulted following the northwest regional orientation, dipping from 45^{o} (La Patria) to 75^{o} (Los Bancos) to either northeast or southwest. Normal faults serve as paths for the fluid migration and host the mineralization, especially at the intersection with other structures or in areas of dilation due to inflection points by changing strike and/or dip (Sillitoe, 2010; Birak and Blair, 2012).

3.6 ICA GEOLOGY

The geology and mineralization at the ICA deposit is similar to those observed in the rest of the Palmarejo – Guadalupe graben. The host of the mineralization is a combination of volcanic andesites, amygdaloidal basalt flows, and laminar andesites, intruded by porphyritic andesites and younger rhyolitic domes and dikes (Figure 3.4). The relationship observed by Ramirez (2016) in his geologic model has the laminated andesitic flows deposited at the base, followed by a thick sequence of amygdaloidal basalts, which are intercalated with thin layers of laminated andesites. The top units comprise andesitic sandstones with polymictic conglomerates divided into two volcano- sedimentary units, and an andesitic porphyry rock cut across these volcano-sediments. The younger rhyolitic porphyry (ToPR) is cross-cutting all the units (Figure 3.5). The mineralization is inferred to be younger than this last intrusive body, therefore the Independencia and Los Bancos veins were placed on top in the geochronological order of events. The Independencia and Los Bancos veins have a general northwest orientation of ~ 325^{0} which is

congruent with the general trend observed in the Palmarejo district. The surface expression of the Independencia structure is indicated by a high-argillic, low-quartz, metal-barren, alteration zone. The mineralization, at depth, is comprised of quartz veins, quartz-vein breccias, hydrothermal breccias, and hematitic tectonic breccias. The dominant sulfide minerals include silver sulfosalts, pyrite, sphalerite, and galena.

The association of visible gold, in the form of electrum, with hematite and goethite has been documented. The oxidation of pyrite was the most likely source explanation and petrography made by Perez (2013) suggests that the goethite comes from the oxidation of pyrite, but later careful examination did not reveal evidence of pyrite and suggests a different scenario, where the hematitic limonite may have evolved from primary high temperature and gold-bearing solutions (Ramirez, 2016).

3.7 GEOCHRONOLOGY AND MINERALIZATION.

According to Ferrari et al (2002), the bulk of ignimbrite forming the UVS was emplaced in two distinct events; the first occurred in early Oligocene, from 32 to 28 Ma, and the second at Early Miocene (24 to 23 Ma). Murray et al (2013) had identified three discrete Late-Oligocene to Early Miocene volcanic pulses at the Guazaparez area, just a few kilometers east of the Palmarejo district. The oldest of these three pulses is represented by the Parajes Formation, which is an around 1-kilometer-thick package of silicic ignimbrites, dated at 27.5 Ma (Murray and Busby, 2015). Another pulse of intermediate composition, interpreted as an andesitic volcanic center, has been dated between 27 - 24.5 Ma. The youngest volcanic pulse identified by Murray et al (2013) is composed by “silicic vent facies ignimbrites to proximal ignimbrites, lavas, plugs, dome-collapse deposits” labeled as the Sierra Guazaparez Formation. The age of this formation is from 24.5 to 23 Ma (Murray et al, 2013). These dates are fully equivalent to those obtained by Galvan (2012) from the La Patria rhyolitic dike (23.0 ± 0.5 Ma) and the Guadalupe rhyolitic dome (24.2 ± 0.4 Ma).

The new zircon U-Pb age data from Ramirez (2016) are consistent with the ignimbrite ages observed in the Guazaparez and Palmarejo regions. The U-Pb age data from Guerra Al Tirano at 23.4 ± 0.4 Ma and Guadalupe Norte at 23.7 ± 1.1 are attributed to the Early Miocene ignimbrite pulse. Age data from the San Francisco area recorded at 28.1 ± 1.0 Ma, is consistent with Early Oligocene ignimbritic pulse of the Parajes Formation (Murray and Bugsy, 2015). The timing of the ignimbrite pulses in Guazaparez coincides with the ages observed in the Palmarejo district, which points toward the conclusion that both areas were affected by the same volcanic event. From the structural ground preparation, Goodell (1995) states that the extensional stress has created pull-apart basin geometries, bounded by large-scale lineaments (e.g., Goodell, 1995; Galvan, 2005; Feinstein, 2007), that provided the main ground preparation for the later hosting of mineral deposits. This extensional event was coincident with the emplacement of the above volcanic events, and this coincidence of factors favors the emplacement of the mineralization at regional scale. Using the cross-cutting relationship analysis by Ramirez (2016) between the rhyolitic dikes and mineralized veins at the Independencia and Los Bancos deposits, it is inferred that the most likely age of mineralization for the Palmarejo district is Early Miocene.

3.8 CONCLUSIONS

The ICA deposit, like the rest of the Palmarejo district, is defined to be epithermal type, intermediate-sulfidation affinity as defined by Hedenquist et al (2000). The deposits are structurally controlled by a set of parallel NW-SE trending normal faults, while the ore shoots occur at the inflections of structures, or at the intersection with a secondary set of faulting oriented NNW. Researchers concluded that the Oligocene to Early Miocene volcanism that forms the SMO is coincident and genetically liked to the post-Laramide extensional regime (Murray and Busby, 2015, Ferrari et al, 2007). U-Pb analysis from Galvan (2012), Murray et al (2013) and Ramirez (2016), records two main pulses of rhyolitic volcanism in the area. The oldest of these comprises the rocks from 28.1 to 24.5 Ma, and records the emplacements of the bulk of the rhyolitic UVS

rocks of the area. The second is from domes and dikes between 24.5 to 23 Ma, which is the most likely age of mineralization.

3.9 ACKNOWLEDGMENTS

This study is the result of a scientific collaboration between Castulo Molina and Arturo Ramirez. We wish to thank Mitch Krebs, Hans Rasmussen, and Frank Hanagarne for granting the permission to use data in this article and in the UTEP MS thesis “Geology, Geochemistry and 3D Geological modeling of the Independencia - Los Bancos Ag-Au Epithermal vein systems in the Palmarejo District”, (Ramirez, 2016).

Figure 3.1 Location map of the Palmarejo District, Chihuahua.

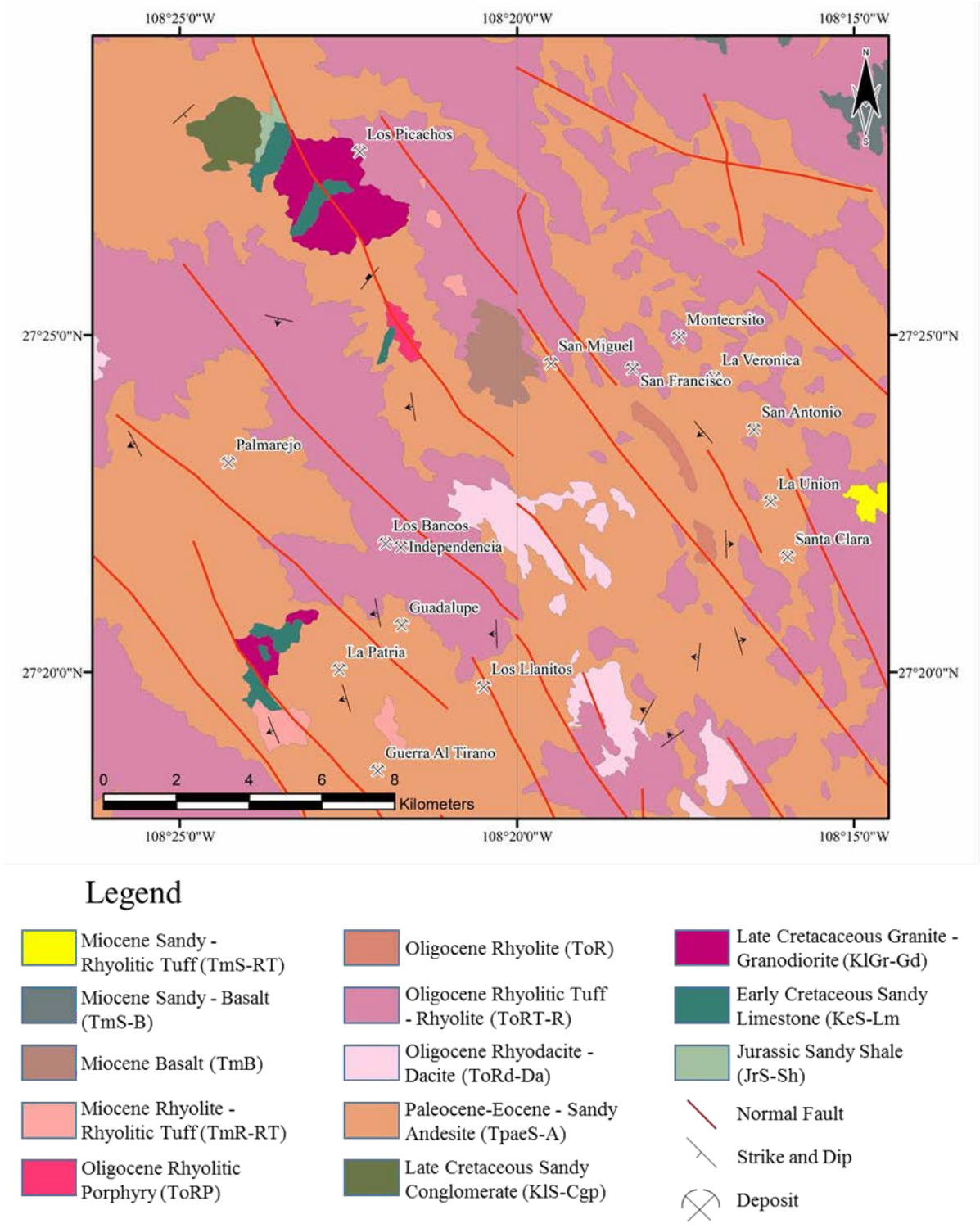

Figure 3.2 Geology of the Palmarejo District. Regional map modified from the Mexican Geological Survey (CRM, 2004, in Ramirez, 2016).

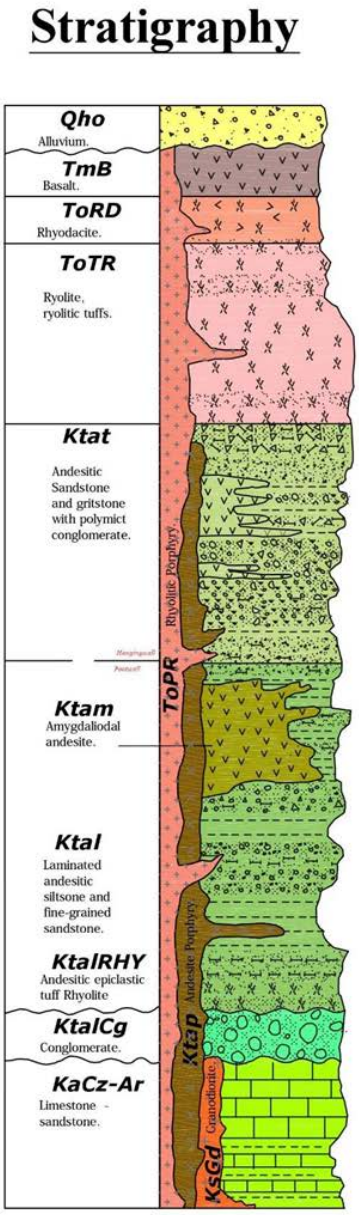

Figure 3.3 Stratigraphic section of the Palmarejo district, showing the most important lithologic units (Kerr et al, 2015, in Ramirez, 2016).

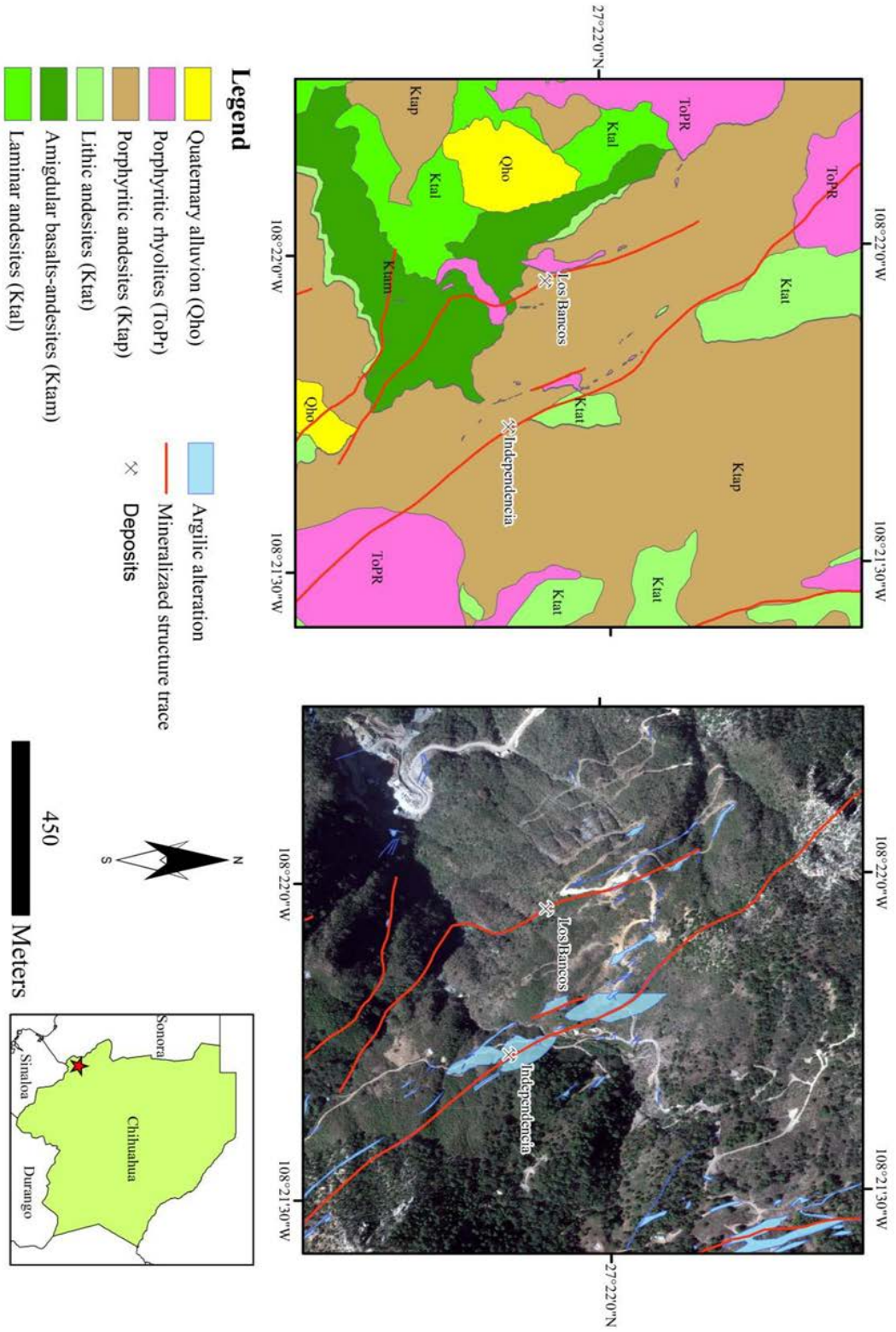

Figure 3.4 Geology and Alteration map of the Los Bancos – Independencia (ICA) epithermal vein deposit (in Ramirez, 2016).

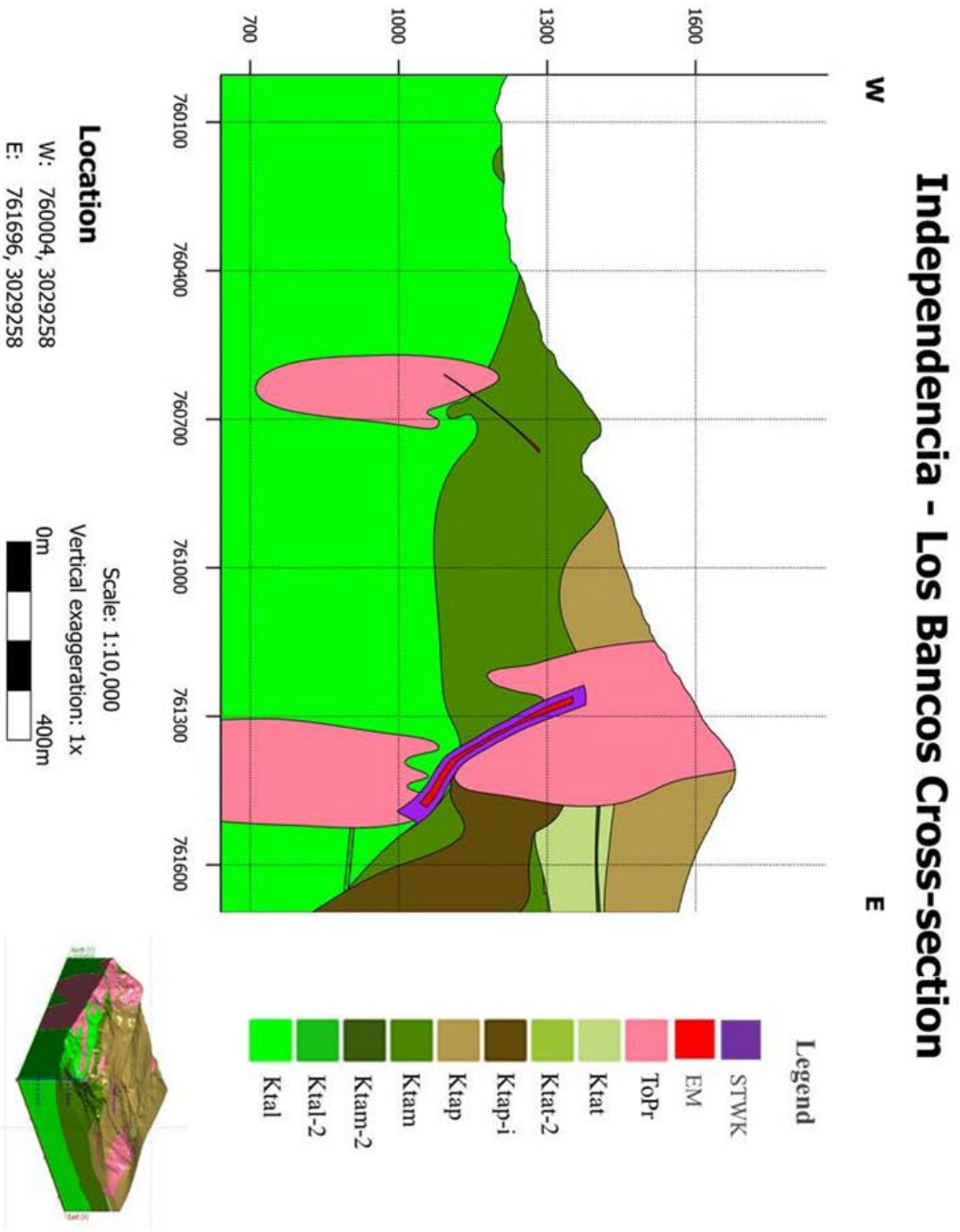

Figure 3.5 Cross-section of the Independencia – Los Bancos veins (ICA), showing the cross-cutting relationships of the rhyolitic porphyry (ToPr) with respect to the veins. Legend: STWK – stockwork; EM – mineralized structures; ToPr – porphyritic rhyolite; Ktat – lithic andesites; Ktap – porphyritic andesite; Ktam – amygdaloidal basaltic andesites; Ktal – laminar andesites (in Ramirez, 2016).

Chapter 4: Selection of Exploration Targets Using Field Data and GIS, in the Palmarejo District.

4.1 ABSTRACT

A combination of remote sensing techniques, field data, and the review of previous studies were used to define areas of interest within the Palmarejo District. Many factors were considered for this purpose, such as the location of the andesitic section, which is the most favorable host rock; the known occurrences of high-grade ore shoots within the district, clearly formed at the intersection of faults with different strikes and dips; blind ore shoots being overlain only by clay-altered caps; the recognition of the top and bottom of the mineralization window, for which the level of erosion and the elevation of the outcrop are critical; the hypothesis that the Palmarejo vein system extends out from the Espinazo del Diablo; and finally, the fact that the vein system in the Palmarejo-Guadalupe area is bounded by a set of northwest-trending normal faults defining distinctive grabens.

The data was introduced into thematic maps by means of ArcMap 10.3. The purpose was to: 1) Use all of the above criteria and look for the intersection of favorable structures (e.g. Palmarejo mine), or standalone veins (e.g. Guadalupe mine); 2) Map and associate epithermal argillic alteration to structures or lineaments; 3) To determine the influence that the rhyolitic domes and the Espinazo del Diablo played in the mineralization process; and 4) To determine the continuity towards the southeast of the Palmarejo-Guadalupe vein system.

The final result of this study consists of the delimitation of discrete areas of interest, and the prioritization of those with higher possibilities of containing mineralization. This approach has proved to be highly efficient in cost/benefit terms, since the study covered approximately 12, 000 hectares, and it was fully accomplished in less than 90 days.

4.2 GEOLOGIC SETTING AND MINERALIZATION

Sierra Madre Occidental is considered the largest silicic ignimbrite province (SLIP) in the world (Bryan and Ferrari, 2013). It consists of an undeformed core at the center oriented NW-SE, and two extensional sub-provinces: basin and range (BR) to the east and Extensional Province of

the Gulf (EPG) to the west (Henry, 1975). The Palmarejo District (PD) is located between the EPG and the undeformed core.

4.2.1 Mineralization type

The ore deposits of the PD have been classified as epithermal intermediate sulfidation-style, hosted mostly in the andesites of the Lower Volcanic Complex (LVC). The veins are located in a sequence of andesitic to basaltic composition rocks, from Eocene to early Oligocene in age. From the base upward, the lithologic units consist of laminated epiclastic sedimentary rocks of broadly andesitic composition, amygdaloidal basalt flows, and andesitic lithic tuffs. This sequence constitutes an angular unconformity with the upper volcanic sequence (UVS) dominated by rhyolitic ignimbrite flows and tuffs, of mid- to late Oligocene age (Murray 2009). Andesitic dikes and sills intrude the lower volcanic sequence, whereas rhyolitic dome complexes and dikes cut both the lower and upper sequences.

4.2.2 Mineralization controls

The epithermal mineralization is structurally controlled, and the discontinuities in the PD are mostly due to normal faulting, although Corbett (2006) and Sillitoe (2010) have considered strike-slip displacements. The main high-grade ore shoots at the Palmarejo District were clearly formed at the intersection of faults with different strikes and/or dips. This crossing of faults created extensional areas in the form of triangular blocks, bounded by veins on two sides, and the mineralized stockwork is infilling the triangle (Figure 4.1). Clavos Rosario and 76 are the classical examples, of mineralization in triangular-shapes, in which the ore deposition is facilitated because of the upright position of the triangle which helps the expansion (Sillitoe, 2010). This triangular “ore-shoot model” likely occurs in other vein arrays in the district, hence is fundamental knowledge to be used in the exploration of ore-bodies in the district.

4.2.3 Deep-seated intrusion and mineralization

The intrusive engine considered the temperature source for the mineralization in the Palmarejo District is located two kilometers to the west of the Palmarejo mine in the area known

as Espinazo del Diablo (Figure 4.2). This advanced argillic lithocap is overlying a hypothetical porphyry intrusive and according to Sillitoe (2010) “likely to host porphyry copper-style alteration and mineralization”. The location of the Espinazo del Diablo lithocap with respect to the Palmarejo vein system strongly suggests that the graben faults acted as the principal conduits for upward and outward flow of mineralization fluids from the inferred porphyry center.

The Espinazo del Diablo intrusive helps to explain the presence of high-sulfidation mineral such as enargite and luzonite, and the relatively higher temperature of the La Patria graben, but raises some questions on the role of the rhyolite domes and dikes in vein formation. Although the relationship between the intrusion and the rhyolitic domes is not clearly understood at this time, it is clear that both played a role in the mineralization on the district.

4.2.4 Rhyolitic intrusions and mineralization

The Palmarejo District is located in an area of volcanic transition characterized by the conspicuous presence of rhyolitic domes, outlining the location of silicic magma reservoirs at depth. These extruded bodies are intruding the volcano-sedimentary sequence along the main NW-SE listric faults, and at the intersection of transcurrent ones (Corbett, 2006). The plasticity of the intrusions, throughout expansion and contraction during solidification, produced both horizontal and vertical movements in the overlying volcano-sedimentary package. A steady spatial relationship between veins and dikes has been documented, although their genetic relationship has not been fully established. The veins cut the rhyolitic domes and dikes, therefore the mineralization age should be younger or contemporaneous to the dome-dike event.

4.2.5 Mineralization zoning and alteration

Another exploration tool at the district and mine scale is the mineralization zoning and the argillic alteration. The downward increment of silver/gold ratios in the Palmarejo and Guadalupe veins (Molina and Goodell, 2015) has been fully documented, and helps to locate the deposit, with respect to the window of mineralization. On the other hand, after the discovery of the first blind orebody at the Palmarejo mine (Clavo 76) in 2004, mapping at the surface returned no evidence

of a vein structure outcropping, only a few meters of argillization along the trace of the fault projected from below. Mapping the surface expression of these blind veins (Guadalupe, Clavo 108, Los Bancos, Independencia) has shown the presence of smectite, a low temperature clay, mixed with supergene kaolinite. A further analysis of drill core has shown that the clay varies in abundance with kaolinite by the middle of the mineralization window, and to illite to the bottom of the system. These two observations (decreasing of the silver/gold ratio with depth, and clay variation from low to high temperature) are very useful when comparing the different deposits within the district, and actually helps us to arrive at the conclusion that the La Patria mine, with Ag/Au ~10, is located in a relatively deeply eroded structure.

4.2.6 Mineralization belts

The vein system in the Palmarejo District is bounded by a set of post mineralization, northwest-trending normal faults that locally define two main graben structures (CRM, 2004), that are two distinct mineralization belts (Figure 4.3). The northernmost is the Palmarejo-Guadalupe graben, which is 3 km wide and comprises the most important veins: La Blanca, La Prieta, San Juan, Los Bancos, Independencia, Guadalupe and La Curra. The graben to the southwest is slightly smaller, 2.5 km wide, and comprises the Cerro de los Hilos, Todos Santos, La Patria and Guerra al Tirano veins (Figure 4.2).

4.3 METHODOLOGY - DATA ACQUISITION AND PROCESSING

The approach to get additional information from the exiting data was applied to the above criteria and the following characteristics were sought: a) intersection of favorable structures (e.g. Palmarejo mine), or standalone veins (e.g. Guadalupe mine); b) map the associate epithermal argillic alteration to structures or lineaments; c) map and show the association of rhyolitic domes and structures; and d) map the likely continuity towards the southeast of the Palmarejo-Guadalupe vein system.

Data from different levels was merged to create the basic database for this study. A combination of remote sensing and field data was classified and placed in an Excel™ spreadsheet

for later GIS manipulation. All the data was divided in four categories: a) Lineaments, b) Structural data (dikes, mineralized structures, banded flow, shear zones, stockwork and faults), c) Kinematics, and d) Mineralogical (argillic alteration). Using a combination of all the former data, eight thematic maps were created to assist with the interpretation.

4.3.1 Thematic maps of lineaments

The first thematic map shows the lineaments (Figure 4.3) which had orientation, but no dip. This map was generated from mapping, satellite imagery analysis (SRK, 2014) and geophysics (Vizcarra, 2012). The map shows the internal lineaments within the Palmarejo-Guadalupe graben (PG-G), and the regional faults mapped by the Mexican Geological Service (CRM, 2004) that bounds it; Saucillo de Lugo to the northeast and Los Llanitos to the southwest.

Using the lineaments map as a base, the second thematic map is showing the estimated azimuths and mineralized structures (Figure 4.4). The assembly of this map included the estimation of azimuths for all lineaments, in order to have a clear idea of the structural dynamics. The azimuths were acquired using a combination of Excel™ and ArcMap™, and the mapped vein systems were also included. Using field data and the former estimation of azimuth of the lineaments, a kinematic map was constructed (Figure 4.5). This map shows, by directional arrows, the relative lateral movement of the structures, and essentially the split of all the lineaments into two categories, right kinematics and left kinematics.

4.3.2 Thematic maps of blocks

The former thematic map (kinematics) and other specific features allowed the distinction of diverse blocks within the grabens. Figure 4.6 is a map showing the extensional grid developed from a step over of two main dextral strike-slip faults. There are two structural systems at the northern portion of the Palmarejo – Guadalupe graben. The first one is oriented NWW and the second strikes NNW. These systems configure at Palmarejo into a strike-slip basin with mineralized ore shoots concurring at the intersections, e.g. Clavo Tucson, Clavo Rosario and Clavo 076. In general terms, the norther portion of the Palmarejo–Guadalupe graben (Palmarejo mine)

belongs to the first group, while the southern portion (Guadalupe and ICA mines) belongs to the second.

Considering the different domains of deformation from the former map (Figure 4.6), and overprinting the younger regional faults that vertically displaced the grabens (Figure 4.3), five distinctive blocks can be defined as shown in Figure 4.7. The general limits between blocks are oriented NW-SE, following the trace of the regional younger faults, while the limit between blocks 2 and 4 is oriented roughly N-S. Each block shows specific structural characteristics and mineralization styles. Block 1 is characterized by compressional stress, e.g. strike-slips, reverse faulting. This block does not have identified mineralization. The Espinazo del Diablo lithocap is located within this block, and the mineralization possibilities are restricted to porphyry or high-sulfidation epithermal type.

Block 2 is characterized by a curved lineament and shows rhombohedral features which are diagnostic of strike-slip basins. At the intersection of the fault systems is where the ore shoots are found. This block encompasses all the Palmarejo mine complex, including Rosario, Tucson, Chapotillo and Clavo 76.

Block 3, like block 2, also shows rhombohedral features which are diagnostic of strike-slip basins. The peculiarities of this block are the presence of the bottom of the stratigraphic section and the exposure of the base of the mineralization window. This block is interpreted as the “horst”, with respect to the Palmarejo-Guadalupe graben. This block contains several mines and prospects, such as Maclovia, La Patria, Convirginia, Todos Santos, and Cerro de Los Hilos.

The structural dynamics of Block 4 is mainly characterized by a series of rhyolitic dikes parallel to the main faults. Within this block are the mineralized structures of Guadalupe-Animas-La Curra; Los Bancos-Nacion and Independencia-Don Ese.

Block 5 is located northwest of the Saucillo de Lugo fault, the structural dynamics are likely to be similar to block 4, but the younger rhyolitic package conceals possible mineralization.

4.3.3 Thematic maps of alteration

SRK (2014) conducted an alteration survey, and along with previous alteration data from Bolnisi and Coeur, two alteration maps were generated. The first is a thematic map of kaolinite indexes (Figure 4.8), which was generated from historical and field data obtained for kaolinite, using a portable analyzer. The data was interpolated using the Kriging process module included in ArcMap. The same procedure was used to generate the illite indexes thematic map shown in Figure 4.9.

The thematic maps of alteration are showing the areas where the hydrothermal alteration is more intense inside the Palmarejo – Guadalupe graben. The Kaolinite indexes map (Figure 4.8) shows how the kaolinite is concentrated in four areas; Palmarejo (1); the eastern extension of the Cerro de Los Hilos (2); The Guadalupe – La Curra corridor (3); and the Independencia – Los Bancos area (4). The Illite indexes map (Figure 4.9) is showing the highest values associated with rhyolitic domes, the smaller area at Guadalupe Norte (1), and the largest at Los Bancos (2).

4.4 RESULTS

The thematic map overlaying and cross referencing of information is critical to determined areas of interest and to their prioritization. After analyzing critical factors such as gold-silver metal ratios, mineralogy, alteration assemblages, and younger regional tectonics, tested against the mineralization model, it was determined that the Palmarejo – Guadalupe graben has better potential to contain silver – gold than the adjacent La Patria corridor. Figure 4.10 is a thematic map showing the prioritization of exploration areas inside the Palmarejo – Guazaparez graben. The prioritization of areas is based on the distance and similar characteristics to known mineralization, a favorable structural array, exposure of the mineralization window, and alteration. The areas labeled in red as first priority (targets 1 to 3) are those around the existing mines, Palmarejo, Guadalupe and ICA.

Exploration within those areas should concentrate along the NW-oriented structures: Since the best concentration of minerals are those with several pulses of fault reactivation and

mineralization, one of the keys is to focus on the NW faults with higher displacements. The second clue is to search for the intersection with northing structures, or change in orientation. The third factor is the presence of low temperature illite (smectite) in the argillic alteration at the surface.

Outside of the former three areas with current mining, the most favorable areas for exploration are as follows: 4) La Curra; 5) Palmarejo South, and 6) Palmarejo Central. La Curra, described by Miller and Goodell (1988), as the southern extension of the Guadalupe Vein. The mineralized vein outcrops at La Curra, and using gold/silver ratios it is determined that we are looking from the middle to the bottom of the mineralization window. Therefore, it is recommended to focus the exploration in the shallower portions of the vein, searching for the highest Ag/Au ratio values.

The number 5 exploration target is located to the southeast from the Palmarejo mine. It is characterized by similar framework that formed the Blanca and Prieta veins in Palmarejo, but the erosion level is less intense in this area, hence the exploration should focus on finding the mineralization window around 1000 masl. The search for the main structural controls, such as the continuation to the south of La Blanca vein, along with low-temperature argillic alteration, can be the pathfinder for hidden mineralization in this area.

Block 6 is located in the center of the pull apart basin outlined in Figure 4.6, between the Guadalupe (2), ICA (3) and Palmarejo South (5) exploration areas (Figure 4.10). The suggested exploration approach for this area is to search for the intersection of the NNW structures, with the main NWW trend. The presence of any of those structures with the presence of smectite is worth reconnaissance type (wildcat) drilling.

4.5 CONCLUSIONS

The combination of azimuth data, kinematics, alteration, and structural data such as vein-faults, dikes, stockwork and banded flows have allowed the selection and prioritization of sites for the focus of the exploration inside the Palmarejo District. The use of geographical information systems (GIS) has proven to be a very effective tool in terms of cost/benefit, but there are some

issues that need to be considered in order to have the highest degree of confidence in the results. Any data mining program should be divided into two stages: field data acquisition and interpretation. Gathering the data requires both amount and quality. Interpretation requires the full understanding of the mineralization model and the implication of every factor under consideration.

4.6 ACKNOWLEDGMENTS

This study is the result of a scientific collaboration between Castulo Molina and Carlos Martinez Piña. We wish to thank Coeur's exploration management for the permission for the use of the historical data, and the consultant's internal reports.

Figures Chapter 4

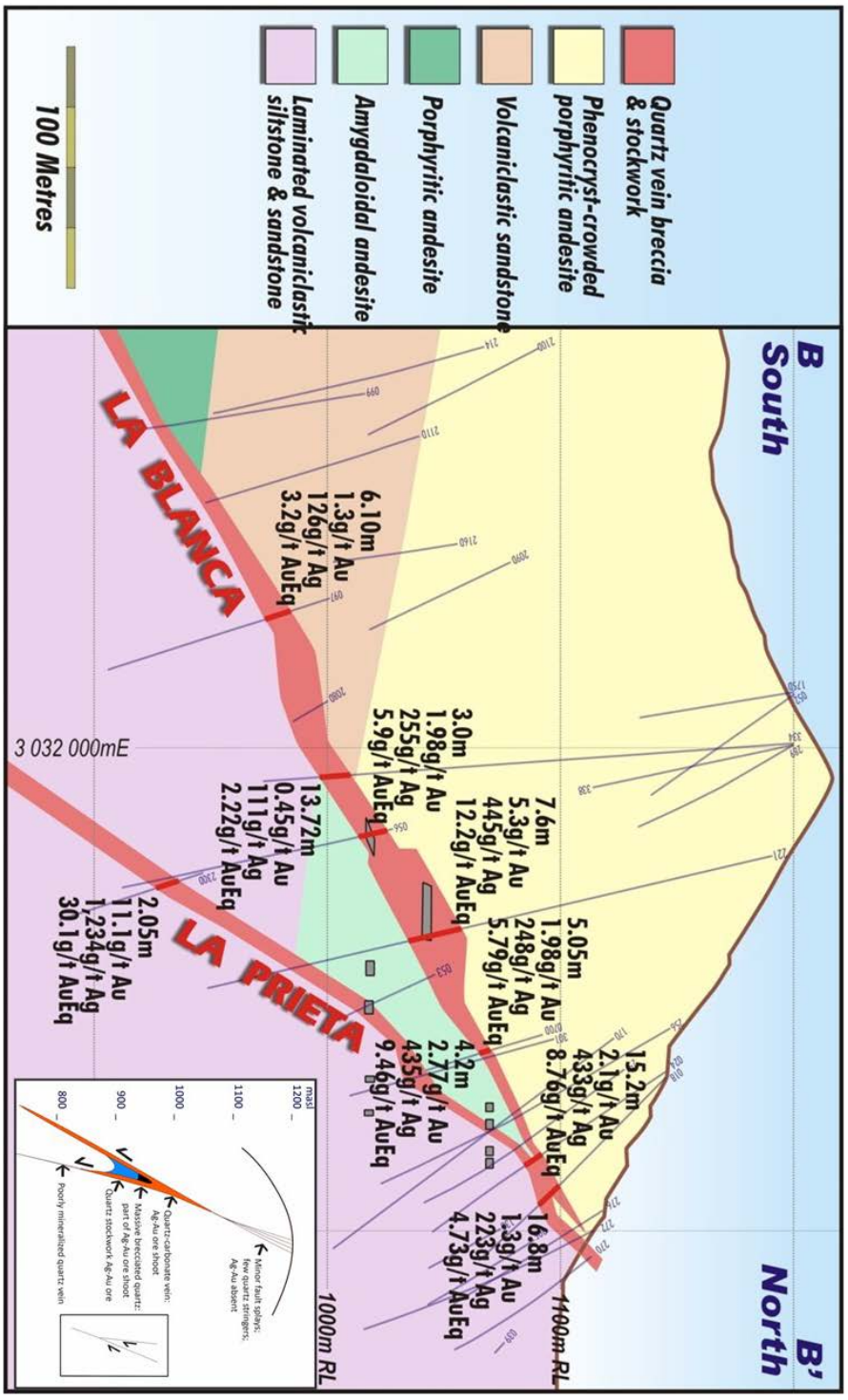

Figure 4.1 Cross section of the Clavo Rosario, as an example of a two structure intersection ore-shoot. Also showing are the drill intercept. The insert is showing a triangular-shaped, ore-shoot development model, as described by Sillitoe (2010).

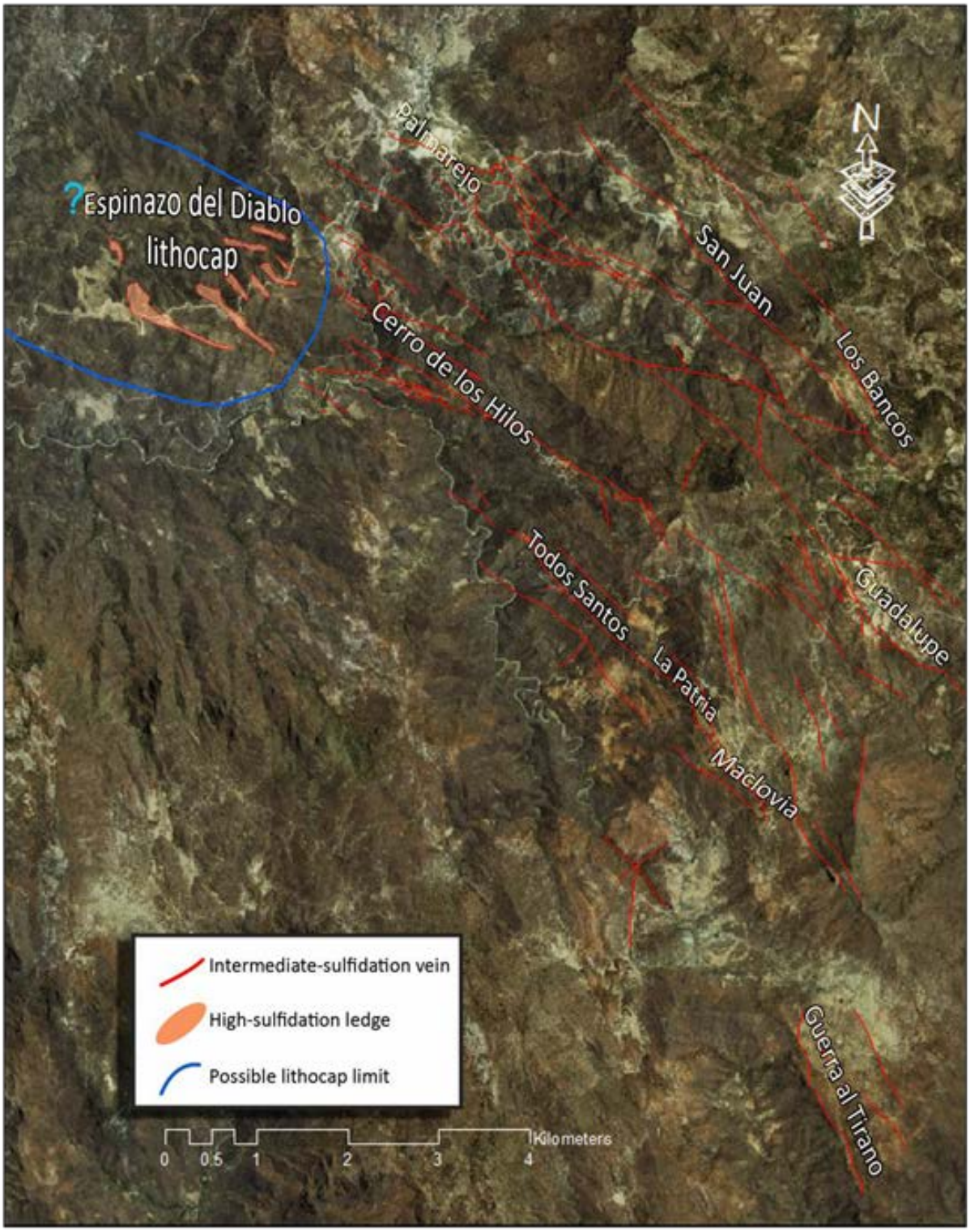

Figure 4.2 Satellite image showing the location of the different veins and the advanced argillic lithocap. (Sillitoe, 2010)

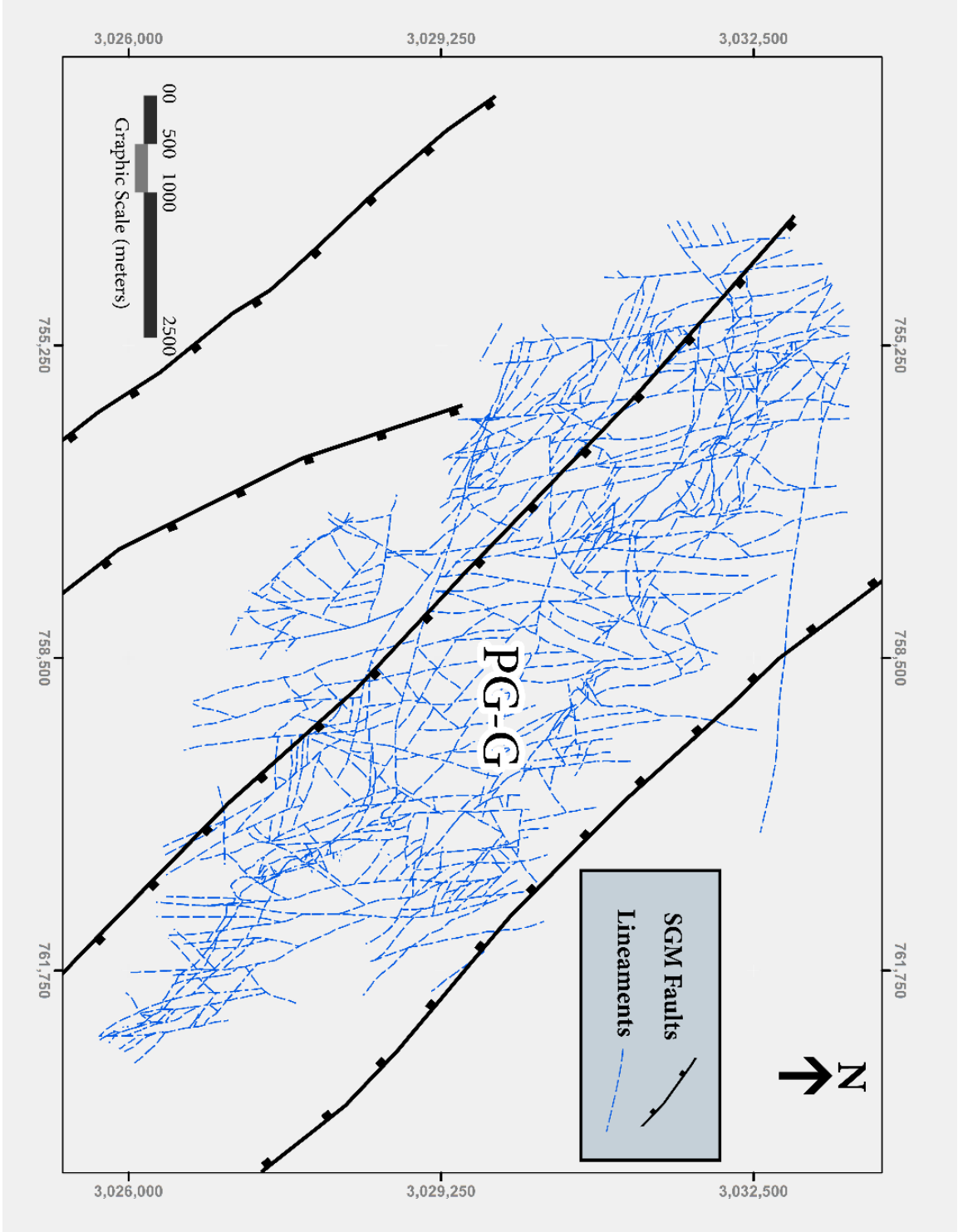

Figure 4.3 Map showing the Palmarejo-Guadalupe graben (PG-G) bounded by regional faults (Saucillo de Lugo to the northeast and Los Llanitos to the southwest). Regional faults drawn from Carta Geológico-Minera Chínipas G12-B38 (2004), lineaments from Coeur's internal reports, SRK (2014), Vizcarra (2012).

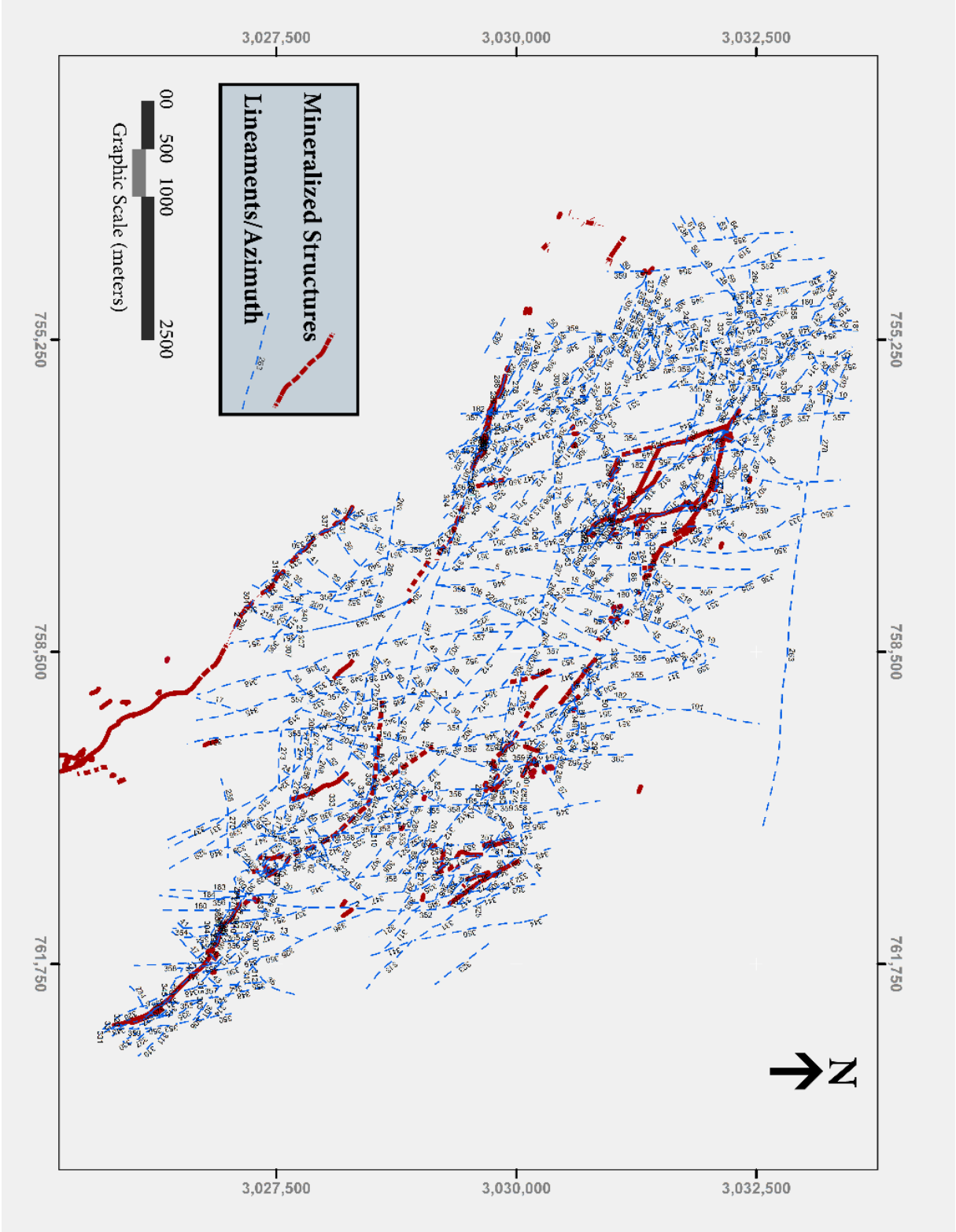

Figure 4.4 Map of estimated azimuth of lineaments. This map is derived from figure 4.3, showing the estimated azimuth of the lineaments obtained from data processing in excel and loaded into ArcMap. The known mineralized structures are also shown.

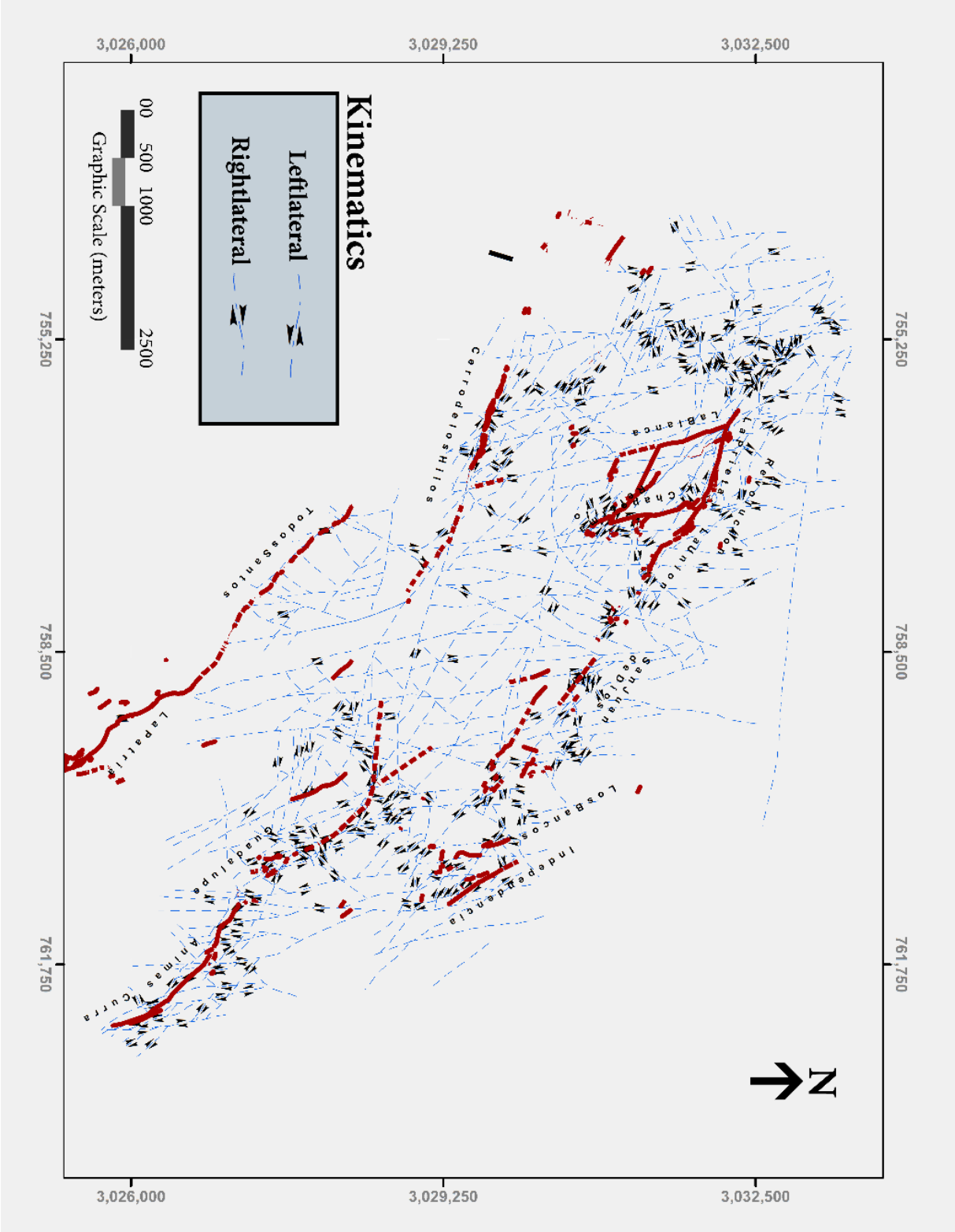

Figure 4.5 Map of kinematics inside the PG-G. This map is blending file data with the former map of lineaments and structures, to estimate the kinematics inside the Palmarejo – Guadalupe Graben (PG-G).

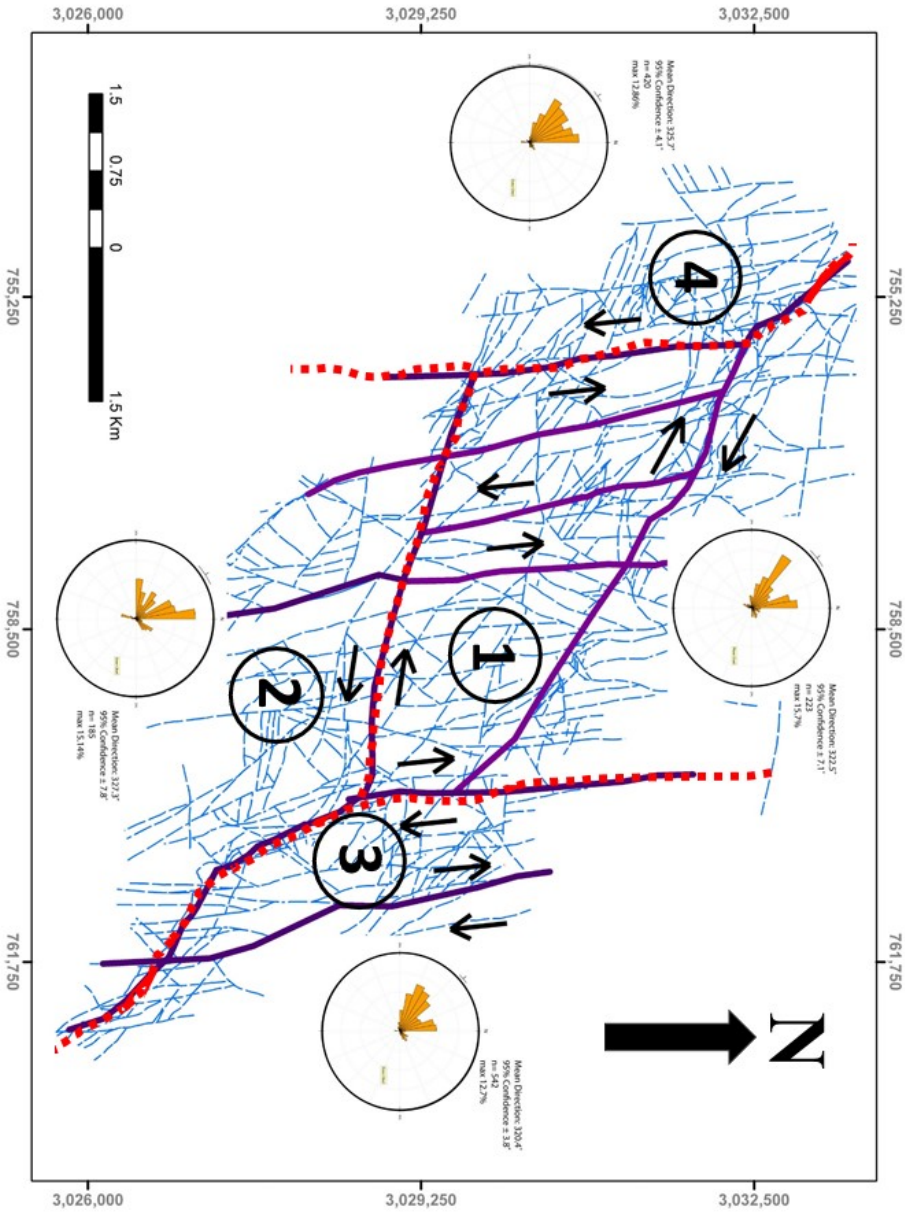

Figure 4.6 Structural map of the Palmarejo – Guadalupe graben, showing extensional grid developed from a step over of two main dextral strike-slip faults. There are two structural systems at the northern portion of the Palmarejo – Guadalupe graben. The first one is oriented NNW and the second strikes NWW. These systems configure at Palmarejo a strike-slip basin with mineralized ore shoots concurring at the intersections, e.g. Clavo Tucson, Clavo Rosario and Clavo 076.

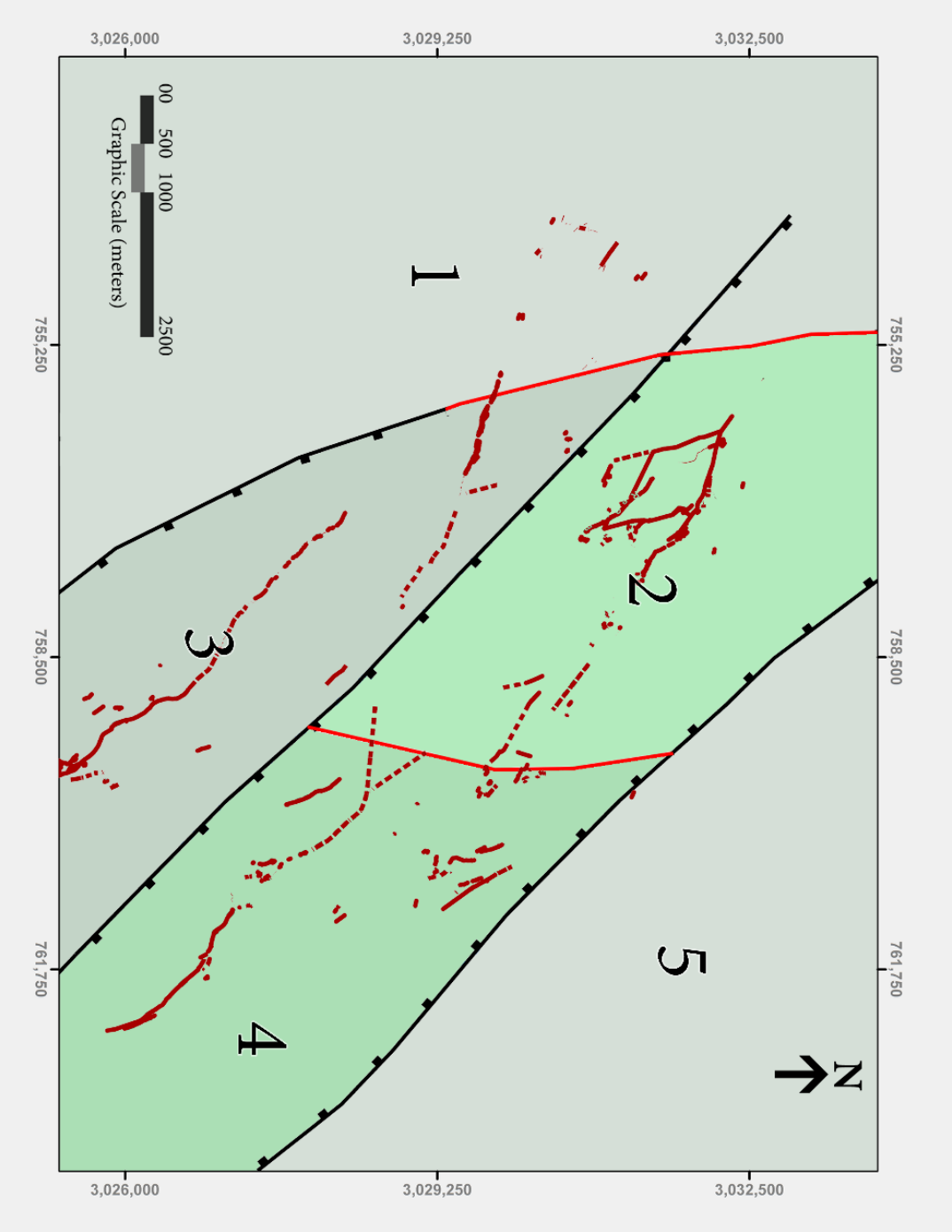

Figure 4.7 Map of structural blocks, showing 5 discrete structural blocks. Each block shows specific characteristics and mineralization styles. The general limits between blocks are oriented NW-SE, following the trace of the regional, younger faults, while the limit between blocks 1 and 2, and, 2 and 4, are oriented roughly N-S.

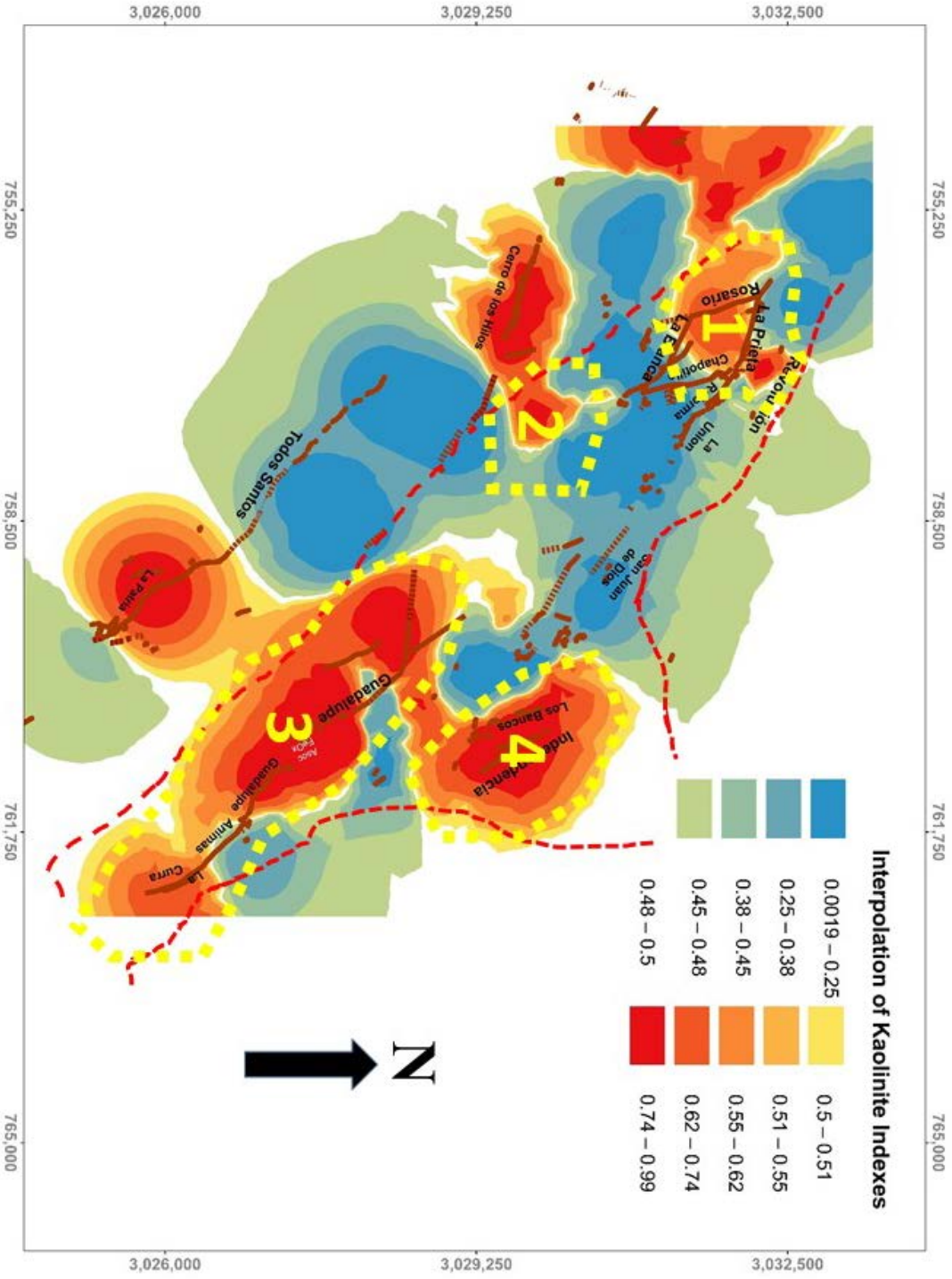

Figure 4.8 Alteration map of kaolinite generated from historical and field data obtained from kaolinite readings and interpolated by Kriging in ArcMap. The kaolinite is concentrated in four areas; Palmarejo (1), the eastern extension of the Cerro de Los Hilos (2), The Guadalupe – La Curra corridor (3), and the Independencia – Los Bancos area (4).

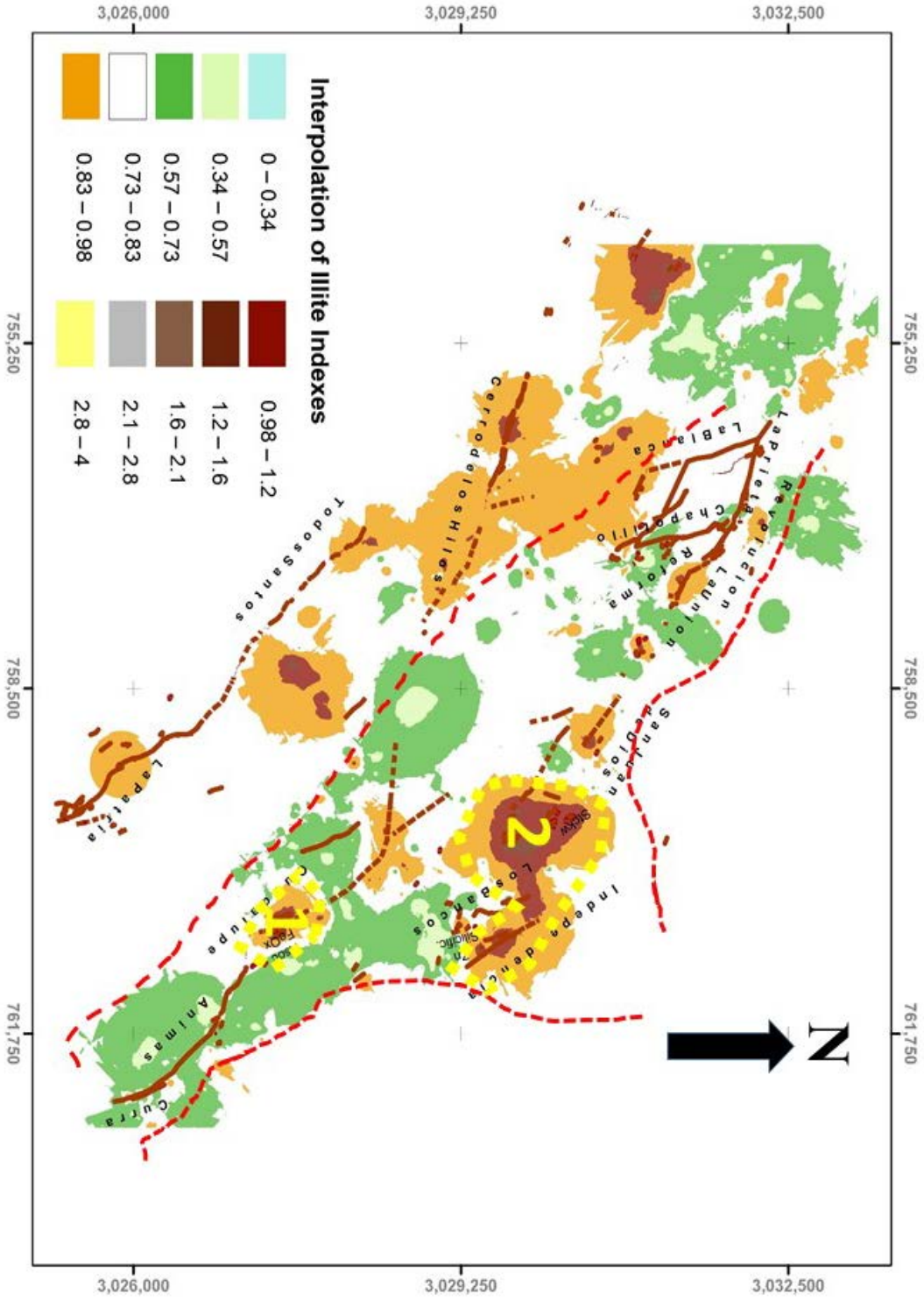

Figure 4.9 Alteration map showing the illite distribution. Map generated from historical and field data obtained from Illite readings and interpolated by Kriging in ArcMap. The highest values are associated with rhyolitic domes and mineralization, such as Guadalupe (1) and Los Bancos (2).

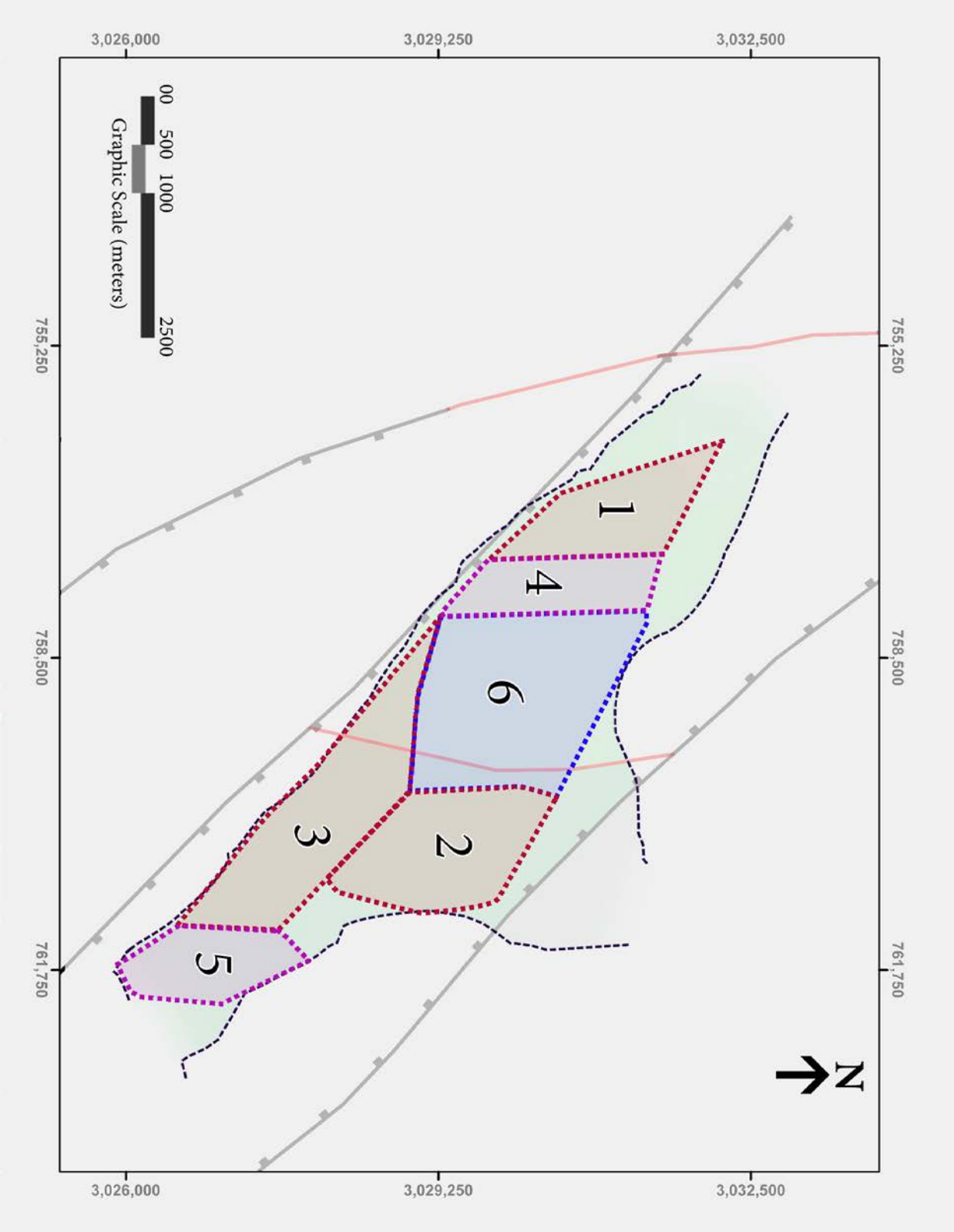

Figure 4.10 Map showing the prioritization, in ascending order from 1 to 6, of exploration targets within the Palmarejo – Guadalupe graben.

Chapter 5: Interpretation of HR Magnetometry Data in the Palmarejo District and Surrounding Areas

5.1 ABSTRACT

This interpretation of high resolution magnetometry data covers the area inside the geographic coordinates from 27°04´ to 27°32´ latitude, and 108°02´ to 108°34´ longitude, encompassing a surface of approximately 1,624 square kilometers, in the Sierra Madre Occidental (SMO). The SMO is characterized by the presence of northeasterly-facing, elongated, asymmetrical and parallel mountains with heights of more than 2000 meters above sea level (masl), dissected by deep canyons. Geologically, the Sierra Madre Occidental (SMO) is composed of two igneous packages, traditionally called the Lower Volcanic Complex (LVC) and the Upper Volcanic Complex (UVC). The LVC ranges in age from 45 Ma to at least about 100 Ma. This sequence is composed mainly of andesitic rocks from the Late Cretaceous to Early Tertiary (Paleocene). The UVC is an extensive sequence of rhyolitic volcanoclastic rocks, with some shallow intrusions that form large, extended sub horizontal plateaus, crowning the higher parts of the SMO. Most of the mineralization inside the SMO is epithermal in origin, structurally controlled, and usually hosted in the andesitic LVC, or is close to the contact with the UVC.

The magnetic data used in this study was derived from two different sources. The most recent data was acquired through an aerial (HRM) geophysical survey in 2015, and covers the area formerly controlled by Paramount Gold de Mexico. That data was integrated with HRM data from a geophysical survey done by Coeur Mexicana in 2012 to perform the total processing of all acquired data with Helimag, in one package, using the platform of Oasis Montaj Geosoft™.

Based on the processed data, for this type of mineralization, it was concluded that the HRM methodology is more suitable for a large scale exploration approach, > 100 square kilometers, rather than a mine scale. The main finding of this research is the supporting evidence for semi-

circular structures at depth that are linked to the mineral occurrences in the area. This genetic model helps to discriminate the less prospective areas, and focuses on those whose structural and tectonic settings have the best chances of containing economic mineralization.

5.1 INTRODUCTION

The aero magnetic survey used in this study, covers 1624 square kilometers over the Chínipas, Guazapares and Urique counties, in the southwestern portion of the state of Chihuahua, México. The shape of the area is an irregular polygon, roughly outlined by the geographical coordinates of 27°04’ to 27°32’ latitude, and 108°02’ to 108°34’ longitude (Figure 5.1).

The zone is located in the Sierra Madre Occidental (SMO) physiographic province, into the sub-province of canyons of Raisz (1964), which is characterized by the presence of northeasterly facing, elongated, asymmetrical, parallel mountains with heights of more than 2000 meters, intersected by deep canyons. The surface area is topographically a sharp volcanic relief, formed at the base by a sequence varying from acid based to mafic- epiclastic rocks, interlayered with andesites, the Lower Volcanic Complex. This is covered by another layer of acidic rocks with a thickness of over 1000 m, the Upper Volcanic Complex, which is characterized by the presence of large escarpments.

5.2 GEOLOGIC SETTING

In general terms, the Sierra Madre Occidental (SMO) is composed of two predominantly igneous sequences, traditionally called the Lower Volcanic Complex (LVC) and the Upper Volcanic Complex (UVC) (Wisser, 1966; McDowell and Clabaugh, 1979). The LVC is the older and ranges in age from 45 Ma to at least 100 Ma (McDowell and Clabaugh, 1979). This sequence is composed of plutonic and volcanic rocks from the Late Cretaceous to the Early Tertiary (Paleocene)

characterized by andesitic volcanic rocks, and in smaller portions dacitic rhyolites. The geological column is composed of a large variety of volcanic rocks, among which, andesite has a predominance, and they are commonly interlayered with some sedimentary rocks. The LVC rocks are better exposed within the canyons of the western margin of the province, where the erosion is more prominent.

The Upper Volcanic Complex is an extensive sequence of volcanic and volcanoclastic rocks, and shallow silicic intrusions, forming large extended, sub-horizontal plateaus. The UVC unconformable covers the LVC, and is usually crowning the higher peaks of the SMO. The entire sequence reaches a thickness of over 1000 meters, and is the result of continued volcanism between 34 and 27 Ma (Swanson and McDowell, 1984; McDowell and Clabaugh, 1979), even though some activity persisted until 23 Ma (McDowell and Clabaugh, 1979). This volcanic sequence is dominated by rhyolitic and rhyodacitic ignimbrites, generally accompanied by rhyolitic domes and flows (Murray and Busby, 2015), and small amounts of mafic lava (McDowell and Clabaugh, 1979; Cameron et al, 1989). Volcanic rocks of intermediate composition have been reported at the base of the felsic rocks in various places along the SMO (Wark et al, 1990; Sellepack, 1997). In adjacent areas, these units were emplaced in the Mid-Tertiary (Wark et al, 1990) by a caldera or cluster of calderas. McDowell and Clabaugh (1979) considered a large quantity of calderas, with diameters of 20 to 30 km, all through the SMO, even though the circular or semi-circular configurations are today obscured by the presence of younger normal faulting, and recent alluvial deposits.

5.3 MINERALIZATION

The majority of the mineral deposits in the area are epithermal type, low-to intermediate sulfidation and in lesser amounts, high-sulfidation affinities. The mineralization controls are usually structural in the form of veins emplaced in fault zones, fissure filling, and stockwork. The

majority of these structures are emplaced following the NW-SE structural system, and sporadically in the E-W system. The mineralized structures can extend from a few meters to 2 or more kilometers in length. Most of the mineral deposits are found hosted in the predominantly andesitic rocks of the LVC, although some deposits (e.g. El Sauzal, Sellepack, 1997) are clearly in contact with or within the UVC rhyolites, like those shown in the geologic map (Figure 5.2) of the study area.

5.4 GEOPHYSICAL METHODS

5.4.1 Data Acquisition

An aerial geophysical exploration campaign was launched in March of 2015 to obtain high resolution magnetic and radiometric data over the Temoris mining district, Chihuahua. For this purpose, a Bell 206L3 helicopter aircraft was employed (Figure 5.3), equipped with an advanced navigation system, a Cesium vapor magnetometer, and a gamma ray spectrometer. The collected information was placed cartographically in the Datum WGS 84 referred to a UTM Projection Zone 12 N. The survey collected data along 6,666 linear kilometers, which covered an area of 1460 Km^2. The magnetic sensor was flown at a height of 60 meters from the surface and the flight lines were separated 200 meters. The perpendicular control lines were separated 2000 meters.

Previous HR magnetic data was collected in April 2012 by a 2,571.5 linear kilometers survey (Figure 5.3), which covered an area of 164.6 Km^2, with flight lines every 75 m, and perpendicular control flight lines every 750 m. The lines were surveyed using a Gem System GSM-19TW Over Hauser magnetometer base station, in a place with a low magnetic gradient and away from all cultural noise. The data from both surveys (2012 and 2015) was merged for the current interpretation, therefore, this study area covers a total of 1,624 Km^2, and took 9,237 linear

kilometers of flight to collect the HR magnetic data.

5.4.2 Data Processing

Data processing started in the field by doing corrections to the raw data by heading (effect of magnetic direction), levelling and micro levelling, as preparation to applying the magnetic field day time diurnal variation. This allowed the gathering of a database of the readings of the total magnetic field intensity, tied with the corresponding coordinates of each and every one of the registered points.

Helimag data in this study was processed on the platform of Oasis Montaj Geosoft™, under the filtering system MAGMAP module, an integrated software package, which supports the implementation of common filters in the Fourier domain (Winograd, 1978) on data sorted as a grid. The software gives particular emphasis on Potential fields information (Wiener, 1949; Burg, 1975), such as Magnetic and Gravity data, being able to select and apply appropriate filtering or processing in MAGMAP module (Bhattacharyya, 1966; Spector and Grant, 1970; Gupta, and Grant, 1985). Geosoft, through this module, supports geoscientists who are familiar with methodologies to acquire, process and present information for Geosciences, and who want to use the filtering module and MagMap processing Oasis Montaj to process, analyze, visualize and interpret field data Potential source.

The information was displayed in a magnetic map, showing the variation and shape of the total magnetic field (Figure 5.4). This is built by the sum of the vectors of the induced field, and the magnetization of the rocks of the geologic column, superficial as well as deep, either remnant or permanent, that are existing in the study area.

It was then necessary to place the information in its original position and distribution, as if the measurement had been taken at the magnetic north pole, where the magnetic inclination is

equal to 0,00 degrees, and the magnetic declination is also equal to 0,00 degrees (Figure 5.5). In order to do this, a magnetic model (WMM2015; NOAA, 2015) was used, utilizing an elevation of 2000 masl with a latitude of 27.25° and a longitude of -108.25°, the Magnetic Inclination and Declination of the study area. The following parameters of 54.32781° for the Magnetic Inclination, and 8.51186° for the Magnetic Declination, and a theoretical value at the coordinates of 44,491.9 Nt were used in order to correct or reduce the information to the magnetic north pole.

This process places the magnetic response (high or low) above the source, and does not take into account the distortion of the vector field that is caused by the remnant magnetization. By applying this process, we can observe that the magnetic highs are displaced to the south and slightly displaced of their actual position. The results obtained by the correction of the magnetic pole indicate the presence of high frequency events, that makes the interpretation of the continuity of structures in the area difficult. For this reason, a continuous ascendant filter of 100 m above the earth's surface was selected to remove the magnetic response of shallow sources (High Frequency Noise) and preserve the deeper and wider, magnetic sources. Also, in order to obtain the cleanest product possible, a high pass Gaussian filter (Spector and Grant, 1970) was applied to the information with the purpose of eliminating anomalies or other effects caused by very large or deep bodies, and in this way have a residual effect on the magnetic field (Figure 5.6).

5.5 RESULTS

Based on the processed and corrected information at the magnetic pole, the global magnetic effect was filtered and eliminated, in order to consider only the residual aspect of the magnetic field. Data processing was applied to allow us to emphasize the superficial behavior of the structures and the geological conditions that have a direct correlation with the location of the mineral deposits. Three processing techniques, plus the radiometry and the 3D modelling, were

used to improve the geophysical interpretation, and to help to display the structural conditions that exist within the explored area.

5.5.1 1st Vertical Derivative

This process allows us to emphasize the magnetic response of the high-frequency waves, which are subtle and narrow, caused mainly by low magnetic alignments associated with vein-shaped structures, faults or open fractures with some sort of alteration and/or porosity (Verduzco et al, 2004). This procedure is showing the main structural behavior orientated northwest to southeast, some north-south orientation, also northeast to southwest, and less from east to west. Some circular and semicircular structures are particularly evident, which have been affected by other regional alignments, and can be considered calderas (Figure 5.7).

5.5.2 Analytical Signature

This process analyzes the information by breaking the longitudes of waves in the derivatives, dx, dy, and dz, and considers the extreme magnetic values, either low or high (Roest et al, 1992). The purpose is to locate the possible sources of hydrothermal fluids associated with the economic mineralization. In the study area, those sources are found within circular structures and at the southeaster edge of a main circular structure, starting near Temoris at the southwestern portion, and projecting to the north to conform the veins at the Guazaparez area (Figure 5.8).

5.5.3 Correction of Magnetic Inclination

This is a process of improvement of the superficial signal to amplify and highlight the alignment of the structural trends, which have a very subtle display otherwise (Verduzco et al, 2004). These lineaments can help us to identify the rhyolitic volcanic domes and dikes (Roest et al, 1992) that either outcrop on the surface or remain buried (Figure 5.9).

5.5.4 Radiometry

The radiometric data collected in the 2015 Helimag survey and the information of potassium, thorium and total gamma ray count, supports the magnetometry interpretation.

Analyzing the radiometric information for Potassium, no external anomalies were found and the detected levels of radiation are interpreted as derived from the minerals (K-feldspars) contained in the rocks. Considering that, four distinct domains associated to main lithologic units were traced within the following values of intensity: 1.- Values over 4%, related to diorite or dacitic porphyry. 2.- Values between 2.5 and 4 %, related to granitic intrusions. 3.- Values between 1.75 and 2.5 %, related to extrusive volcanic rocks. 4.- Values below 1.7%, related to sedimentary or metamorphic rocks (Figure 5.10). The radiometric signature of Thorium (Figure 5.11) and total gamma count, support the radiometric domains shown by the Potassium, and both maps shows a circular behavior, which is interpreted in this research as a Caldera (Figure 5.12).

5.5.4 3D Modelling

A 3D modeling exercise was done to support the interpretations, and have a better understanding of the structural behavior. The 3D model is composed of a sequence of magnetic maps at different depths, which serve to analyze the behavior of the bodies and alignments that they follow (MacLeod et al, 1993). The next step was to build vertical sections or profiles to observe the vertical behavior of the structures. These were designed in a radial pattern from the center of the main circular structure (Figure 5.14), in an attempt to perpendicularly cut the outer limits of this feature that can be considered a caldera. In those radial sections an abrupt change in the magnetic behavior is very noticeable (Figures 5.15 to 5.22), from the 0.0 masl elevation, and deepening towards the west, in which we can postulate the location of the Magnetic Basement, that underlies the Sierra Madre Occidental Province.

5.6 CONCLUSIONS

The interpretation of the high resolution magnetic data, along with HR magnetics, radiometry and satellite imagery, lead to the conclusion that the HRM methodology is suitable for large scale exploration approaches, > 500 square kilometers, rather than a mine scale. The most important finding of this research is the identification of the mineralization controls at regional scale (Figure 5.13). It is also important to mention that the radiometric information of potassium (Figure 5.10), thorium (Figure 5.11), and the total gamma rays count (Figure 5.12), contributed to outline the main structures interpreted with the magnetic survey, and it was especially useful to delimitate the structures at the Guazaparez and to locate the border of the Temoris Caldera (Figure 5.23). The outlining of circular structures pointed towards the conclusion of a caldera development, with at least two resurgence stages, as the heat source for the hydrothermal mineralization. The structural controls of mineralization are either at the outer rim of the caldera (e.g. Picachos, Temoris, Millonaria, San Lorenzo), or inter-caldera extensional tectonics associated to a pull-apart regime oriented NW-SE; either between the outer and the resurgent rim, like the Guazaparez, or between the resurgent rim and the central resurgent dome, like the Palmarejo District. The resurgent rhyolitic domes (responsible for the mineralization) are either located at the rim, such as Picachos, (Figure 5.23), or internally, such the domes within the Guazaparez and Palmarejo Districts. The presented approach, constitutes an invaluable tool for the exploration targeting on large areas, and helps to explain the genesis of the epithermal mineralization in this area.

5.7 ACKNOWLEDGEMENTS

This study is the result of a scientific collaboration between Castulo Molina and Mario Vizcarra. We wish to thank Coeur Mining management for the permission to use the HR magnetic data, essential in generating this report.

Figures Chapter 5

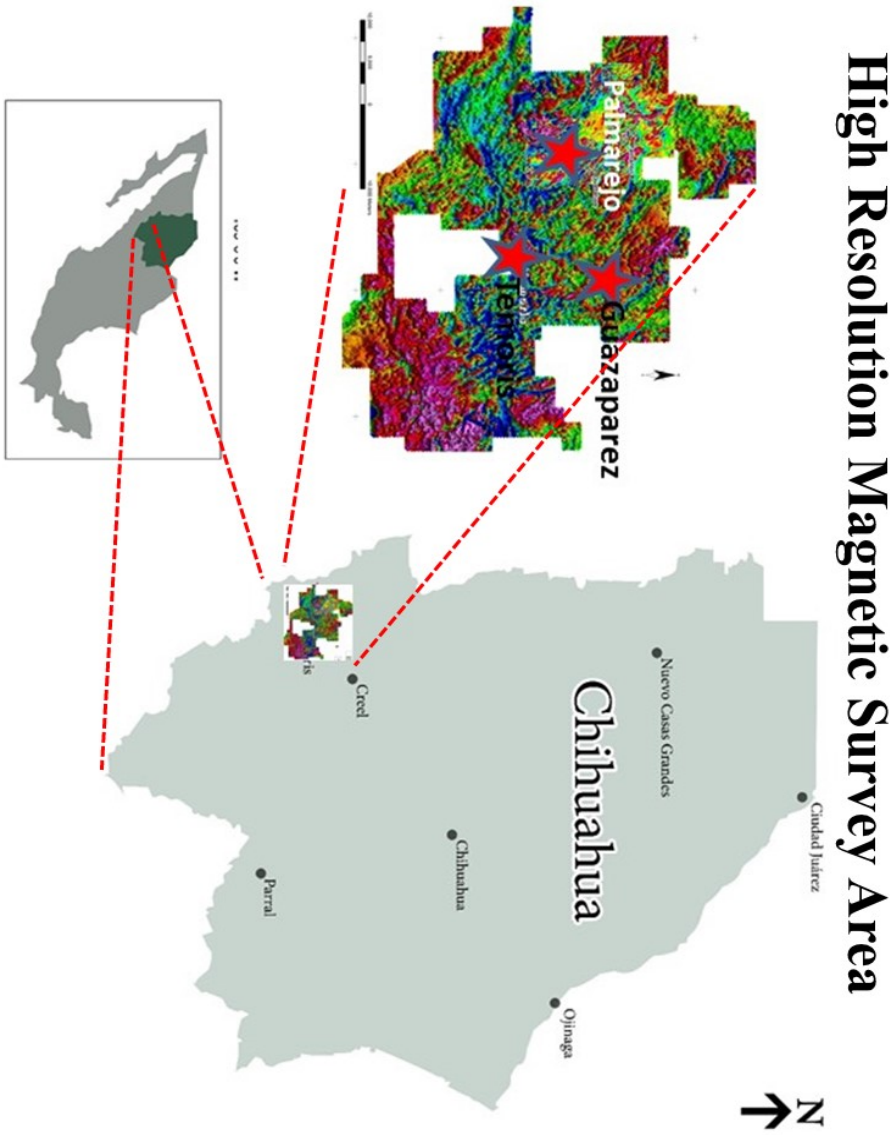

Figure 5.1 Location map, showing the Helimag survey, covering 1624 square kilometers over the Chínipas, Guazaparez and Urique counties, in the southwestern portion of the state of Chihuahua, México.

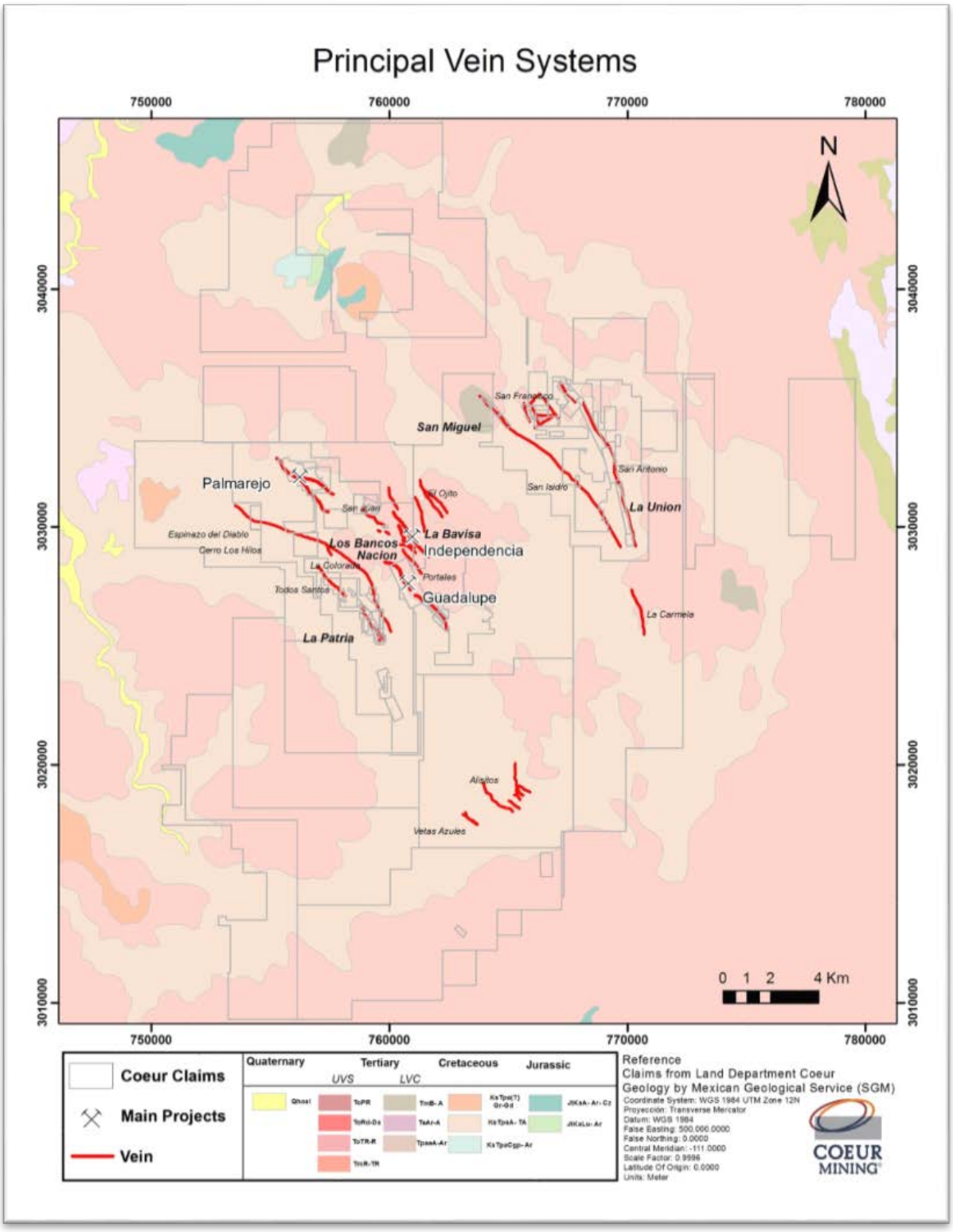

Figure 5.2 Geologic map showing the main veins systems, and mineral claims within the study area.

Figure 5.3 Aeromagnetic survey. Upper photo is showing helicopter collecting high resolution magnetic data over the Palmarejo mine complex in 2012. The lower is the takeoff of the Bell 206L3, from the Temoris airstrip, during the Helimag survey in 2015.

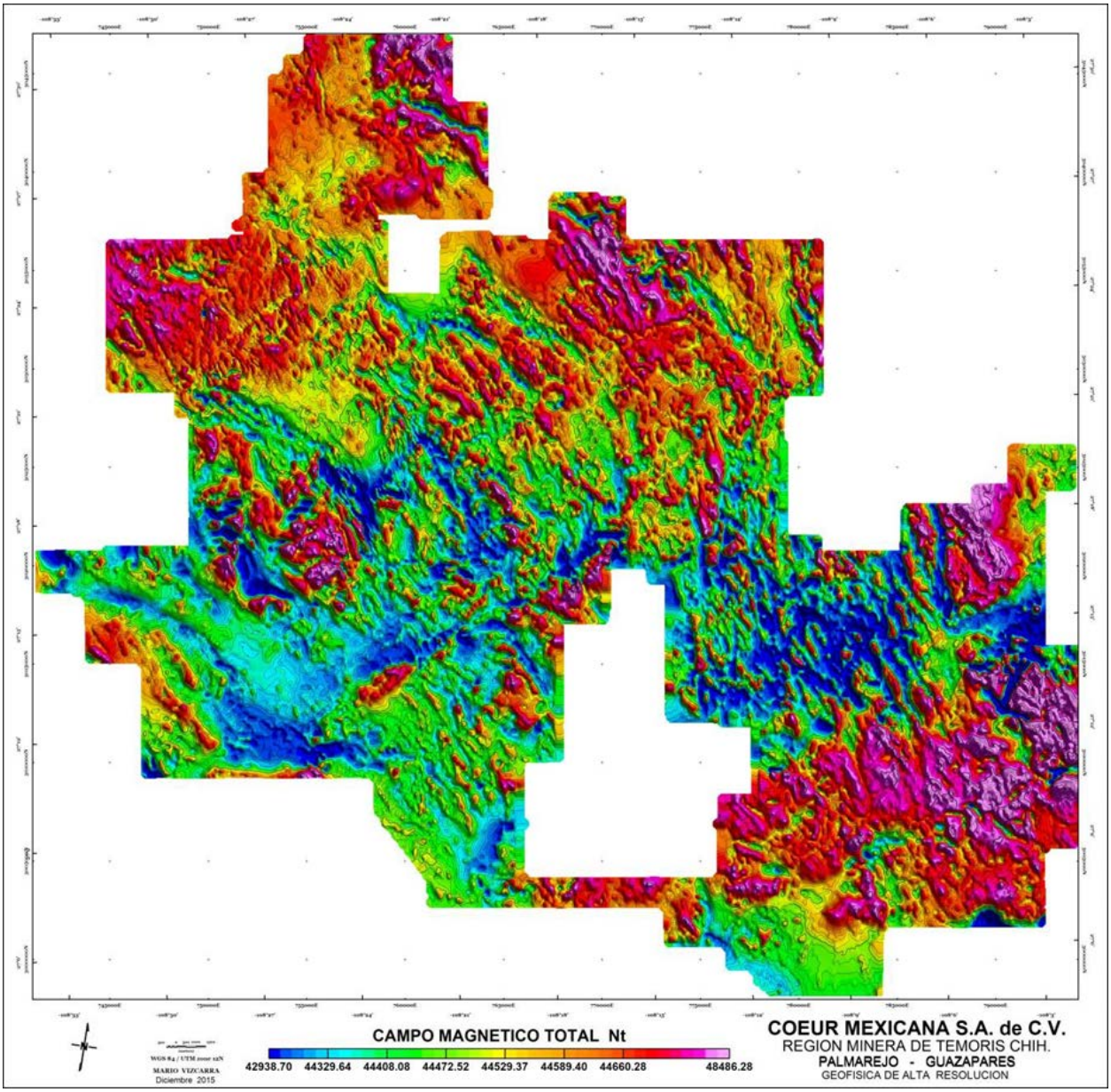

Figure 5.4 Total magnetic field map, showing the sum of the vectors of the induced field and the magnetization of the rocks.

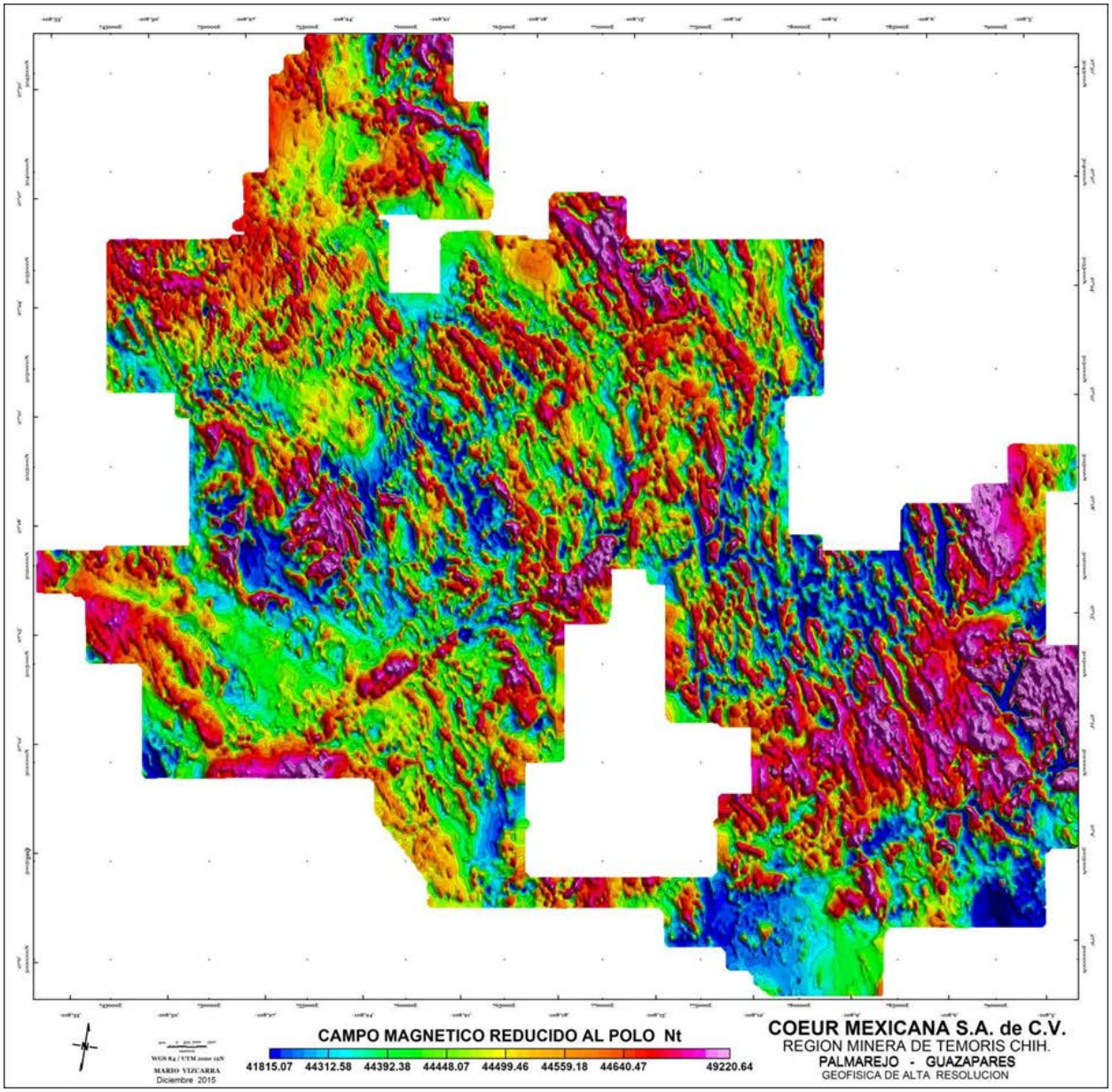

Figure 5.5 Map showing the magnetic field reduced to the north pole, by placing the information in its original position and distribution, as if the measurement had been taken at the magnetic north pole, where the magnetic inclination is equal to 0,00 degrees, and the magnetic declination is also equal to 0,00 degrees.

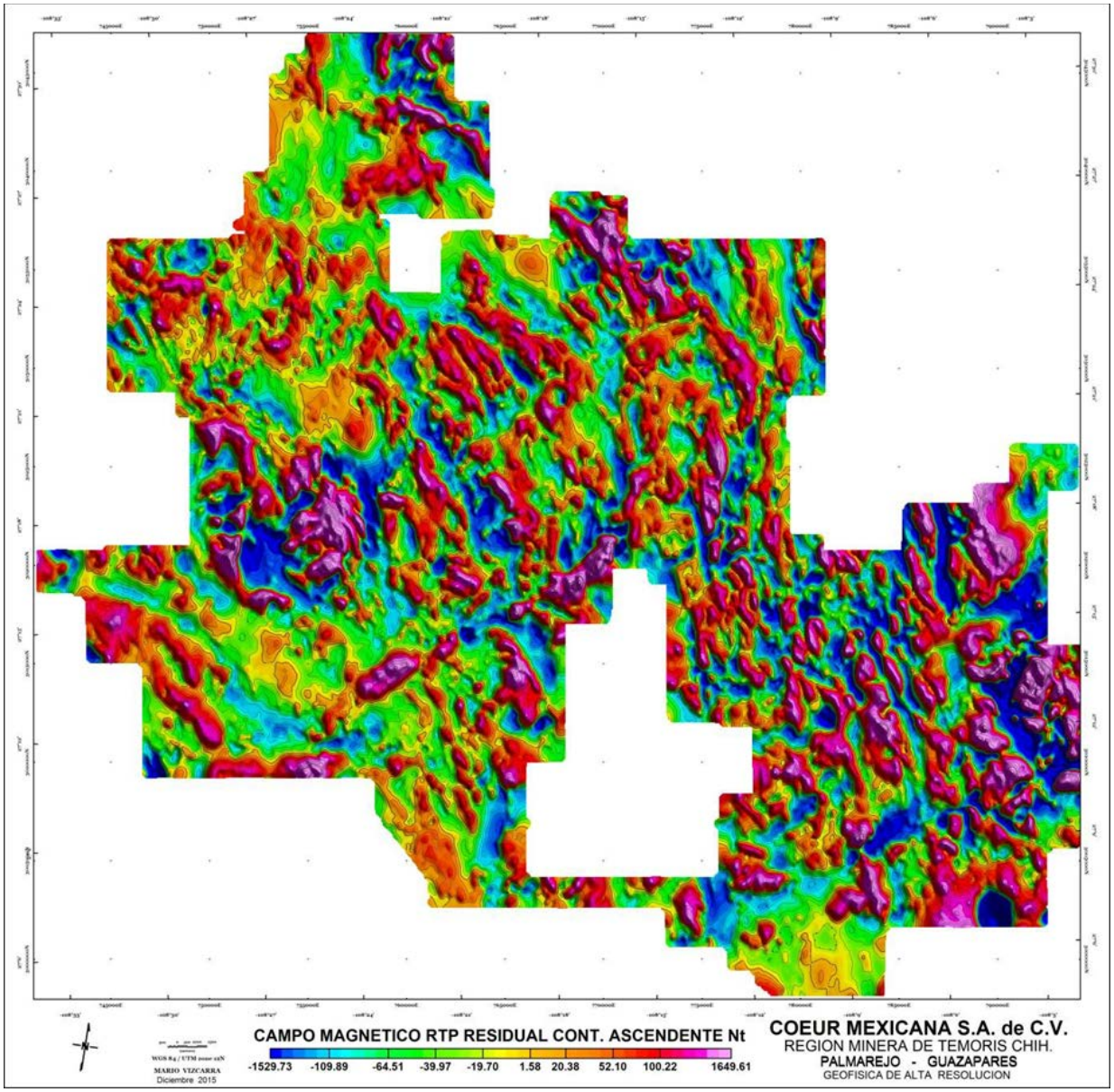

Figure 5.6 Map of the residual magnetic field reduced to the pole and a continuous ascendant filter of 100 m above the surface applied.

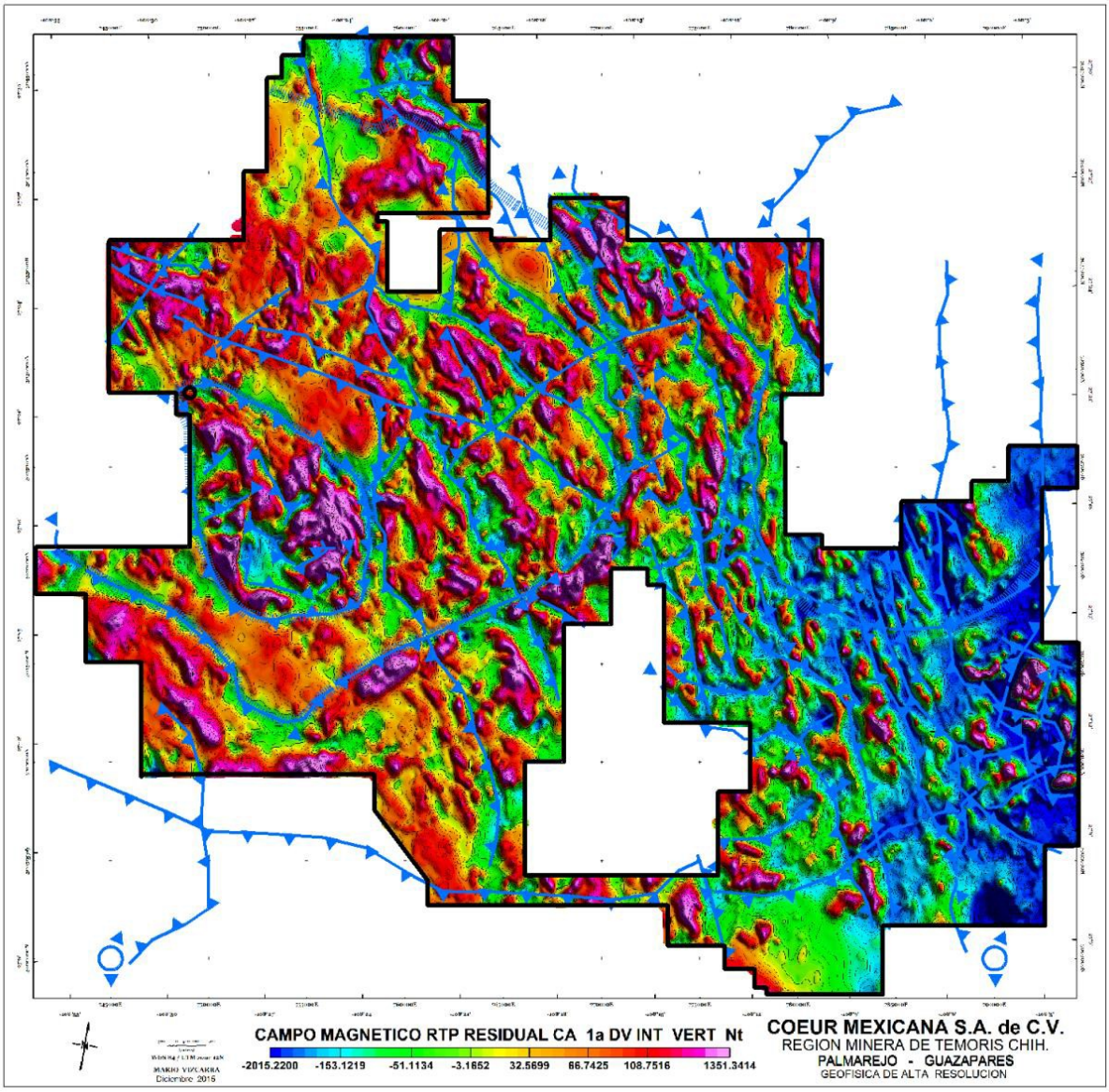

Figure 5.7 1st Vertical Derivative Map, showing the main structural behavior orientated northwest to southeast, some north-south orientation, also northeast to southwest, and less from east to west. Some circular and semicircular structures are particularly evident, which have been affected by other regional alignments, and can be considered calderas.

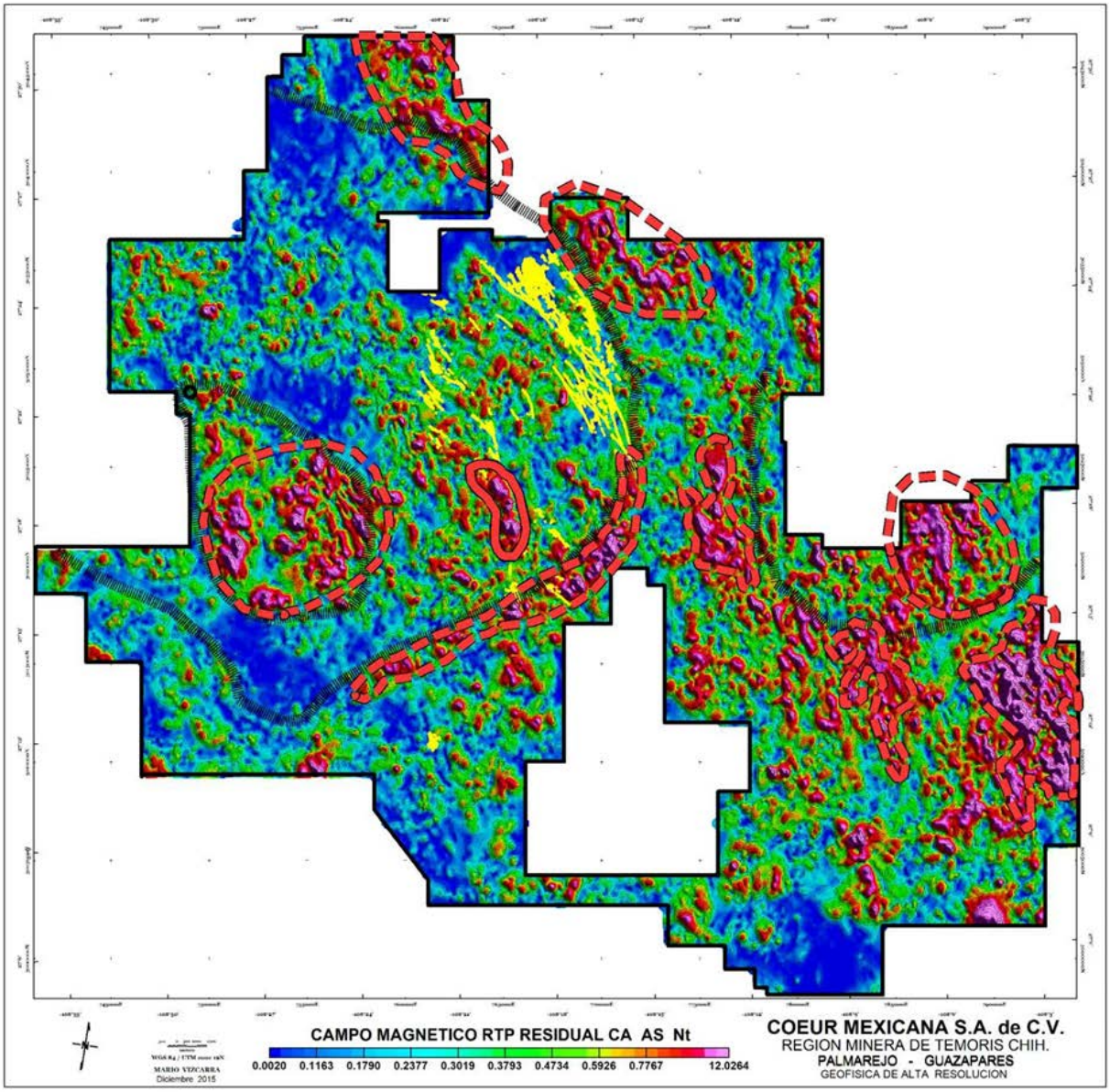

Figure 5.8 Analytical Signature Map, showing the possible sources of hydrothermal fluids associated with the economic mineralization. In the study area, those sources are found within circular structures and at the southeaster edge of a main circular structure, starting near Temoris at the southwestern portion, and projecting to the north to conform the veins at the Guazaparez area.

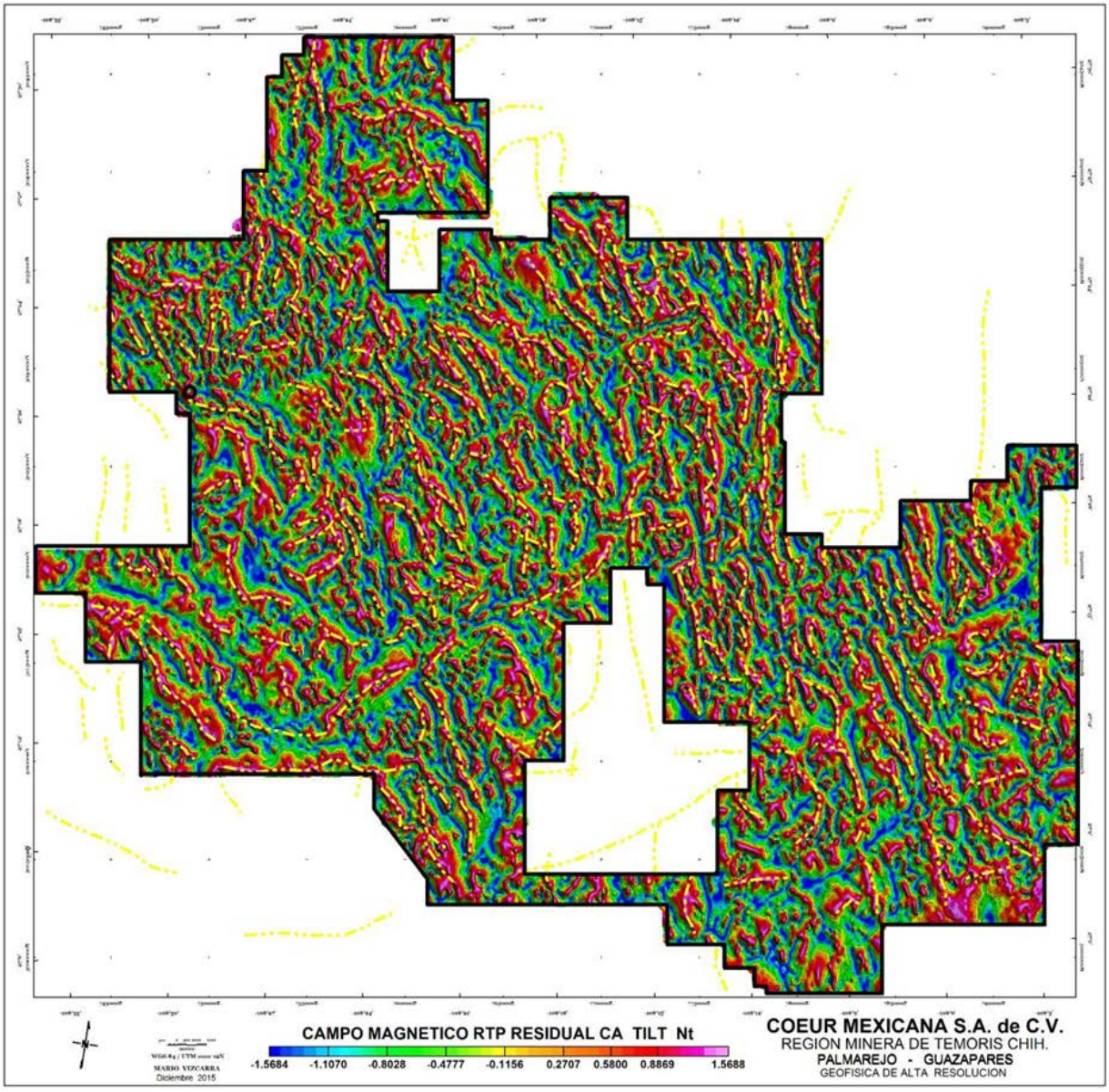

Figure 5.9 Interpreted magnetic inclination map. This interpretation is enhancing the alignment of the structural trends, which otherwise have a very subtle display (Verduzco et al, 2004). These lineaments can help us to identify the rhyolitic volcanic domes and dikes (Roest et al, 1992) that either outcrop on the surface or remain buried.

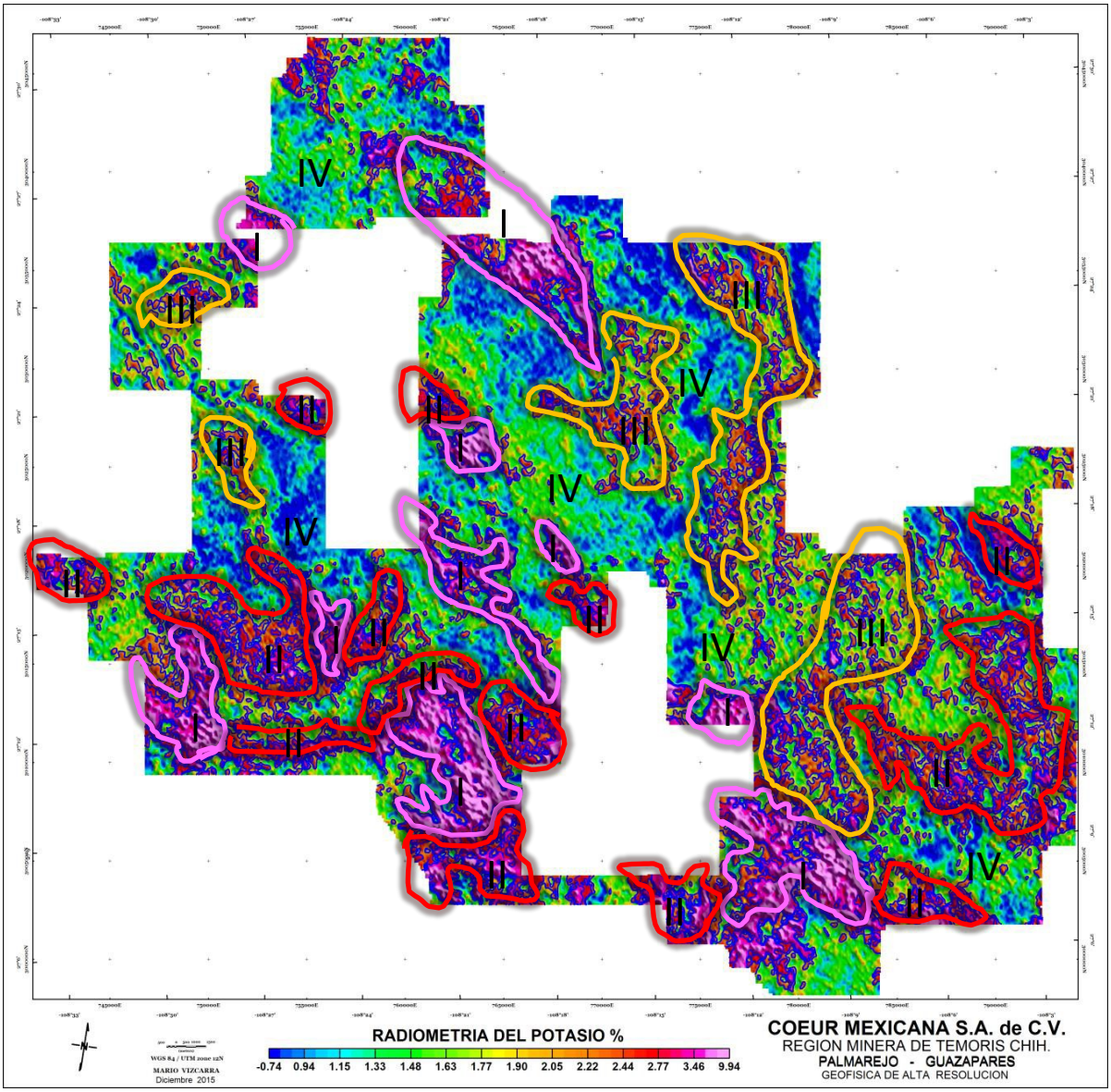

Figure 5.10 Thematic map of Potassium, showing the distinct domains associated to main lithologic units: I.- Values over 4%, related to diorite or dacitic porphyry. II.- Values between 2.5 and 4 %, related to granitic intrusions. III.- Values between 1.75 and 2.5 %, related to extrusive volcanic rocks. IV.- Values below 1.7%, related to sedimentary or metamorphic rocks.

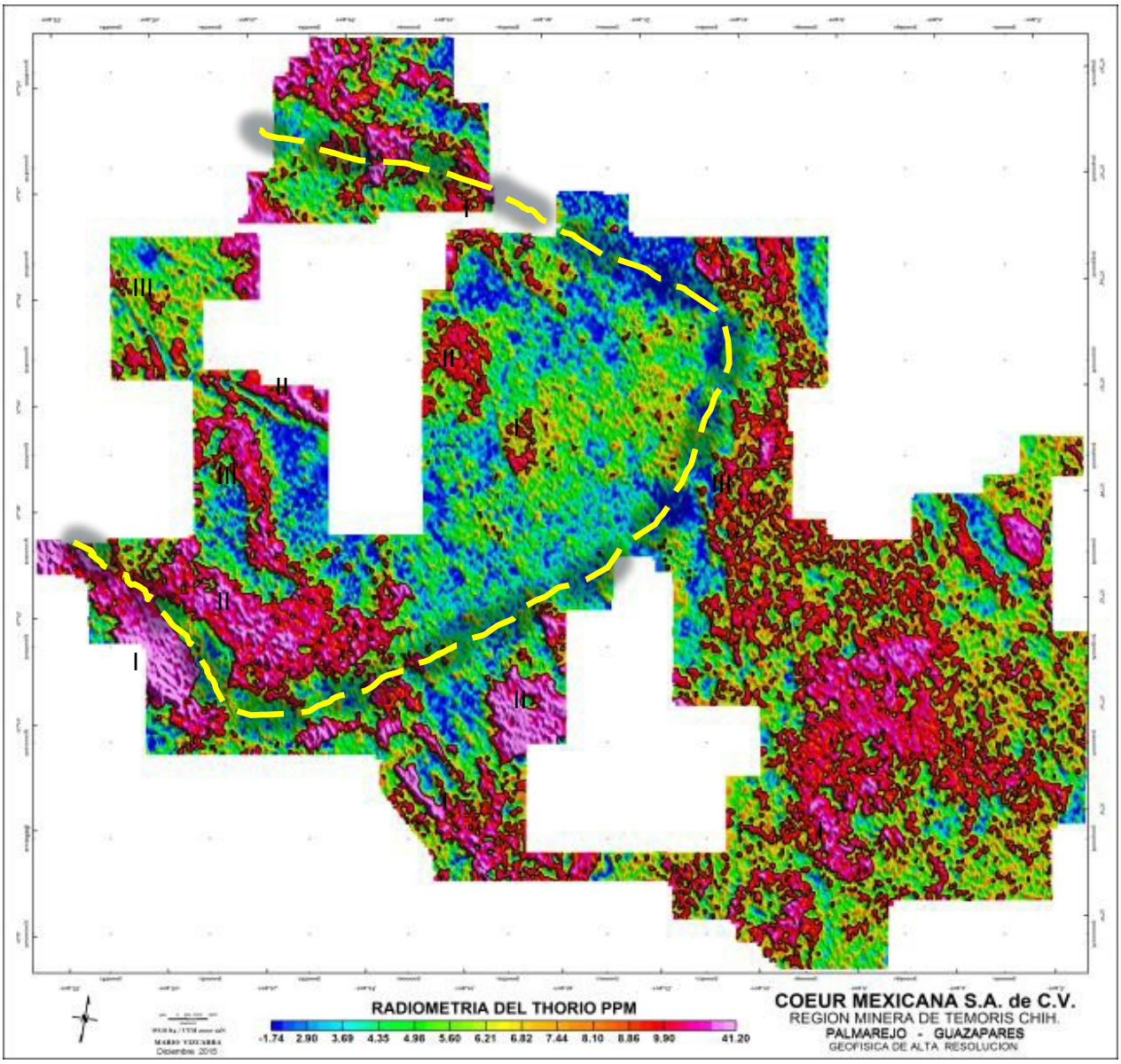

Figure 5.11 Thematic map of Thorium, showing the distinct domains associated to main lithologic units: I.- Values over 30%, related to diorite or dacitic porphyry. II.- Values between 8 and 30%, related to granitic intrusions. III.- Values between 5 and 8 %, related to extrusive volcanic rocks. IV.- Values below 5%, related to sedimentary or metamorphic rocks, and also showing the proposed rim of the Caldera.

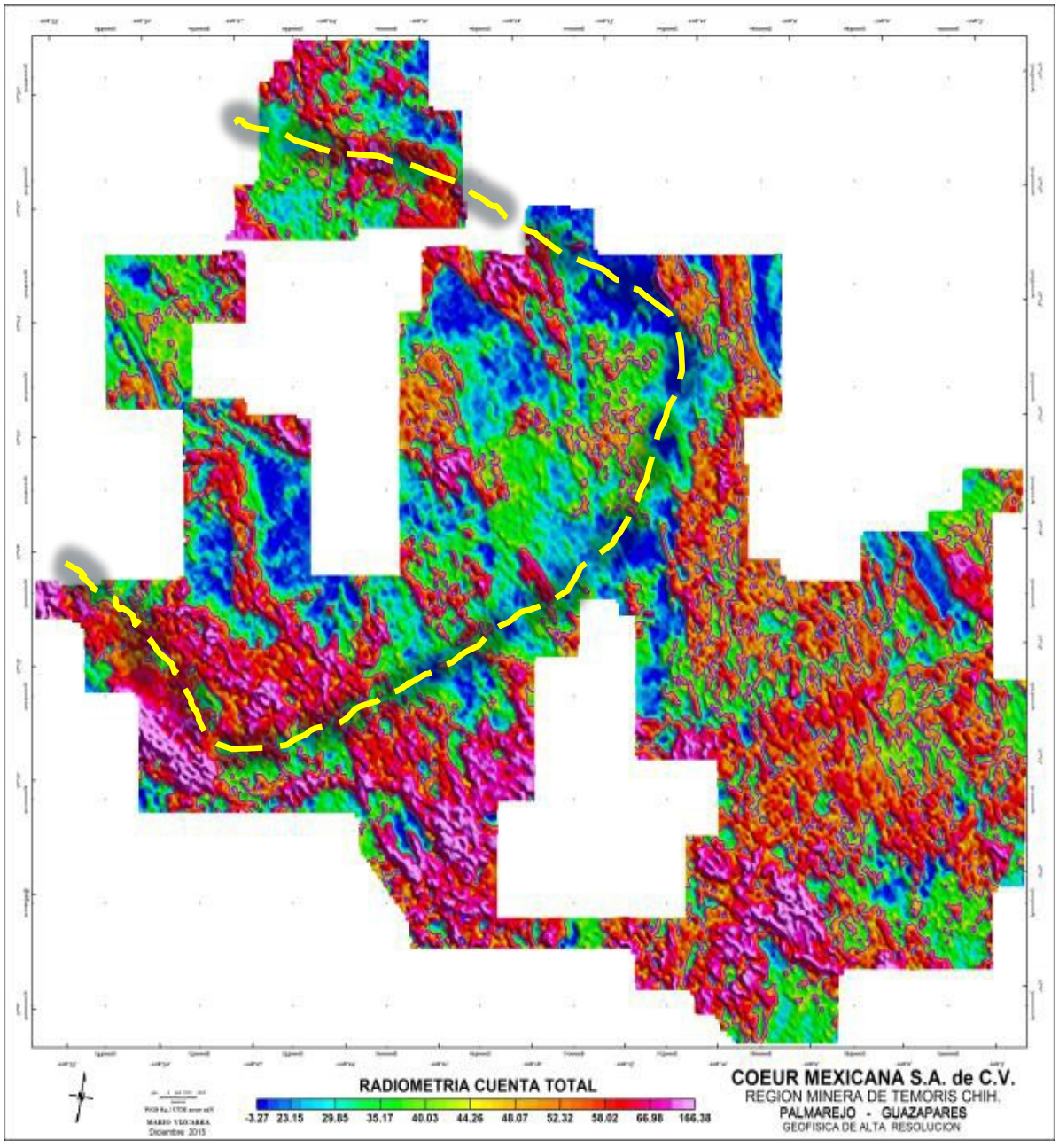

Figure 5.12 Total Gamma Count map, also showing the circular behavior of the data, which is interpreted as the rim of the Temoris Caldera.

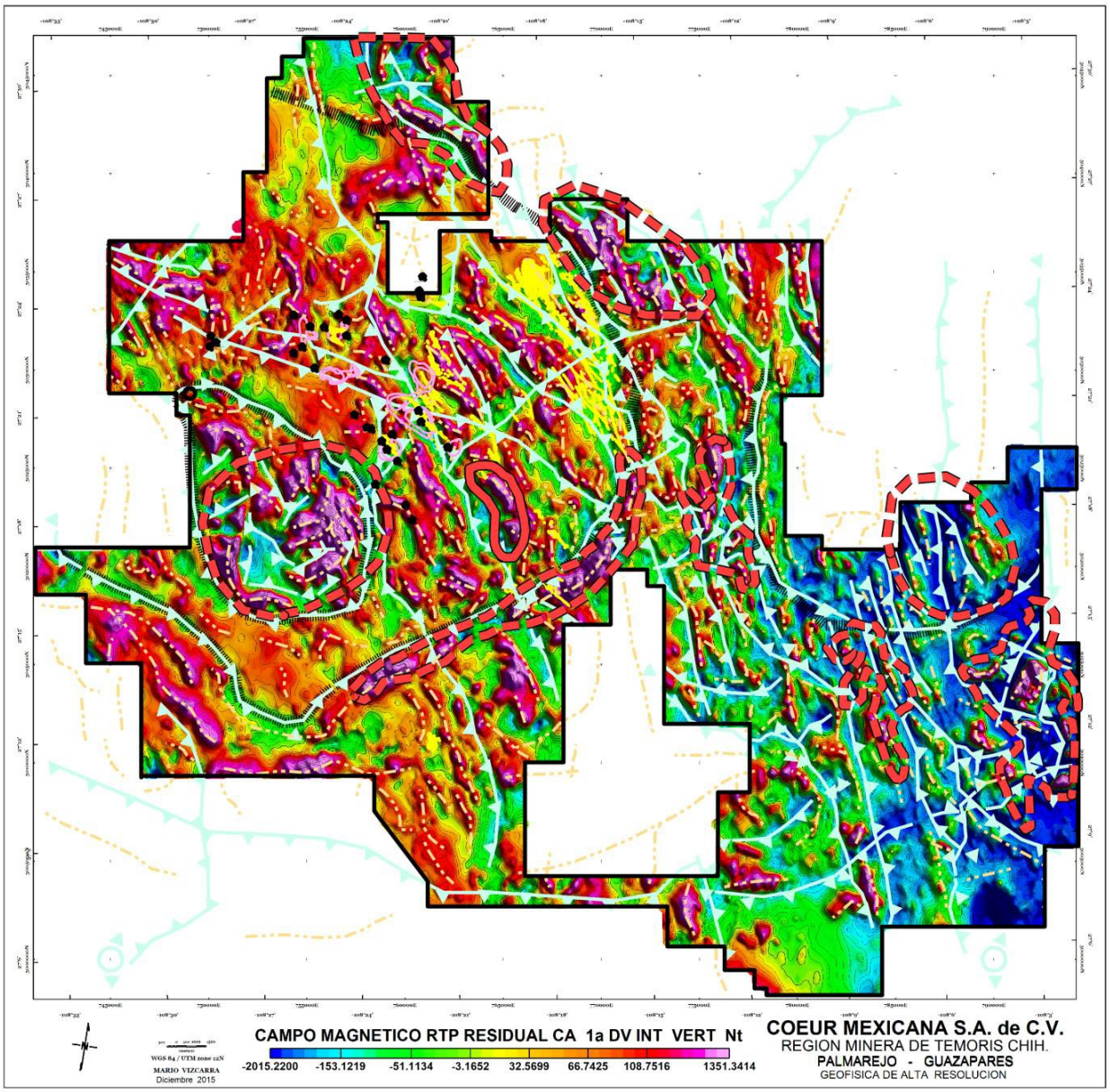

Figure 5.13 Interpretation Map, showing the interpreted faults and fractures in blue lines with triangles, the magnetic lineaments are in two-dotted light-brown lines, whereas the magnetic signatures interpreted as possible source of hydrothermal solutions are marked with thick, dotted red lines. All the above are controlling the epithermal mineralization hosted in veins, shown in yellow lines, within the proposed Temoris Caldera.

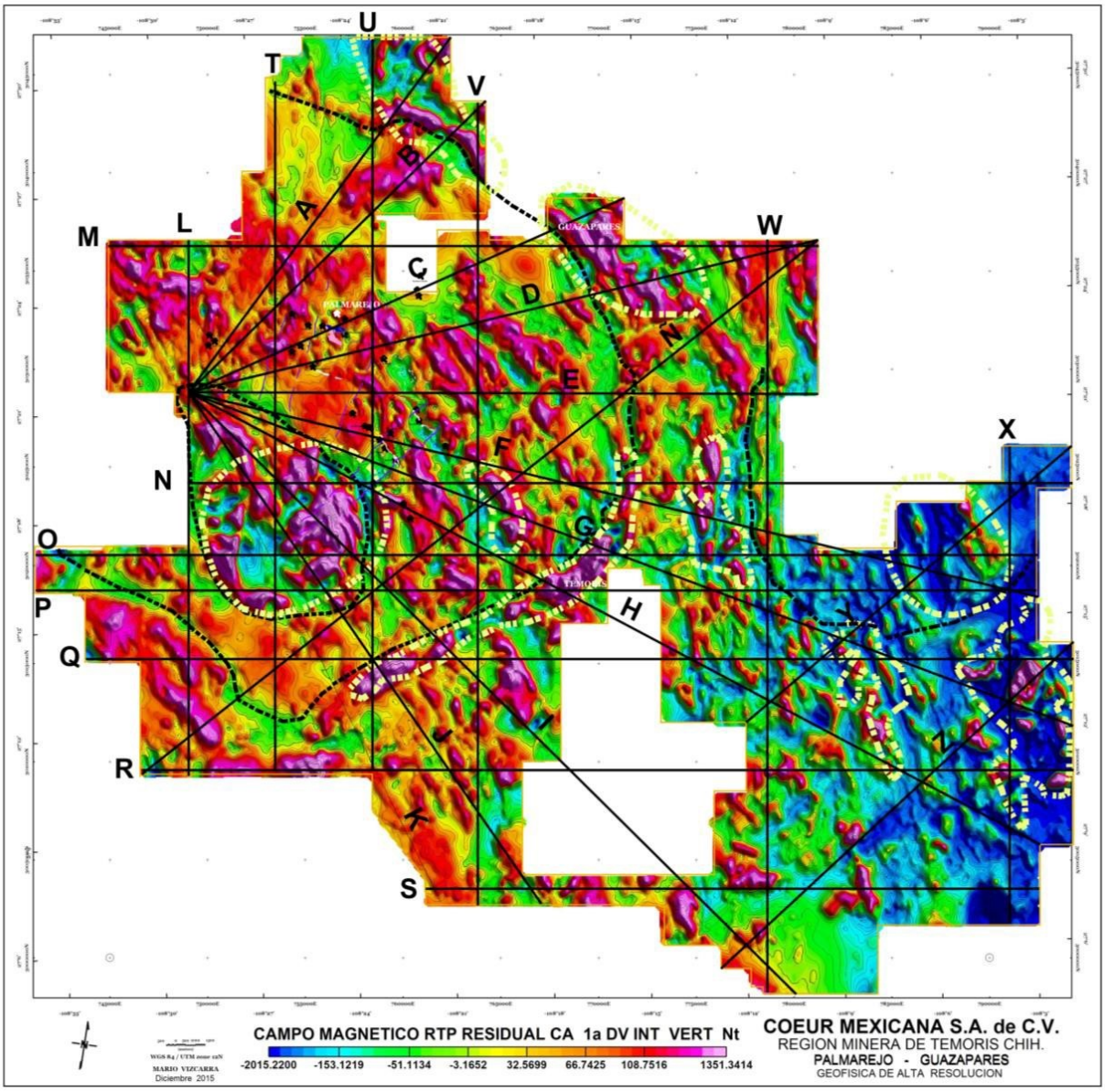

Figure 5.14 Map showing the location of the cross sections generated from the 3D Model, in order to determine the vertical behavior of the structures. Some were designed in a radial pattern form the center of the main circular structure and are labeled from section A to section Z.

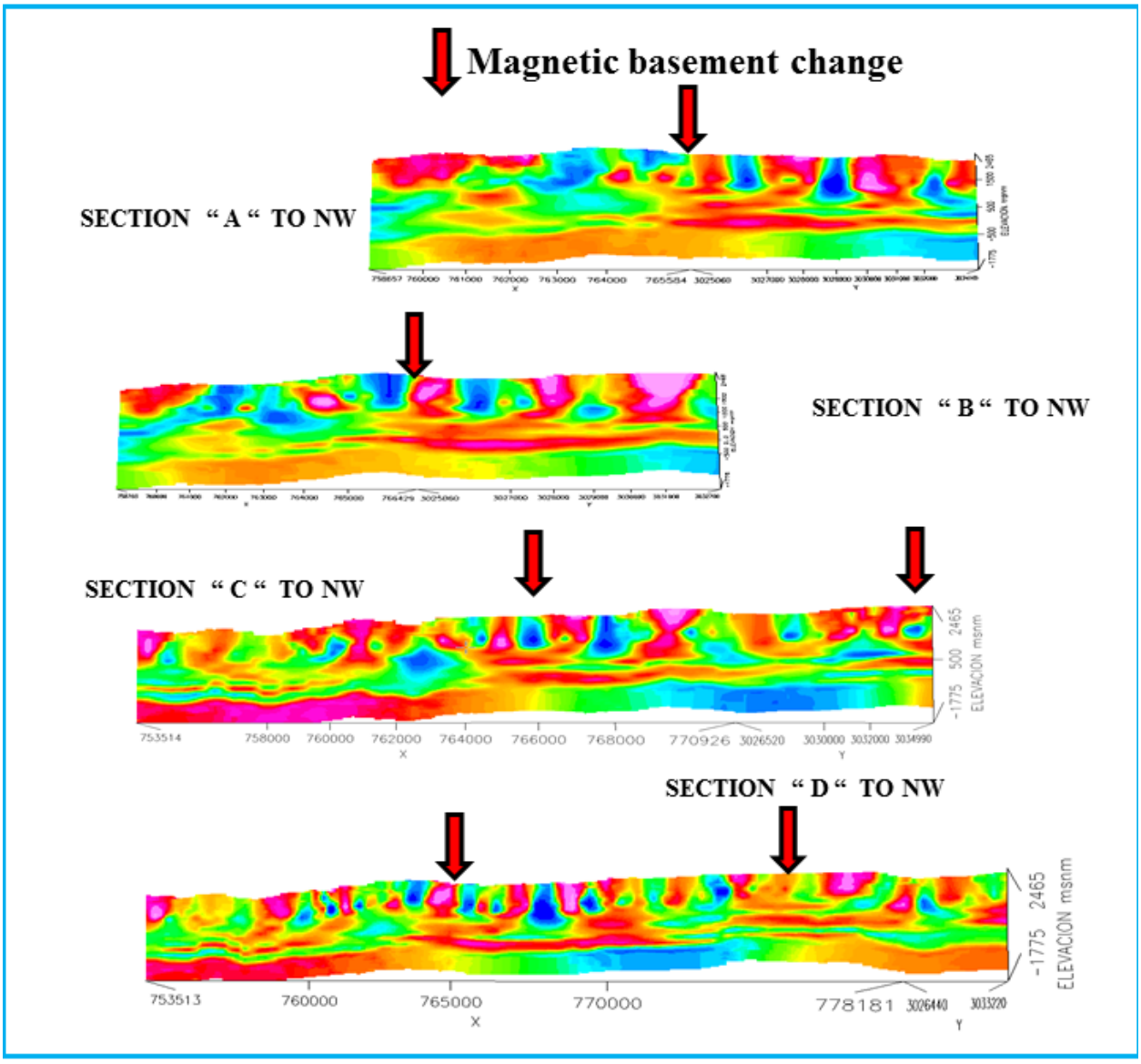

Figure 5.15 Radial sections A to D from the 3D Model, located in the northern portion of the study area. Red arrows indicate changes in the magnetic basement, which can be interpreted as rim-type caldera boundary.

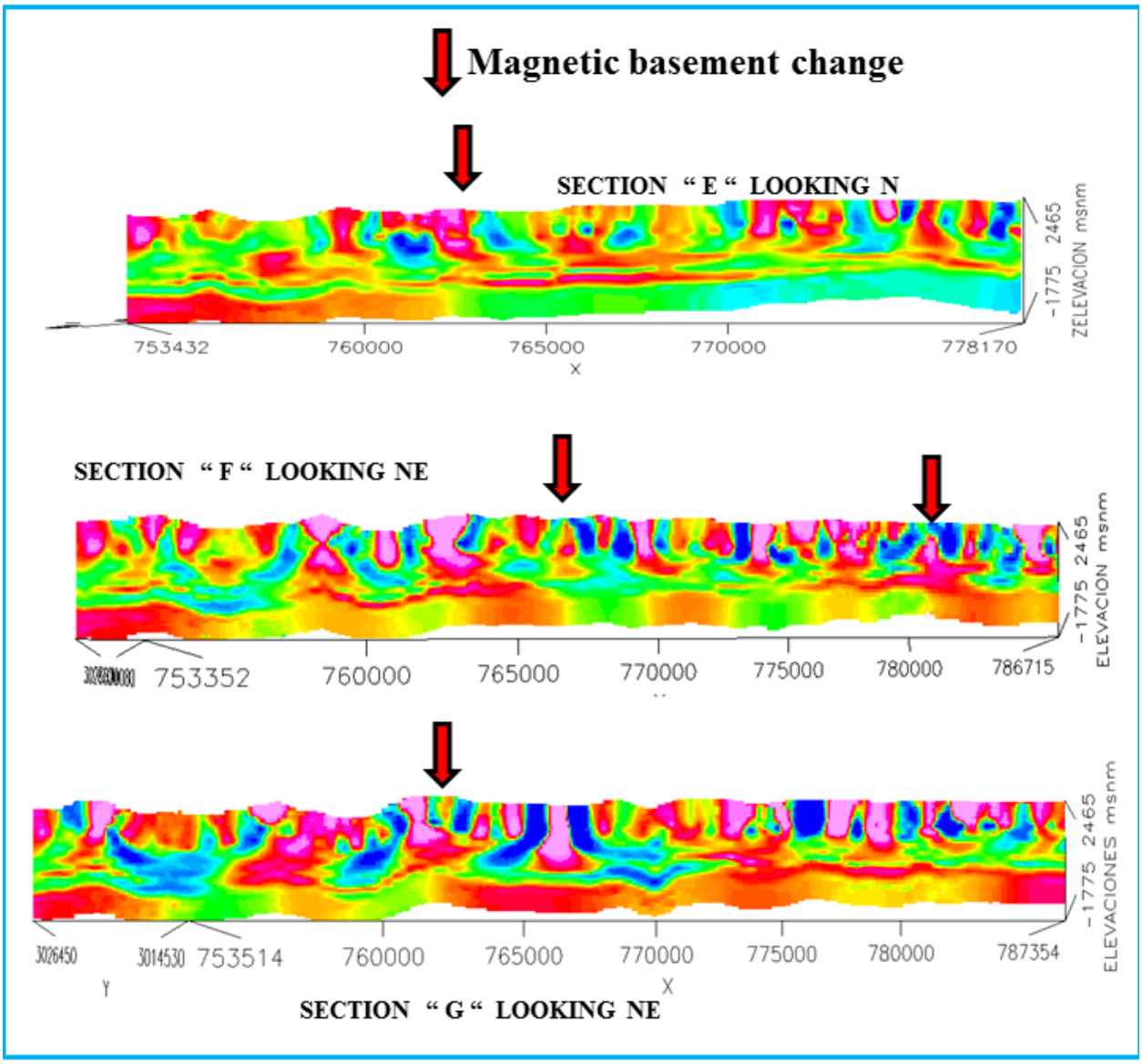

Figure 5.16 Radial sections E to G from the 3D Model, located in the central portion of the study area. Red arrows indicate changes in the magnetic basement, which can be interpreted as rim-type caldera boundary.

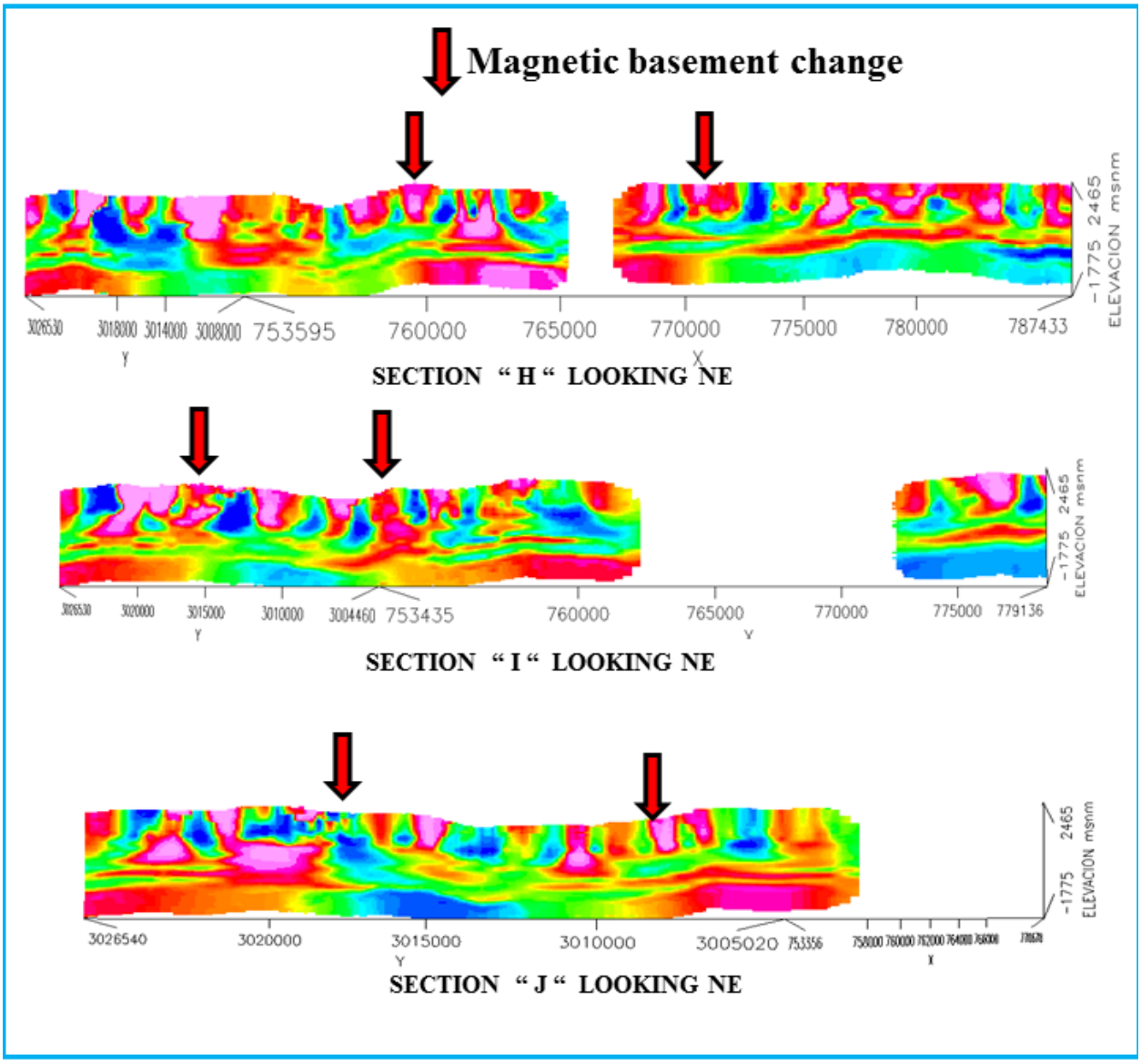

Figure 5.17 Radial sections H to J from the 3D Model, located in the southern portion of the study area. Red arrows indicate changes in the magnetic basement, which can be interpreted as rim-type caldera boundary.

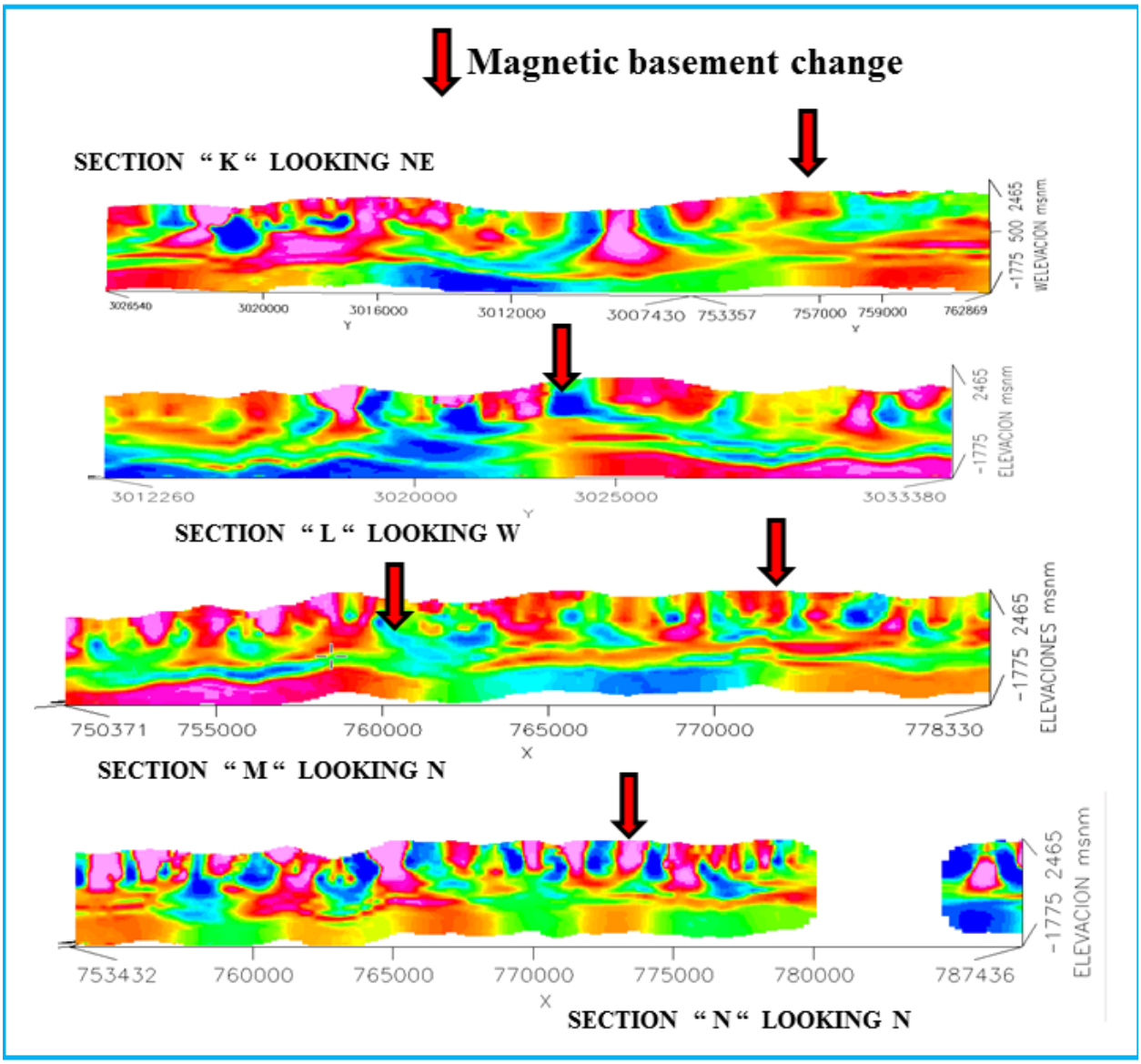

Figure 5.18 Radial sections K to N from the 3D Model, on different locations and orientation. Red arrows indicate changes in the magnetic basement, which can be interpreted as rim-type caldera boundary.

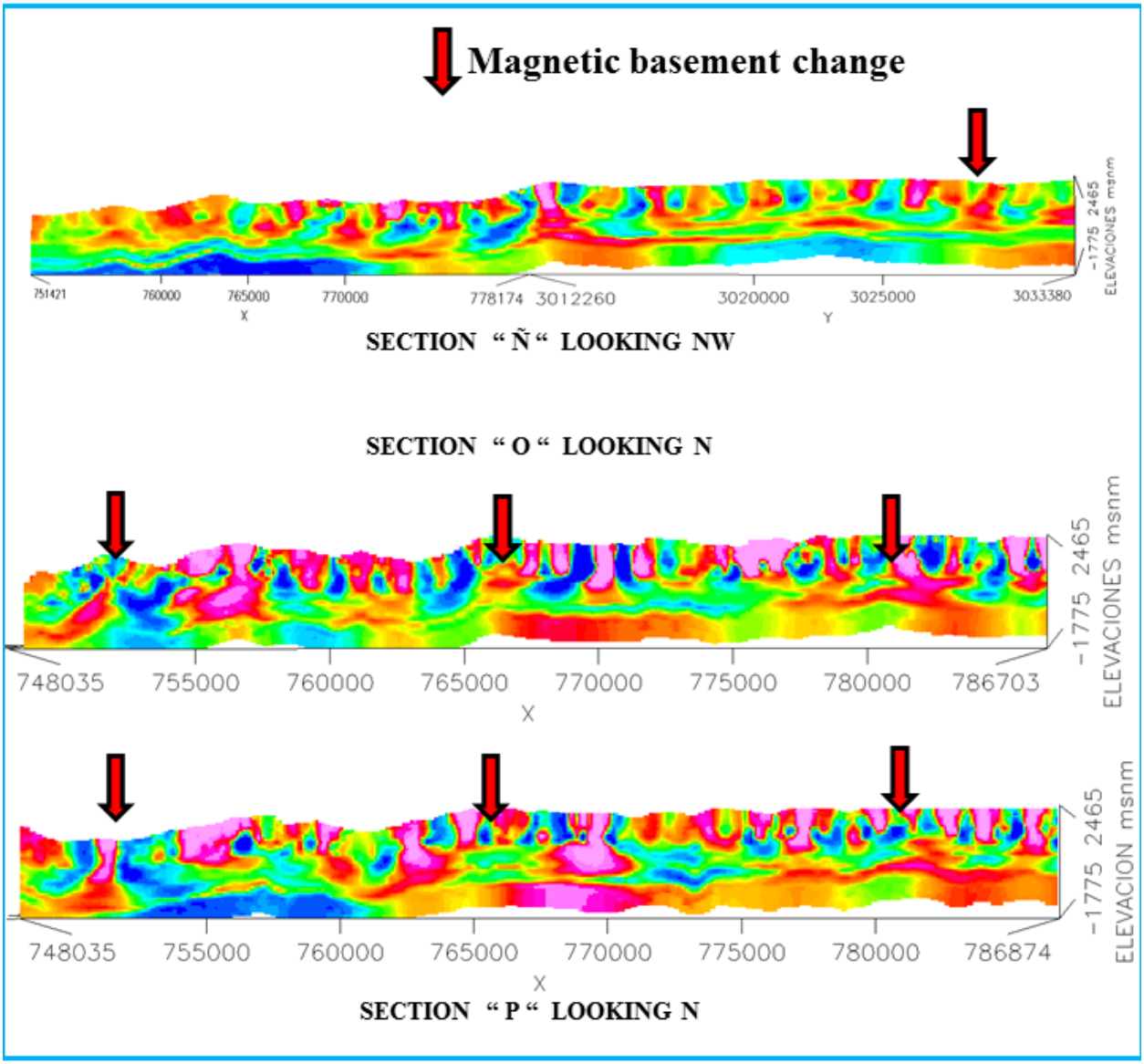

Figure 5.19 Cross sections Ñ to P from the 3D Model, on different locations and orientations. Red arrows indicate changes in the magnetic basement, which can be interpreted as rim-type caldera boundary.

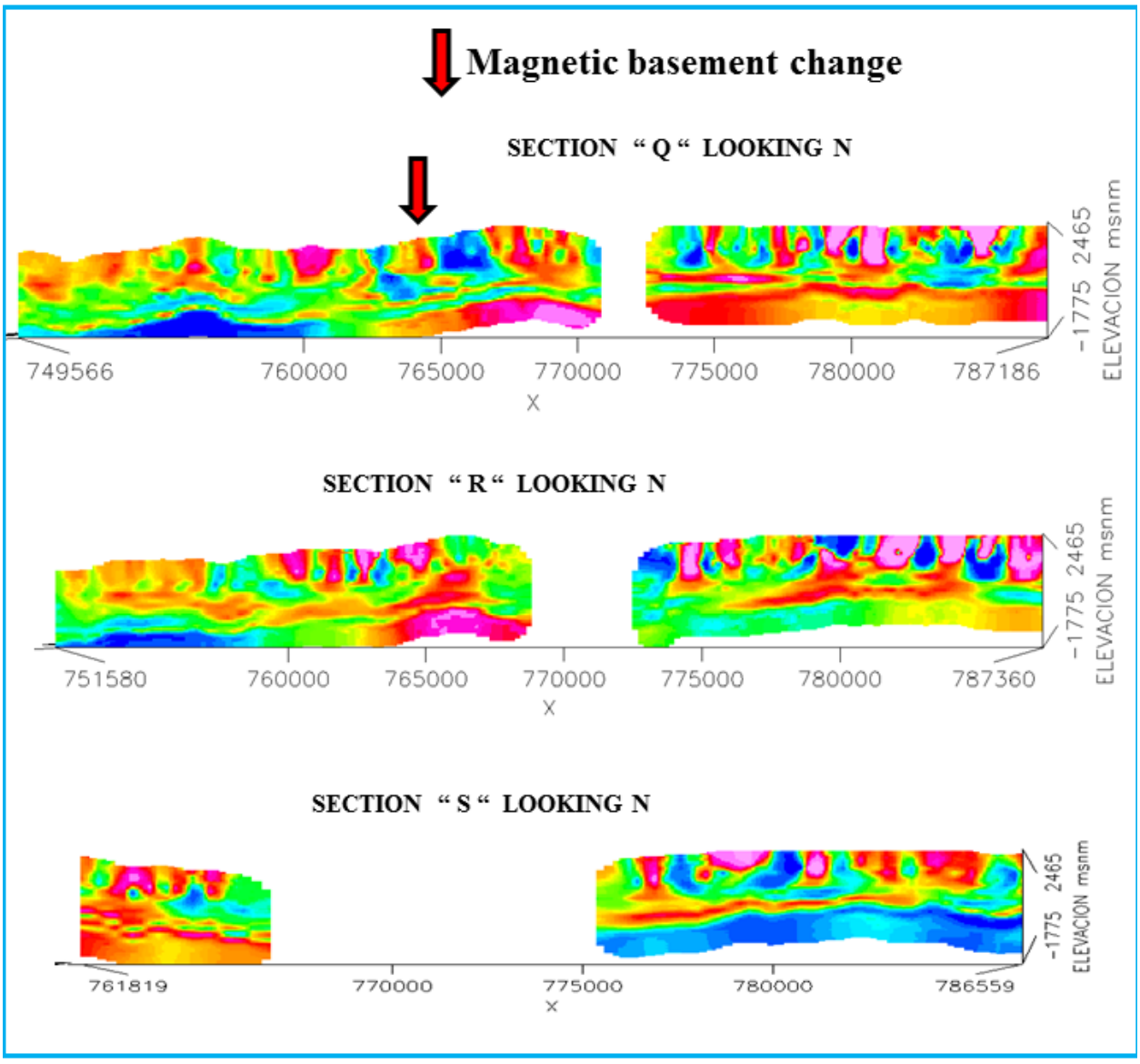

Figure 5.20 Cross sections Q to S from the 3D Model, located on the southern portion, all oriented west-east, and facing to the north. Red arrows indicate changes in the magnetic basement, which can be interpreted as rim-type caldera boundary.

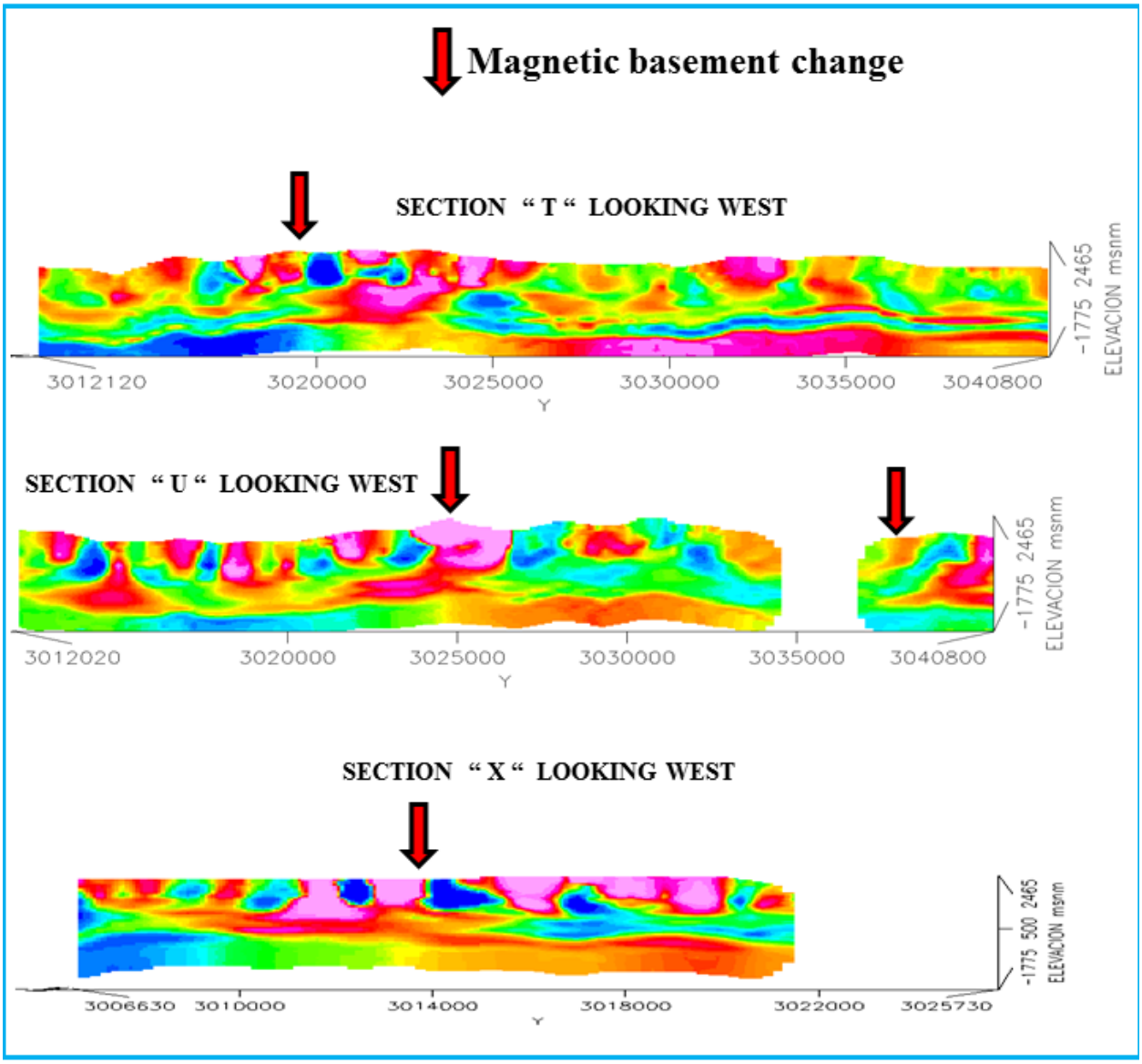

Figure 5.21 Cross sections T, U, and X, from the 3D Model, located on the western and eastern of the study area. The three sections are oriented north-south, and facing to the west. Red arrows indicate changes in the magnetic basement, which can be interpreted as rim-type caldera boundary.

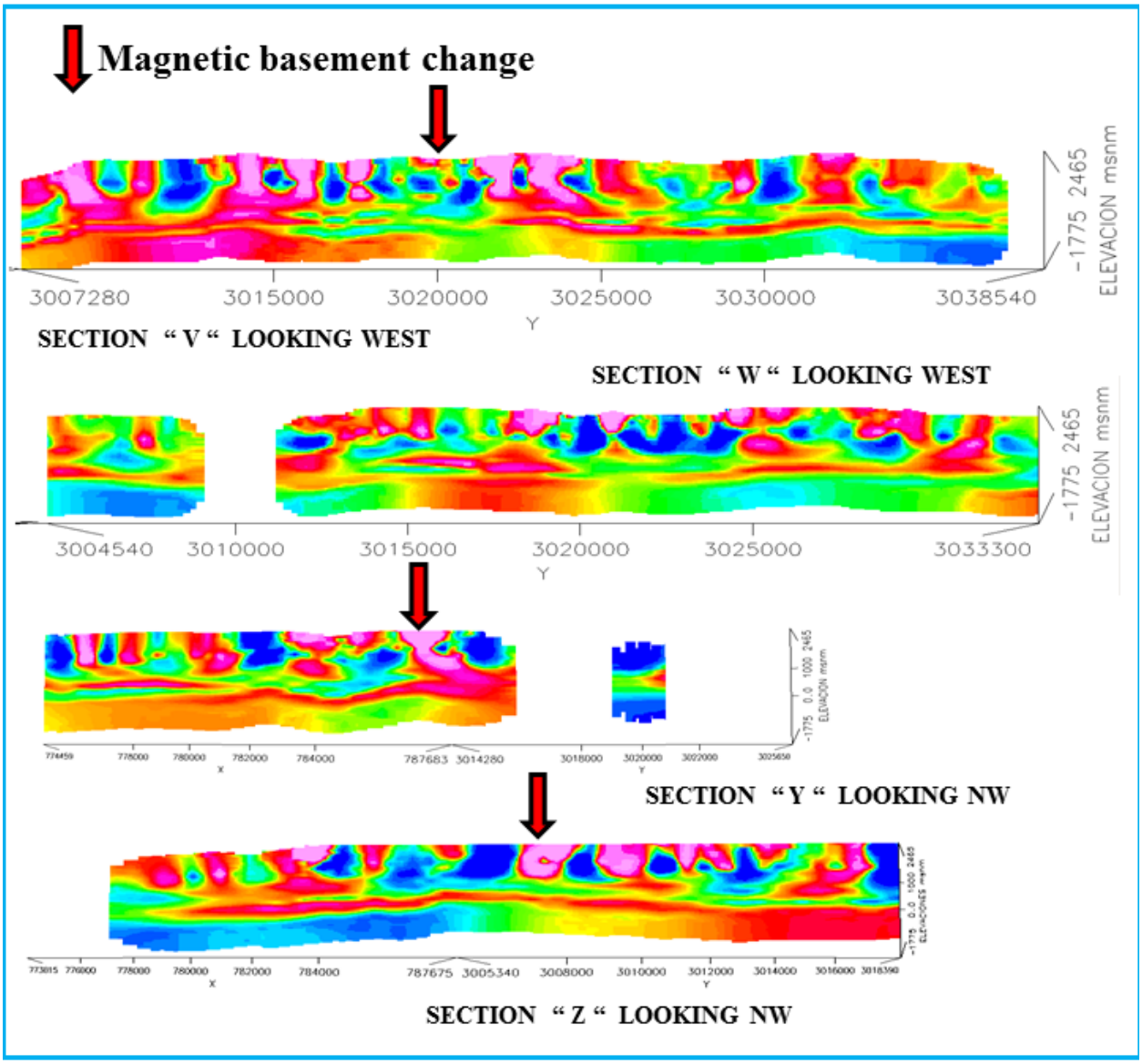

Figure 5.22 Cross sections V, W, Y and Z, from the 3D Model, located on the central and eastern portion of the study area. The first two sections are oriented north-south, and facing to the west. The last are oriented northeast and facing to the northwest. Red arrows indicate changes in the magnetic basement, which can be interpreted as rim-type caldera boundary.

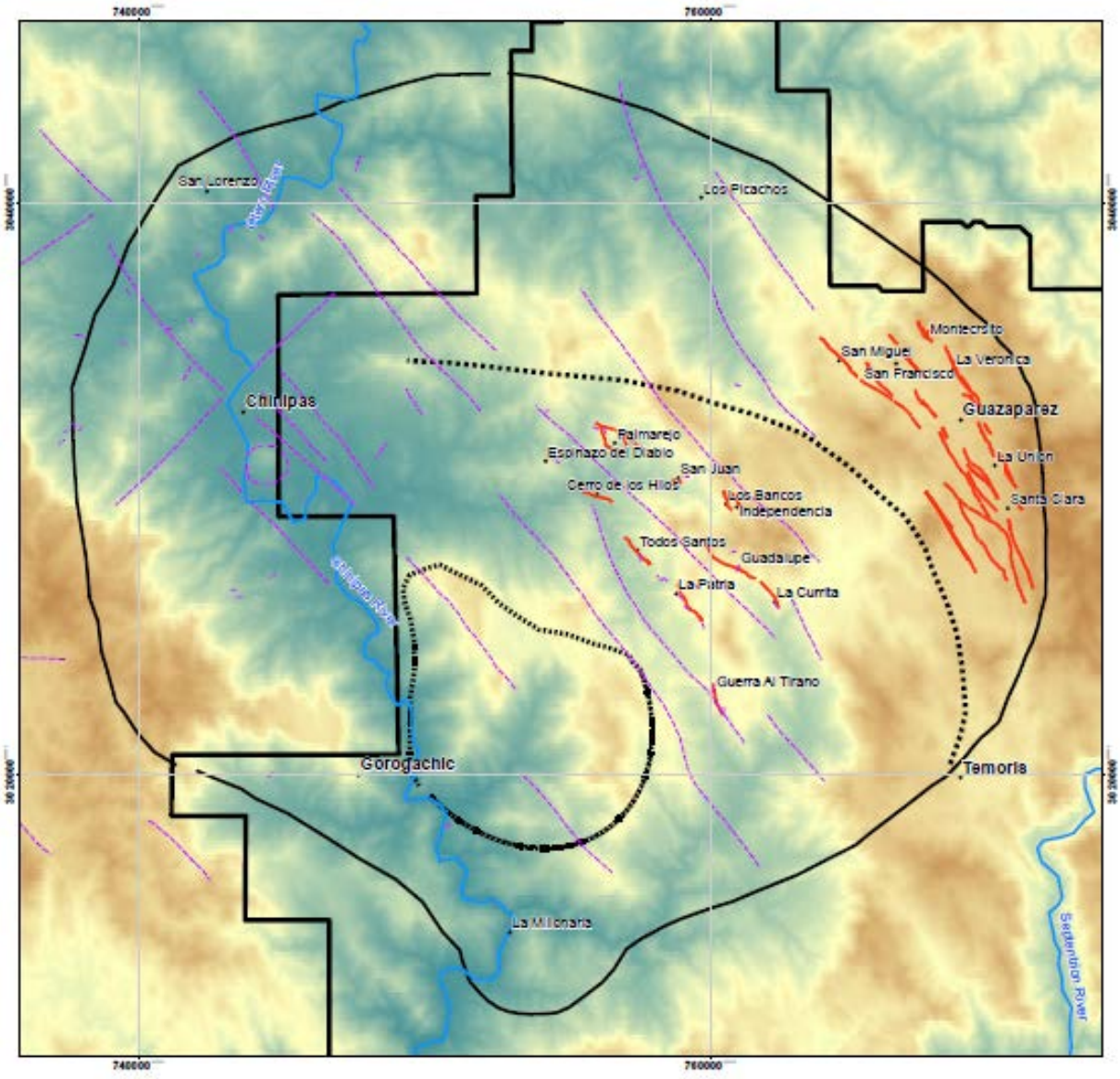

Figure 5.23 Temoris Caldera and resurgent rims, showing the interpretation of the Temoris caldera, and the Palmarejo resurgent rim (dotted line north of the Palmarejo District), and the resurgent dome at the core (west of Gorogachic). Some mineralized areas associated with the outer rim of the Temoris caldera are; Picachos, Temoris, Millonaria and San Lorenzo. The mineralization in the Guazaparez District is located between the outer rim and the Palmarejo resurgent rim. Mineralization between the resurgent rim and the doming are: Palmarejo, Guadalupe, La Patria, and Guerra al Tirano.

Bibliography

Aitchison, J., 1986, The Statistical Analysis of Compositional Data. Chapman and Hall, London - New York 1986, XII, 416 pp.

Beckton, J., 2004, Resource Report Palmarejo, Bolnisi Gold NL Internal Report, 47 p.

Bhattacharyya, B., 1966, Continuous Spectrum of the total Magnetic Field Anomaly due to a rectangular prismatic body, Geophysics Vol. 31, p. 91-121.

Birak, D., Maslowski, M., Molina, C., Melchor, A. and Figueroa, H., 2010, "Geology and Exploration History of The Palmarejo Silver and Gold District, Chihuahua, México", in Society of Economic Geologists, 2014, "Gold and Silver Mines of the Sierra Madre Occidental, Mexico", Guidebook Series, Volume 42.

Birak, D. and Blair, K., 2012. Technical Report for the Palmarejo Project SW Chihuahua State, Mexico. Report prepared for Coeur d'Alene Mines Corp.

Bryan, S., 2007, Silicic large igneous provinces: Episodes, v. 30, no. 1, p. 1 – 12.

Bryan, S. and Ernst, R., 2008, Revised definition of Large Igneous Provinces (LIP): Earth Science Reviews, v. 86, p. 175-202.

Bryan, S., Ferrari, L., Reiners, P., Allen, C., Petrone, C., Ramos, A. and Campbell, I., 2008, New Insight into Crustal Contributions to Large-volume Rhyolite Generation in the Mid Tertiary Sierra Madre Occidental Province, Mexico, Revealed by U-Pb Geochronology. Journal of Petrology, v. 49, p. 47-77.

Bryan, S. and Ferrari, L., 2013, Large Igneous Provinces and silicic Large Igneous Provinces: progress in our understanding over the last 25 years. Geological Society of America.

Burg, J., 1975, Maximum Entropy Spectral Analysis, Unpublished Doctoral Dissertation, Stanford University, 168 P.

Busby, C., 2008, Geology of the Sierra Madre Occidental, Mexico, November 2008 LIP of the Month, International Association of Volcanology and Chemistry of the Earth's Interior.

Cameron, K., Nimz, G., Kuentz, D., Niemeyer, S., and Gunn, S., 1989. Southern Cordilleran basaltic andesite suite, southern Chihuahua, Mexico: A link between Tertiary continental arc and flood basalt magmatism in North America. Journal of Geophysical Research. v. 94, p. 7817–7840.

Clark, K., and De La Fuente L., 1978, Distribution of mineralization in time and space in Chihuahua, México: Mineralium Deposita, v. 13, p. 27-49.

Clark, K., and Fitch, D., 2009, Evolución de los depósitos metálicos en el tiempo y el espacio en México. In: Clark, K., Salas-Piza, G. and Cubillas-Estrada, R. (Eds.), Geología Económica de México, II Edición, Servicio Geológico Mexicano, p. 62-133.

CRM, 2004, Informe Final de la Cartografía Geológico-Minera y Geoquímica, Consejo de Recursos Minerales, Carta Chínipas G12-B38, Escala 1:50,000, Estados de Chihuahua y Sonora.

Coeur, 2013, Coeur d'Alene Mines, NI 31-101 Palmarejo Technical Report, YE-2012.

Coeur, 2010, Coeur d'Alene Mines Corporation corporate public filings on SEDAR.

Corbett, G., 2004, Comments on Palmarejo, El Realito, and Yecora Exploration Projects, Northern Mexico. Internal Report prepared for Bolnisi Gold NL.

Corbett, G., 2006, Comments on Exploration at Palmarejo, Trogan, Cusi, Milpillas, and Namiquipa Projects, Chihuahua Mexico, Internal Report prepared for Bolnisi Gold NL.

Damon, P., Shafiqullah, M., and Clark, K., 1983, Geochronology of the porphyry copper deposits and related mineralization in Mexico. Canadian Journal of Earth Sciences. v. 20, p. 1052–1071.

Dreier, J., 1984, Regional Tectonic Control of Epithermal Veins in the Western United States and Mexico: Arizona Geological Society Digest, Vol 15, p 28-50.

Einaudi, M., Hedenquist, J., and Inan, E., 2003, Sulfidation state of fluids in active and extinct hydrothermal systems: Transitions form porphyry to epithermal environments: Society of Economic Geologists Special Publication 10, p. 285- 312.

Feinstein, M., 2007, Contributions to the Geology of the Cuenca de Oro: Chihuahua, Mexico. Department of Geological Sciences. University of Texas at El Paso, MS Thesis, 168 p.

Ferrari, L., Lopez, M. and Rosas, J., 2002, Ignimbrite flare-up and deformation in the southern Sierra Madre Occidental, western Mexico: implications for the late subduction history of the Farallon plate. Tectonics, v. 21, 1-24.

Ferrari, L., Valencia, M. and Bryan, S., 2007. Magmatism and tectonics of the Sierra Madre Occidental and their relation to the evolution of the western margin of North America. Geological Society of America, Special Papers 442, 1-39.

Galvan, V., 2005, Regional and Local Patterns of Mineralization in the Lower Batopilas and Urique Rivers in Sierra Madre of Chihuahua, Mexico. Department of Geological Sciences. University of Texas at El Paso, MS Thesis, p. 115.

Galvan, V., 2012, Palmarejo Carbonate-Base Metal Epithermal Ag-Au District, Chihuahua, Mexico, Unpublished Ph.D. dissertation, University of Tasmania.

Goodell, P., 1995, Porphyry copper deposits along the Batopilas lineament, Chihuahua, Mexico. In: Pierce, F., and Bolm, J. (Eds.), Porphyry Copper Deposits of the American Cordillera. Arizona Geological Society Digest, v. 20, p. 544.

Gupta, V., and Grant, F., 1985, Mineral Exploration Aspects of Gravity and Aeromagnetic Survey in the Sudbury–Cobalt area, Ontario, Society of Exploration Geophysicists, The Utility of Regional Gravity and Magnetic Anomaly Maps, W.J. Hinze (Editor), p. 392 – 411.

Gustin, M., 2005, Resource estimation report, Palmarejo-Trogan Project, Chihuahua, Mexico: Mine Development Associates (MDA) consultancy report for Bolnisi gold NL.

González Reyna J., 1956, Memoria Geológico Minera del Estado de Chihuahua, XX Congreso Geológico Internacional, pp. 98- 101.

Hedenquist, J., 2014, Observations on Epithermal Ag-Au veins in Palmarejo, Chihuahua, and La Preciosa, Durango districts, Mexico, Internal Report prepared for Coeur Mining, Inc.

Hedenquist, J., Arribas, A., and Gonzalez, E., 2000, Exploration for epithermal gold deposits: Reviews in Economic Geology, v. 13, p. 245-277.

Henry, C., 1975, Geology and geochronology of the granitic batholithic complex, Sinaloa, Mexico: Unpublished PhD Dissert., Univ. Texas, Austin, 158 pp.

Kerr, P., Gustin, M., Hlorgbe, D., Glanvill, J., Mondragon, R., Hoffer, M. and O'Prey, M., 2015, Technical Report for the Palmarejo Complex SW Chihuahua State, Mexico. NI 43-101 Technical Report.

Kürzl, H., 1988, Exploratory data analysis: recent advances for the interpretations of geochemical data. Journal of Geochemical Exploration, Vol. 30, pp. 309-32.

MacLeod, I., Jones, K., Fan Dai, T., 1993, 3D Analytical Signal in the Interpretation of Total Magnetic Field Data at Low Magnetic Latitudes, Exploration Geophysics, Vol. 24(3/4), p. 679 – 688.

Masterman, G., Phillips, K., Stewart, H., Lawrent, I., Beckton, J., Cordery, J., and Skeet, J., 2005, Palmarejo Silver- Gold Project, Chihuahua, Mexico: Discovery of a Ag-Au Deposit in the Mexican Sierra, in Yates, K. (Ed): New Gold 2005, Conference Proceedings, Louthean Media Pty, Perth, Australia, Nov, 28-29, 2005, p 99-115.

McDowell, F. and Clabaugh, S., 1979, Ignimbrites of the Sierra Madre Occidental and their relation to the tectonic history of western Mexico: in, C.E. Chapin and W.E. Elston, (eds.), Ash-Flow Tuffs: Geological Society of America Special Paper 180, p. 113-124.

McDowell, F., Keizer R., 1977, Timing of mid-Tertiary volcanism in the Sierra Madre Occidental between Durango City and Mazatlán, México: Geological Society of America Bulletin, v. 88, p. 1479-1487.

McDowell, F., Mauger, R., 1994, K-Ar and U-Pb zircon chronology of Late Cretaceous and Tertiary magmatism in central Chihuahua State, Mexico. Geological Society of America Bulletin. v. 106, p. 118-132.

McDowell, F. and McIntosh, W., 2012, Timing of intense magmatic episodes in the northern and central Sierra Madre Occidental, western Mexico. Geosphere. v. 8, p. 1502-1526.

Melchor, A., 2005, Mineragraphic Reports on Selected Samples from Palmarejo. Private report prepared for Bolnisi Gold NL.

Melchor, A., 2010, Report on the Mineralogy of Guadalupe Au-Ag Epithermal Vein Deposit, an Au-Ag-Cu-As Vein System. Private report prepared for Coeur d'Alene Mines Corp.

Miller, R. and Goodell, P., 1988, Description of the Los Llanitos Mining District, southwestern Chihuahua, Mexico; in Stratigraphy, Tectonics and Resources of Parts of Sierra Madre Occidental Province, Mexico: El Paso Geol. Soc. Field Conf. Guidebook, p. 287-296.

Molina, C., 2005, ASTER Imagery Processing of the Temoris – Guazaparez District, CMS Image Lab private report prepared for Bolnisi Gold LN.

Molina, C., 2008, Field and logging observations from Guadalupe, Internal report, Coeur Mexicana S.A. de C.V.

Molina, C., 2010, Analysis on rock chip sample spectrometry for clay identifications using Terra Spec, Coeur Mexicana S.A. de C.V., Internal report.

Molina, C., Goodell, P., 2015, "Análisis Geoestadístico de la Mineralización en la Mina Guadalupe, Distrito Palmarejo, Chihuahua, México", AIMMGM, 2015 International Mining Conference.

Murray, B., 2009, Preliminary interpretations of the geologic history of the northern Sierra Madre Occidental in the Guazapares Mining District and vicinity, western Chihuahua, Mexico. Santa Barbara, CA: University of California, Department of Earth Science.

Murray, B., Busby, C., Ferrari, L. and Solari, L., 2013, Synvolcanic crustal extension during the mid-Cenozoic ignimbrite flare-up in the northern Sierra Madre Occidental, Mexico: Evidence from the Guazapares Mining District region, western Chihuahua. Geosphere, v. 9, no. 5.

Murray, B., and Busby, C., 2015, Epithermal mineralization controlled by synextensional magmatism in the Guazapares Mining District of the Sierra Madre Occidental silicic large igneous province, Mexico. Journal of South American Earth Sciences, v. 58, 18 p.

Niton, 2008, Mining Exploration and Geochemical Analysis of Mining Samples: Thermo Scientific Niton XL3t Series Handheld XRF Mining Analyzers, Thermo Fisher Scientific Inc.

NOAA, 2015, National Oceanic Atmospheric Administration, WMM2015, World Magnetic Model.

Perez, E., 2013, Caracterización de oro en las muestras: 133676, 79963, 77782, 132877, 134510 y 132629 de Paramount Gold de México. Private Report.

Raisz, E., 1964, Landforms of Mexico, U. S. Office of Naval Research, Geography Branch.

Ramirez, A., 2016, Geology, Geochemistry and 3D Geological modeling of the Independencia - Los Bancos Ag-Au Epithermal vein systems in the Palmarejo District, Department of Geological Sciences. University of Texas at El Paso, MS Thesis, 124 p.

Rasmussen, H., Nasi, C., Molina, C. and Hohbach, P., 2014, "Geology and Exploration History of The Palmarejo Silver and Gold District, Chihuahua, México", (Revised Version), in Society of Economic Geologists, 2014, "Gold and Silver Mines of the Sierra Madre Occidental, Mexico", Guidebook Series, Volume 42.

Reimann, C., Filzmoser, P., Garrett, R. G., and Dutter, R., 2008, Statistical Data Analysis Explained: Applied Environmental Statistics, John Wiley & Sons, Ltd., 362p.

Reimann, C. and Filzmoser, P., 2000, Normal and lognormal data distribution in geochemistry: death of a myth. Consequences for the statistical treatment of geochemical and environmental data. Environ. Geol. 39, pages 1001–1014.

Rhys D., 2009; Evaluation of Structural and Geological Controls on Vein-Hosted Gold Mineralization at the Palmarejo Deposit, Chihuahua State, Mexico. Internal report prepared for Coeur D'Alene Mines Corp.

Roest, W., Verhoef, J., and Pilkington, M., 1992, Magnetic Interpretation using the 3D Analytical Signal, Geophysics, V.57(1), p. 116 – 125.

Ross, K. V., 2009, Petrographic Study of Palmarejo Deposit, Chihuahua State, Mexico. Internal report prepared for Coeur D'Alene Mines Corp.

Rubio, M. and Albinson, T., 2005; Paragenetic and Microthermometric Survey on Veins Located in the Mining District of Palmarejo, Chinipas, Chihuahua, Mexico.

Sall, J., Creighton, L., and Lehman, A., 2005, JMP® Start Statistics, copyright SAS statistics, Cary, NC, 3rd Edition, 560p.

Sellepack, S., 1997, The geology and geochemistry of the El Sauzal gold prospect, southwest Chihuahua, Mexico. Department of Geological Sciences. University of Texas at El Paso, MS Thesis.

Sillitoe, R., and Hedenquist, J., 2003, Linkages between Volcanotectonic Settings, Ore-Fluid Compositions, and Epithermal Precious Metal Deposits in Volcanic, Geothermal, and Ore-Forming Fluids: Rulers and Witnesses of Processes within the Earth: Society of Economic Geologists Special Publication No. 10, p. 315-345.

Sillitoe, R., 2010, Comments on Geology and Exploration of the Palmarejo Epithermal Silver-Gold Deposit and Environs, Chihuahua, Mexico, Internal Report for Coeur D'Alene Mines Corp., 14 p.

Sillitoe, R., 2013, Further Comments on Geology and Exploration of the Palmarejo Epithermal Silver-Gold Deposit and Environs, Chihuahua, Mexico, Internal Report for Coeur D'Alene Mines Corp., 9 p.

Spector, A., and Grant, F., 1970, Statistical Models for Interpreting Aeromagnetic Data, Geophysics, Vol.35, p. 293-302.

SRK Consulting, 2014, Geological Mapping Program and Aeromagnetic Interpretation of the Palmarejo Property, Chihuahua State, Mexico. Internal Report for Coeur Mining, Inc., 105 p.

Staude, J., and Barton, M., 2001, Jurassic to Holocene tectonics, magmatism, and metallogeny of northwestern México: Geological Society of America Bulletin v. 113, p. 1357-1374.

Stephens, M., 1974, EDF Statistics for Goodness of Fit and Some Comparisons, Journal of the American Statistical Association, American Statistical Association, 69 (347), P. 730–737.

Swanson, E. and McDowell, F., 1984, Calderas of the Sierra Madre Occidental volcanic field, western Mexico: Journal of Geohysical Research, v. 89, p.8787-8799.

United Nations, 2006, Reports of International Arbitral Awards, "The Palmarejo and Mexican Gold Fields (Ltd.) (Great Britain) v. United Mexican States, 6 August 1931, Volume V, pp. 298-302.

Verduzco, B., Fairhead, D., Green C., and Mackenzie, C., 2004, New Insights into Magnetic Derivatives for Structural Mapping, The Leading Edge, 23(2), p.116-119.

Vizcarra, M., 2012, Estudio Geofísico de Magnetometría de Alta Resolución, Proyecto Palmarejo Chihuahua, México. Internal Report for Coeur Mexicana S.A. de C.V.

Wark, D., Kempter, K. and McDowell, F., 1990, Evolution of waning subduction- related magmatism, northern Sierra Madre Occidental, México: Geological Society of America Bulletin, v.102, p. 1555-1564.

Wiener, N., 1949, Extrapolation and Smoothing of Stationary Time Series: With Engineering Applications, Cambridge, MIT Press.

Winograd, S., 1978, On computing the Discrete Fourier Transform, Mathematics of Computation, Volume 32, Number 141, p. 175-199.

Wisser, E., 1966, The Epithermal Precious Metal Province of Northwest Mexico: Nevada Bureau of Mines Report 13, p. 63-92.

Zhang, C., Manheim, F., Hinde, J., and Grossman, J., 2005, Statistical characterization of a large geochemical database and effect of sample size, Applied Geochemistry, Vol. 20, pages 1857-1874.

Zumlot, T., Goodell, P. and Howari, F., 2008, Geochemical mapping of New Mexico, USA, using stream sediment data, Journal of Environmental Geology, Vol. 58, p1479-1497.

Vita

Castulo Molina Sotelo, the son of Cástulo and Ofelia, was born in Villa de Iturbide, Nuevo León, Mexico. He earned his Engineer in Geology degree from the Universidad Autónoma de Chihuahua in 1987. He attended the graduate school at the University of Texas at El Paso and got his MS degree in 1997. Afterwards, while working as a private consultant, Cástulo had the privilege to teach courses on Mineral Deposits, Mining Geology and Petrography at the UACH. As a consultant, his professional career has been mostly in mining management and mineral exploration. His background includes much experience in epithermal gold-silver targets and mining business management. Castulo returned to UTEP in Spring 2003 to pursue a PhD degree, and after the completion of the required course load, he was enrolled by Bolnisi (an Australian Junior) in 2005 as a consultant to participate in the exploration of the Palmarejo district. After the successful exploration at “Guadalupe”, Cástulo was promoted to District Manager, then to National Exploration Manager. The Bolnisi Gold's assets were sold in 2008 to Coeur Mining (the largest U.S. silver mining company), and he was asked to remain in charge of the Exploration in Mexico, under Coeur’s ownership. In 2012 Cástulo promoted to Administrative Vice-President of Coeur Mexicana, and now functions as Senior Vice-President of Coeur in Mexico. All this work experience has allowed him to successfully participate in national and international mining conferences and projects, and to continue his education by taking appropriate courses. It has also allowed him to publish several articles in professional and scientific mining and geological journals.

Contact Information: cacho_molina@hotmail.com

This dissertation was typed by Cástulo Molina Sotelo.